US 20160282427A1

(19) **United States**

(12) **Patent Application Publication**

Heidmann

(10) **Pub. No.: US 2016/0282427 A1**

(43) **Pub. Date: Sep. 29, 2016**

(54) **INTEGRATED OPTICAL NANOSCALE PROBE MEASUREMENT OF ELECTRIC FIELDS FROM ELECTRIC CHARGES IN ELECTRONIC DEVICES**

(71) Applicant: **Infinitum Solutions, Inc.**, Santa Clara, CA (US)

(72) Inventor: **Juergen Heidmann**, Salinas, CA (US)

(21) Appl. No.: **15/179,742**

(22) Filed: **Jun. 10, 2016**

Related U.S. Application Data

(63) Continuation-in-part of application No. 14/952,852, filed on Nov. 25, 2015, which is a continuation-in-part of application No. 14/542,410, filed on Nov. 14, 2014, Continuation-in-part of application No. 14/532,992, filed on Nov. 4, 2014, which is a continuation-in-part of application No. 14/184,610, filed on Feb. 19, 2014, now Pat. No. 8,885,301.

(60) Provisional application No. 61/950,596, filed on Mar. 10, 2014.

Publication Classification

(51) **Int. Cl.**
G01R 33/26 (2006.01)
G01N 21/64 (2006.01)

(52) **U.S. Cl.**
CPC ***G01R 33/26*** (2013.01); ***G01N 21/64*** (2013.01)

(57) **ABSTRACT**

A diamond probe is suitable to be attached to an Atomic Force Microscope and is created with a tip that incorporates a one or more Nitrogen Vacancy (NV) centers located near the end of the tip. The probe arm acts as an optical waveguide to propagate the emission from the NV center with high efficiency and a beveled end directs excitation light to the NV center and directs photoluminescence light emanating from the NV center into the probe arm. The probe tip is scanned over an area of a sample with an electric charge, such as a field effect transistor or flash memory. Optically Detected Spin Resonance (ODMR) is measured as the probe tip is scanned over the area of the sample, from which a characteristic of the area of the sample with the electric charge may be determined.

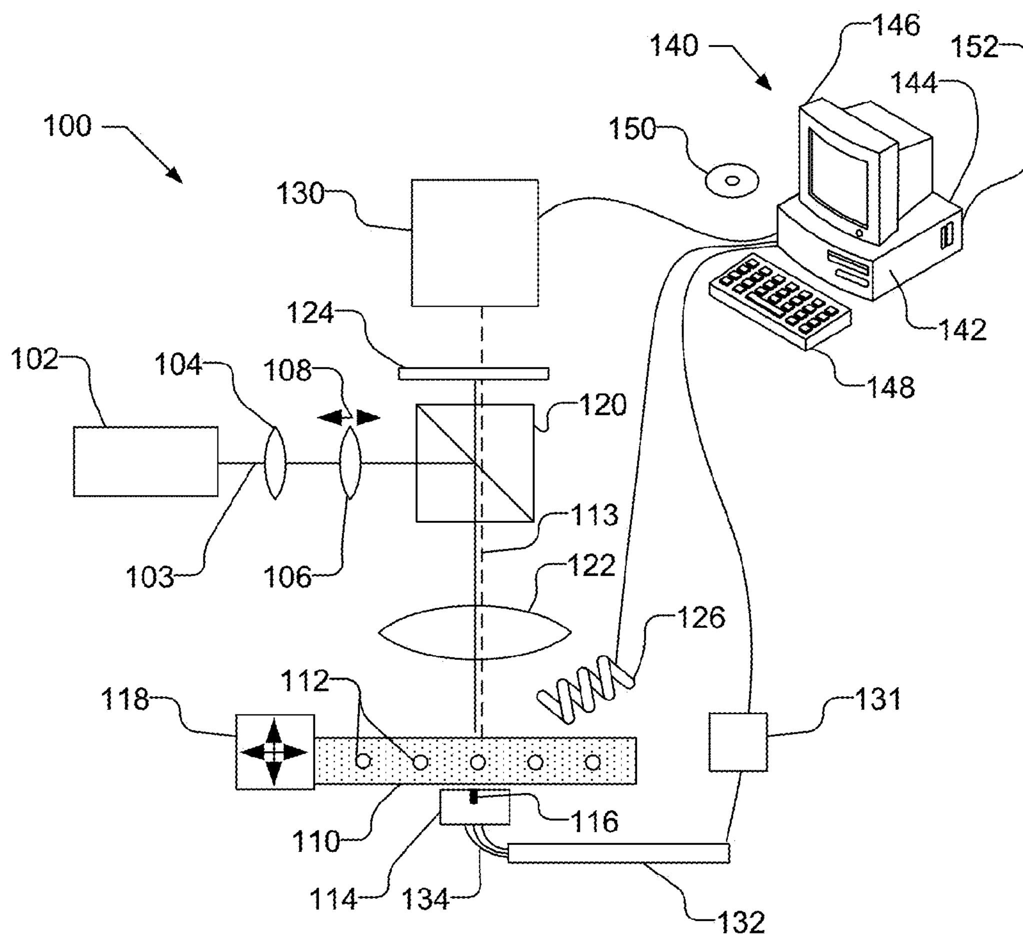

Fig. 1

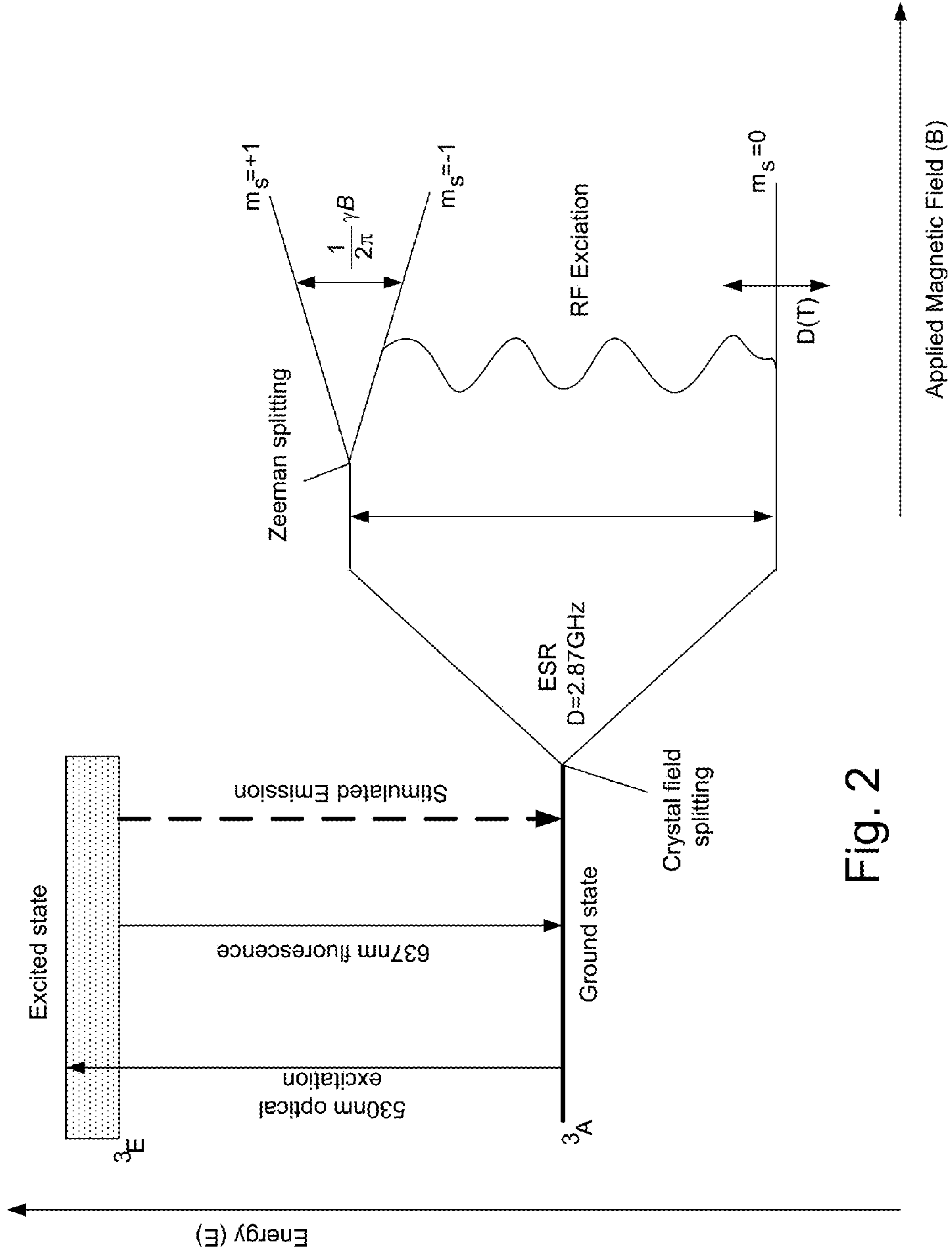

Fig. 2

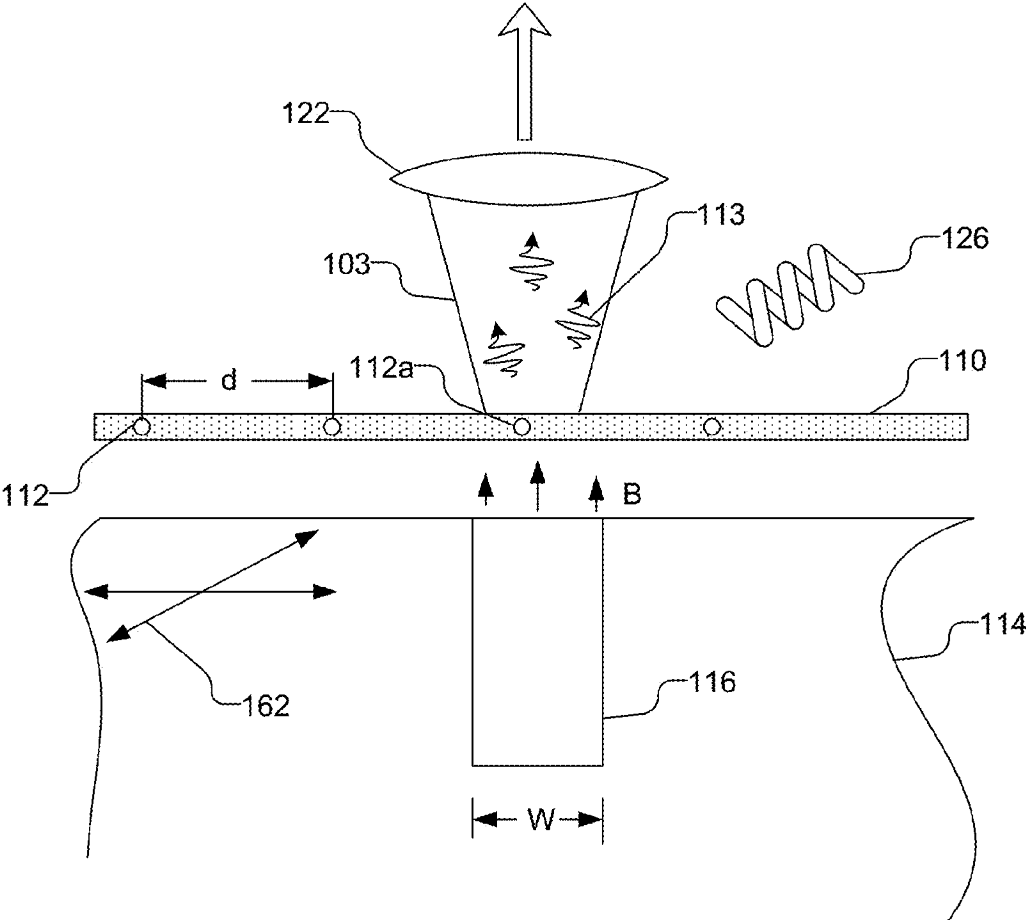

Fig. 3

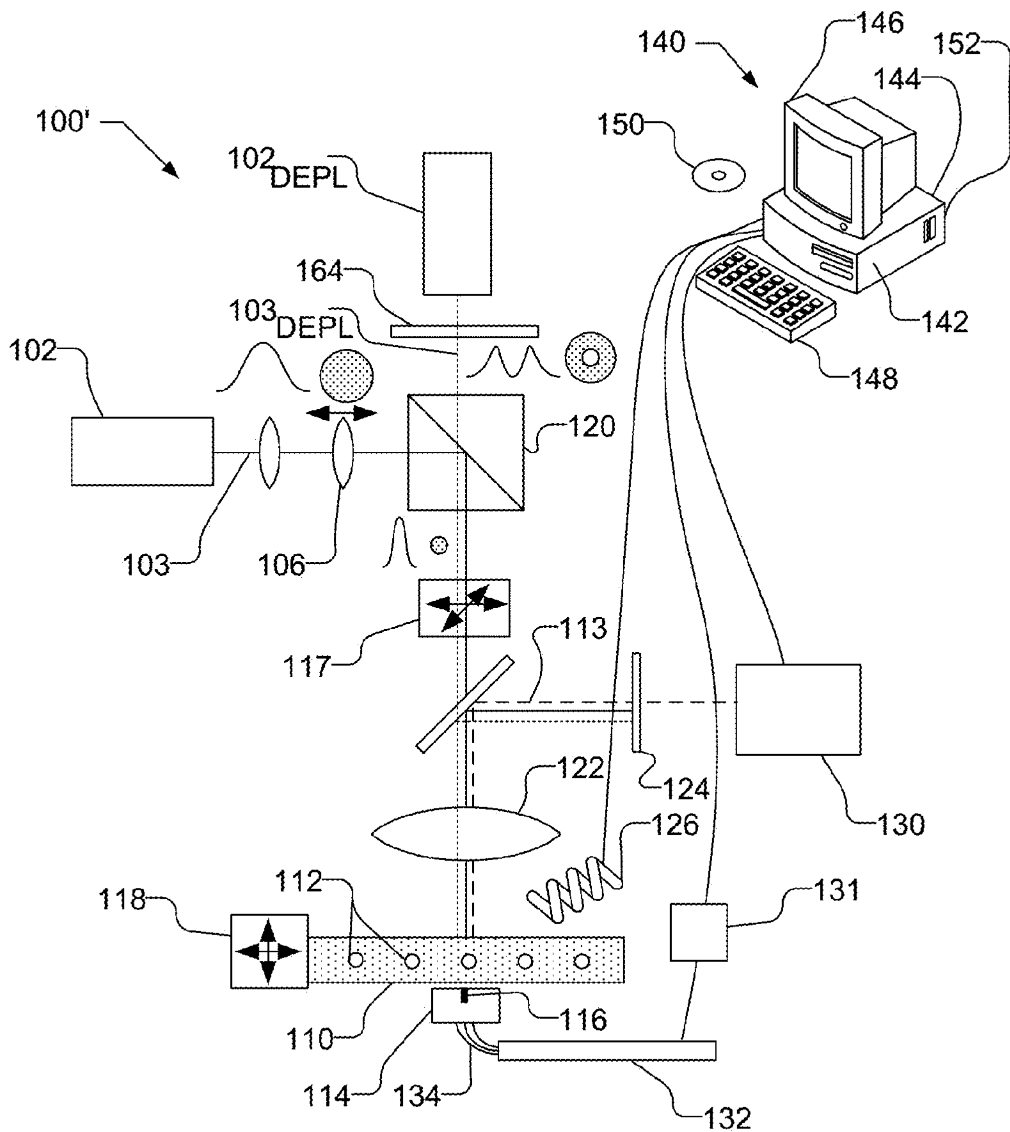

Fig. 4

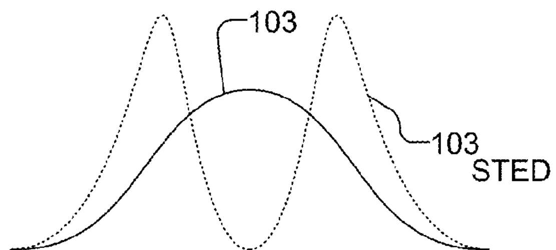

Fig. 5

Fig. 6

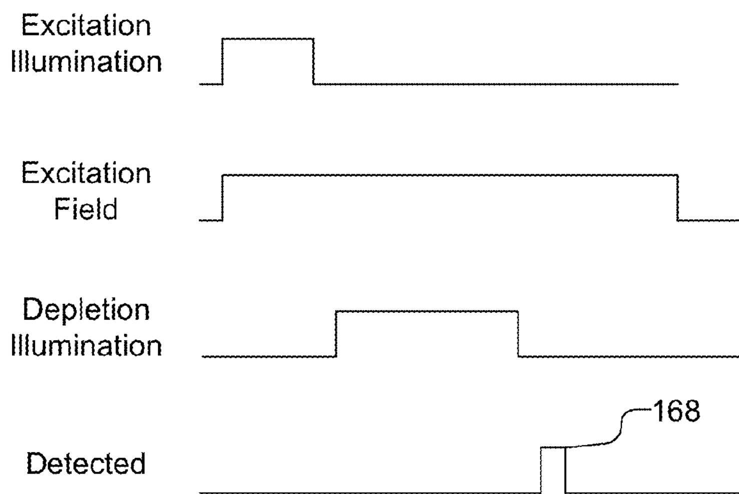

Fig. 7

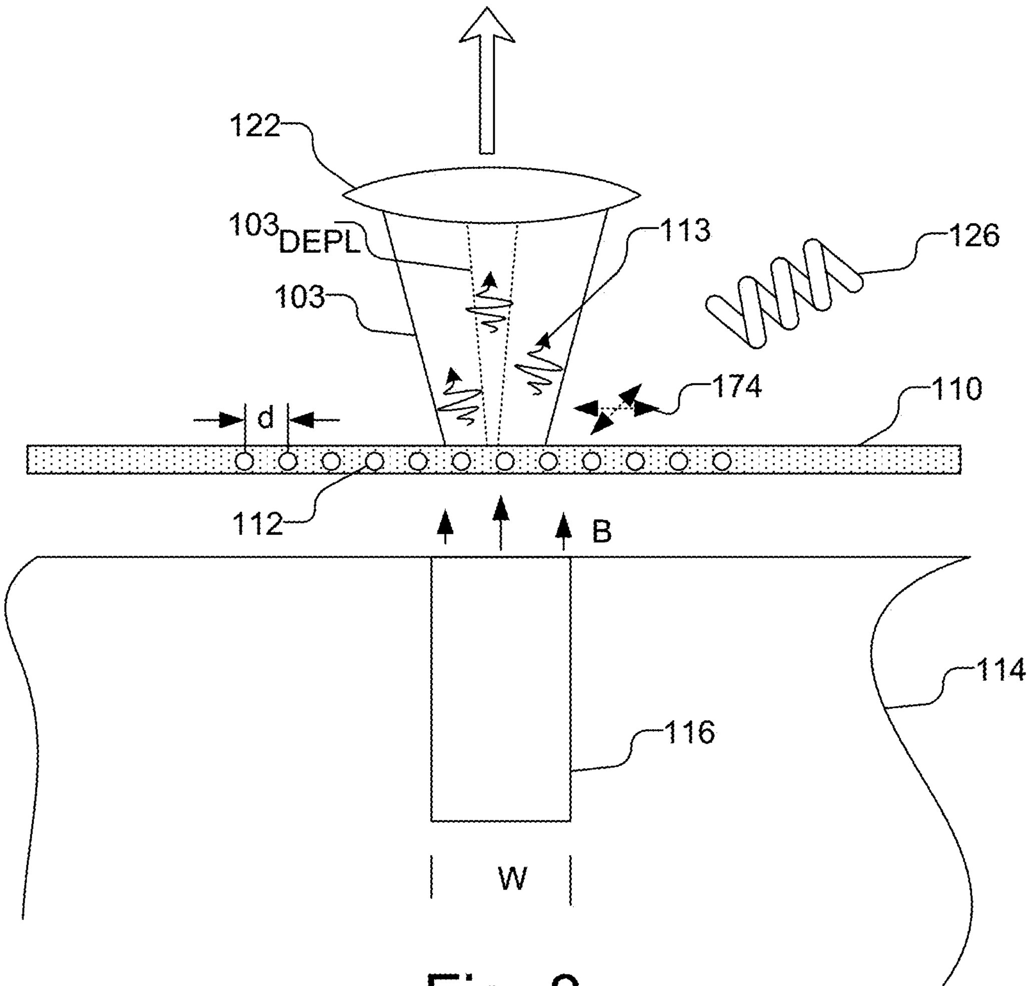

Fig. 8

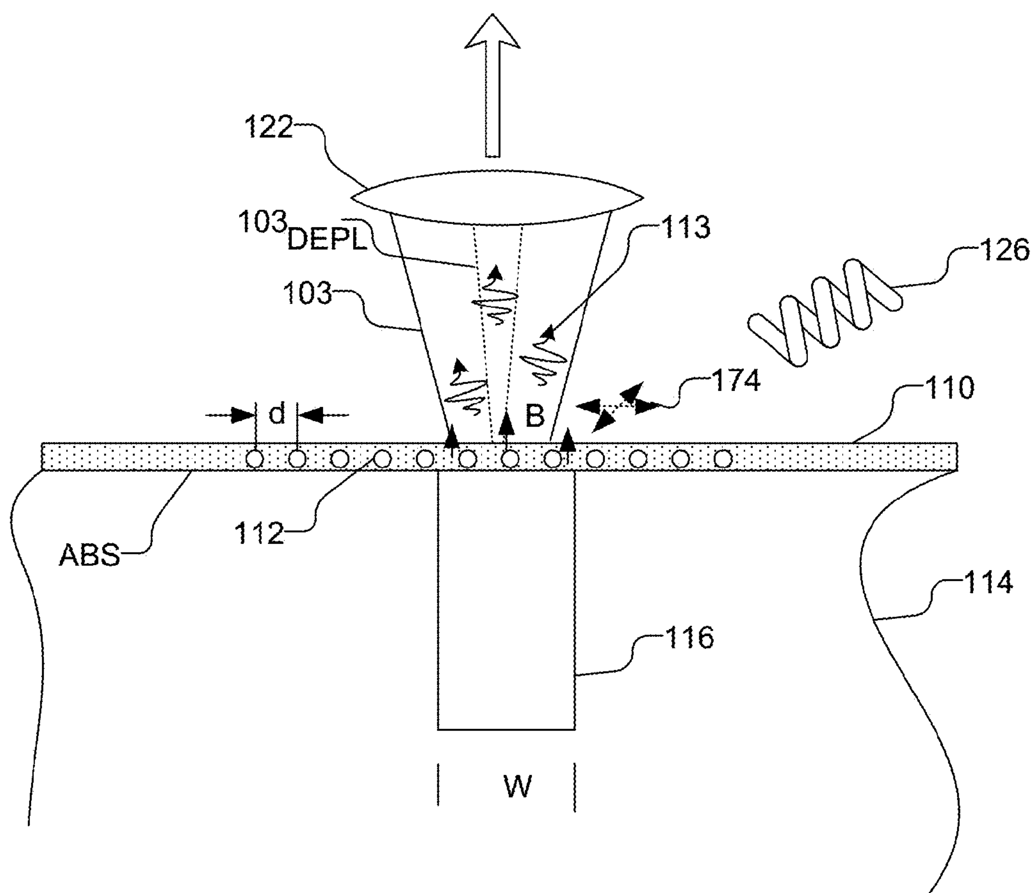

Fig. 9

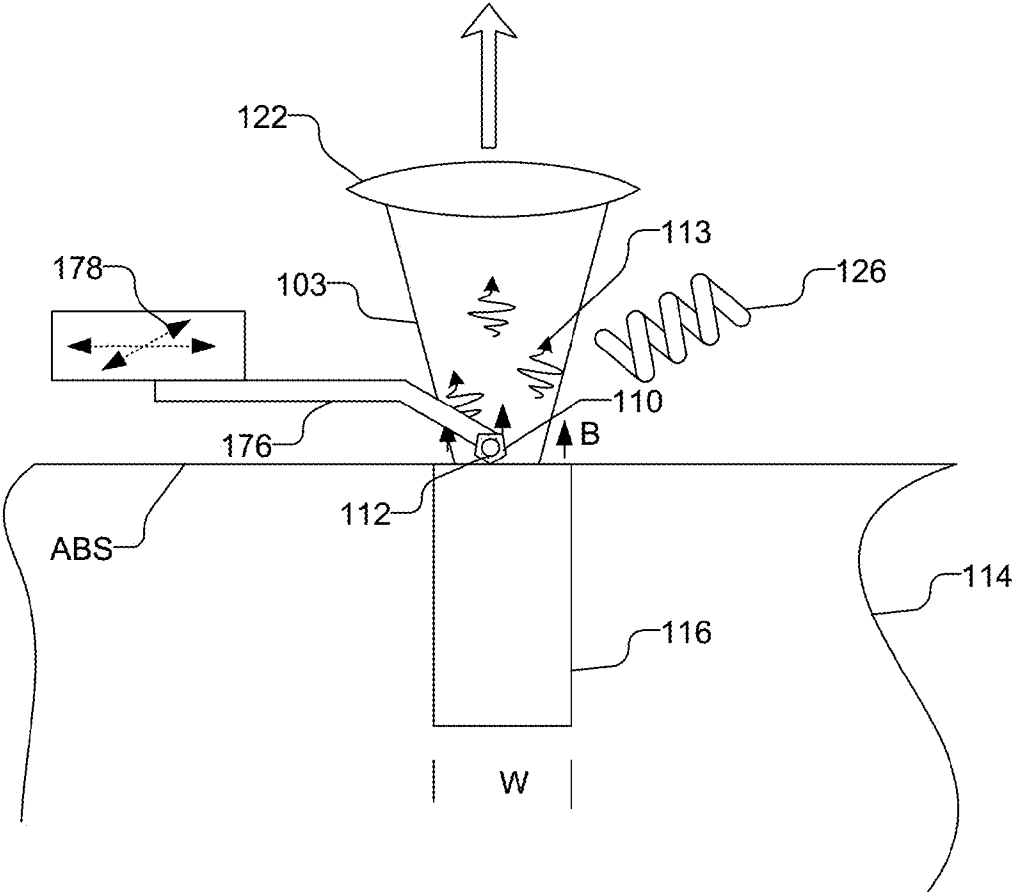

Fig. 10

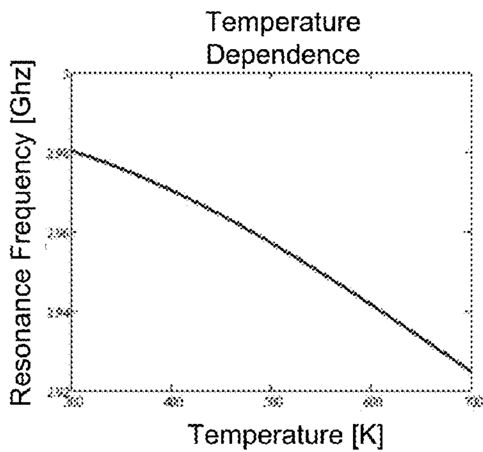

Fig. 11A

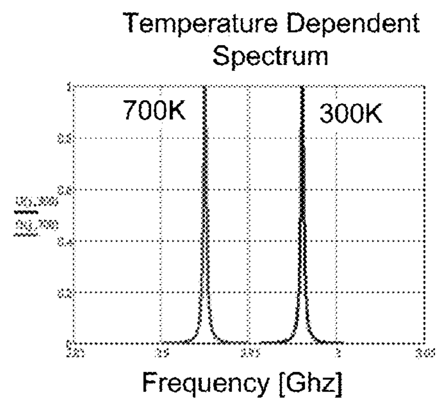

Fig. 11B

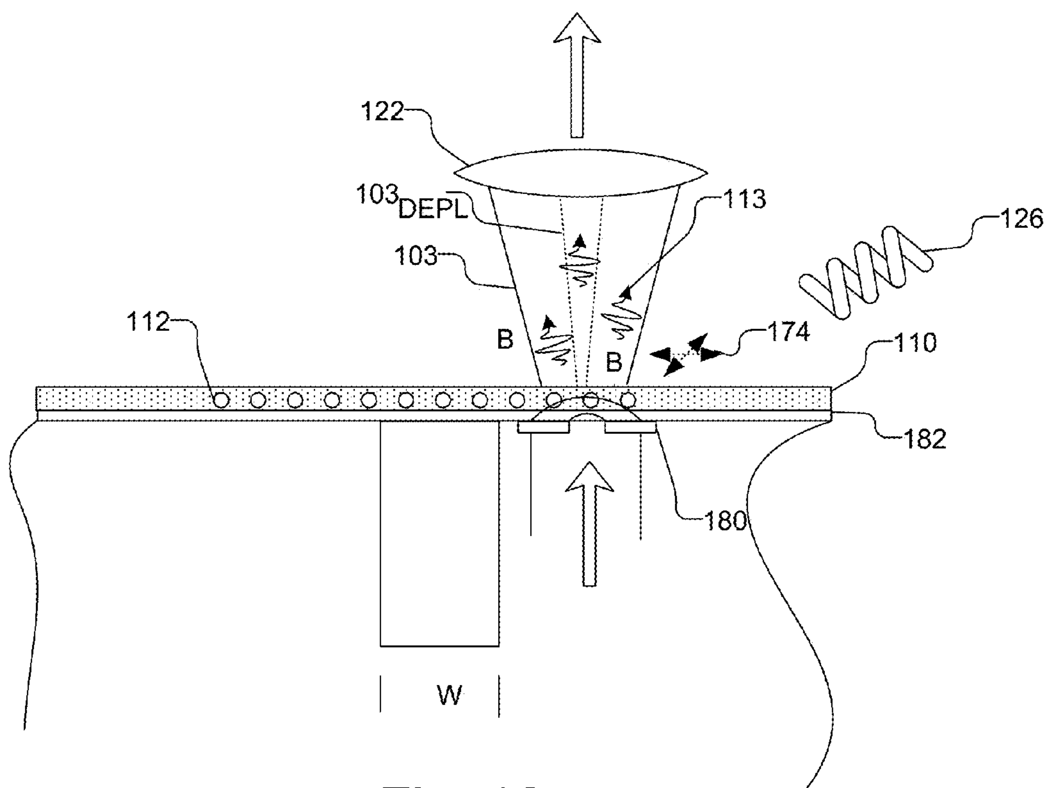

Fig. 12

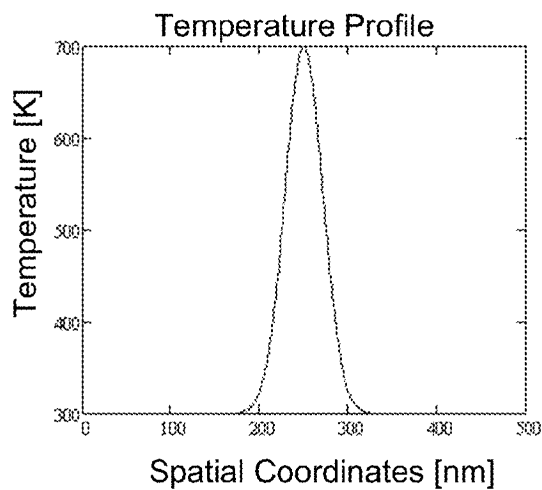

Fig. 13

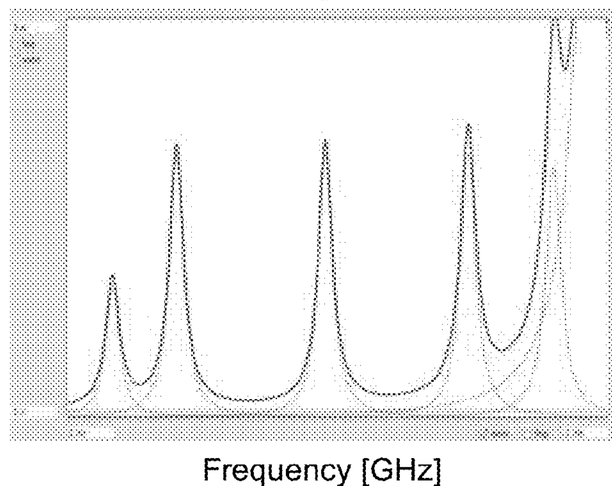

Fig. 14

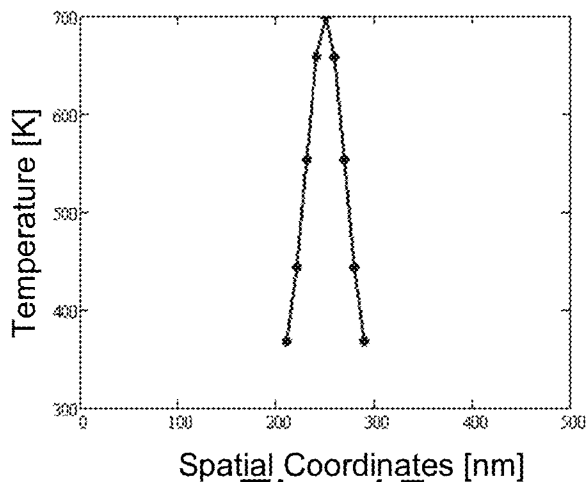

Fig. 15

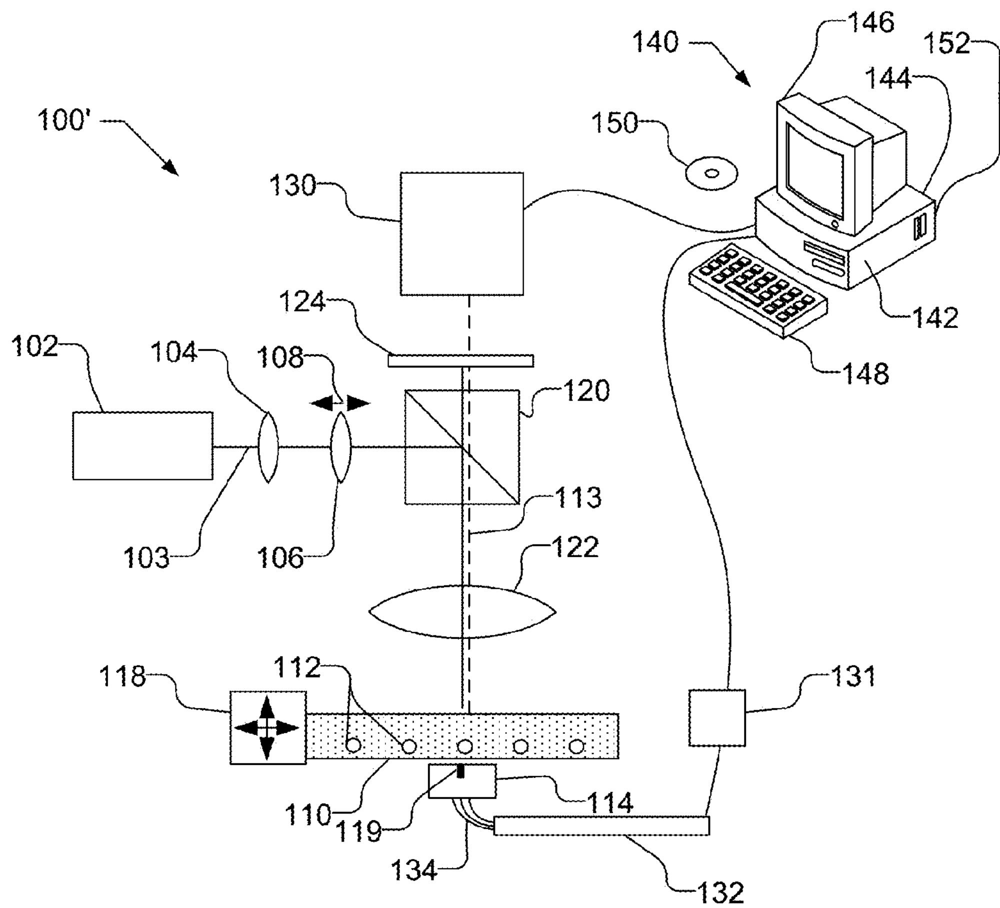

Fig. 16

Fig. 17A

Fig. 17B

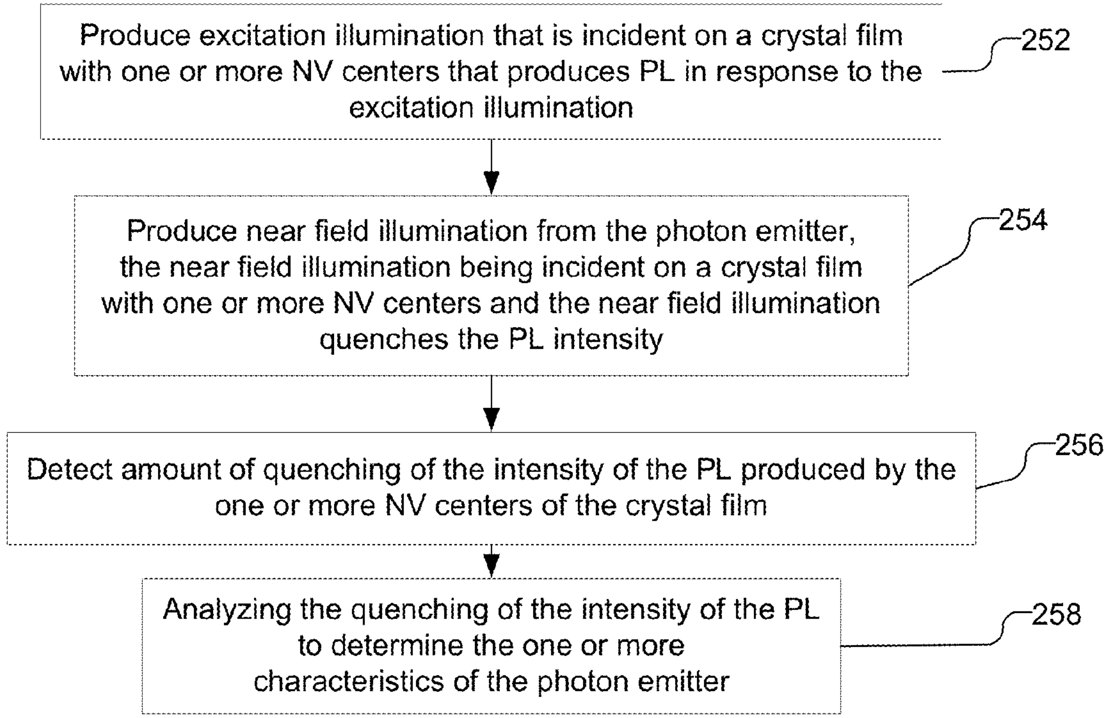

Fig. 18

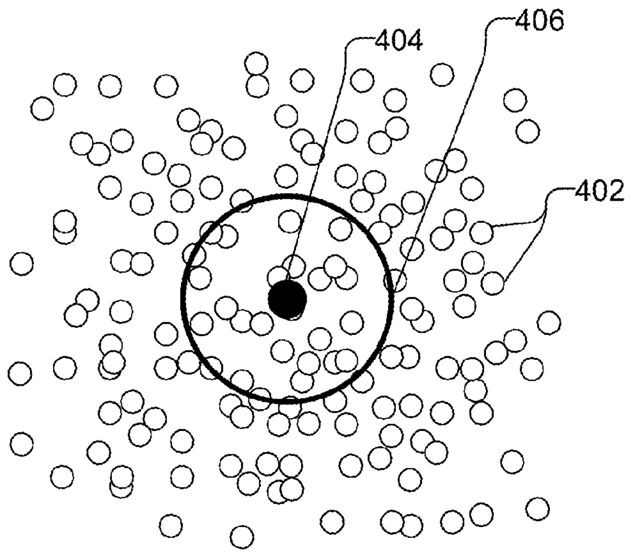

Fig. 19

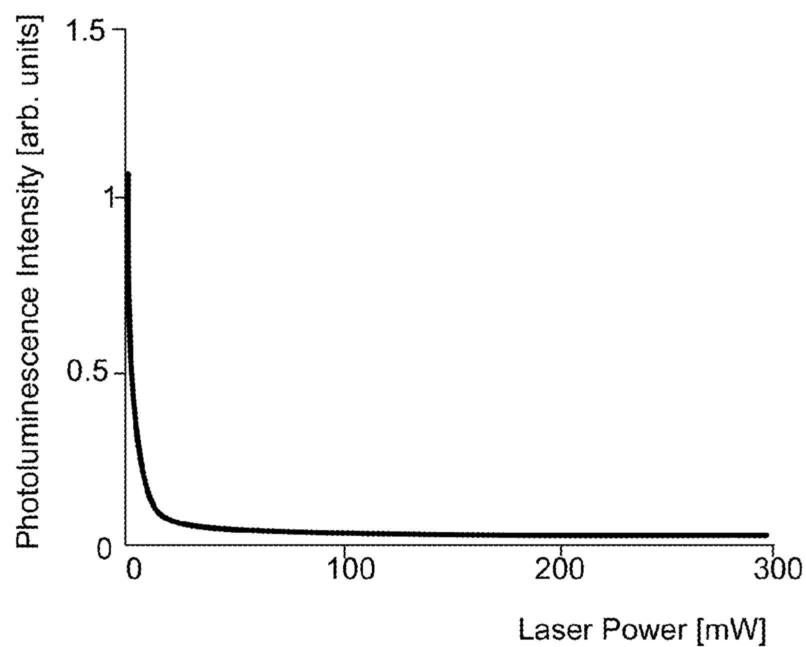

Fig. 20

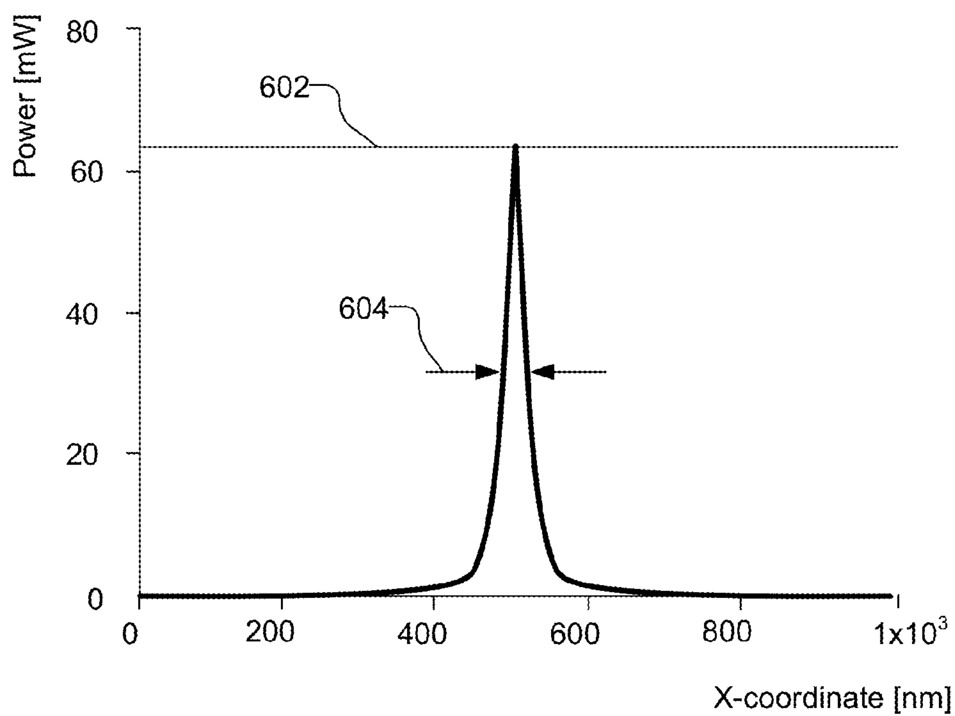

Fig. 21

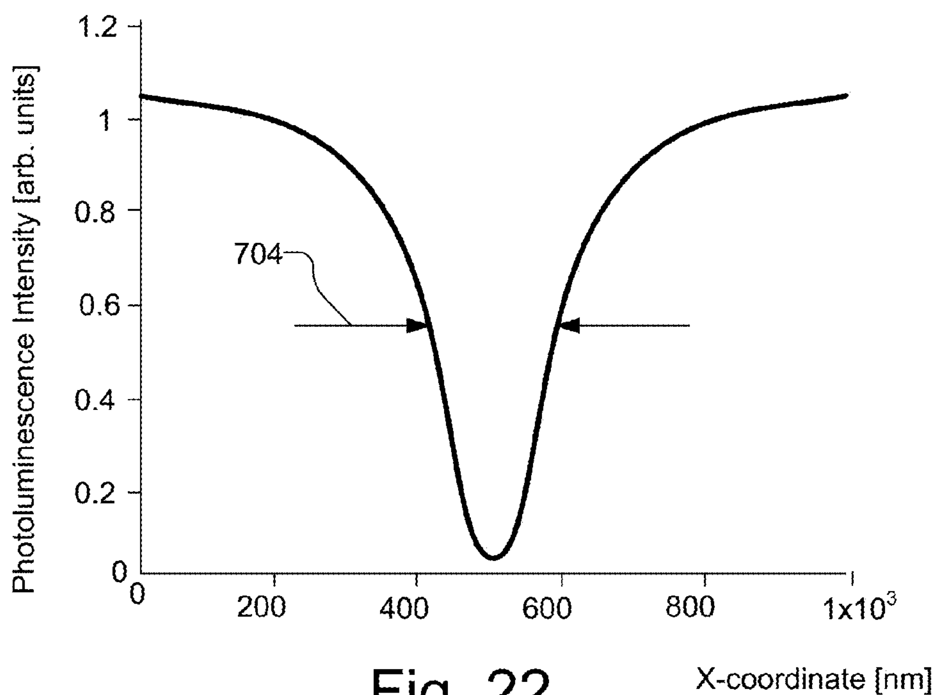

Fig. 22

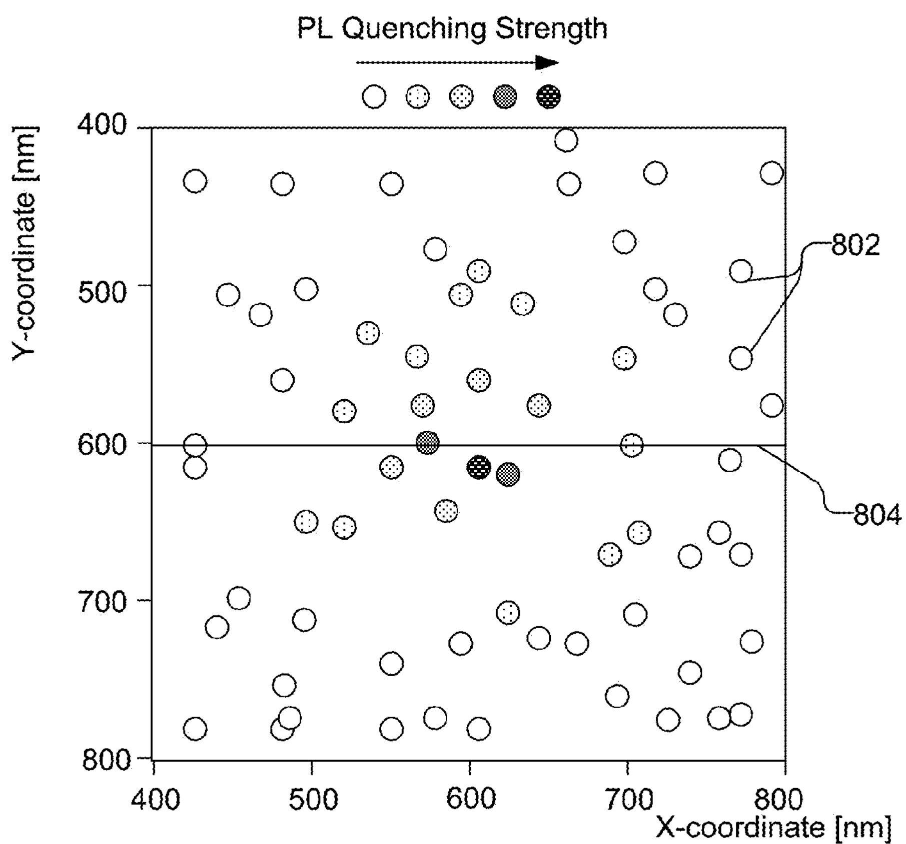

Fig. 23

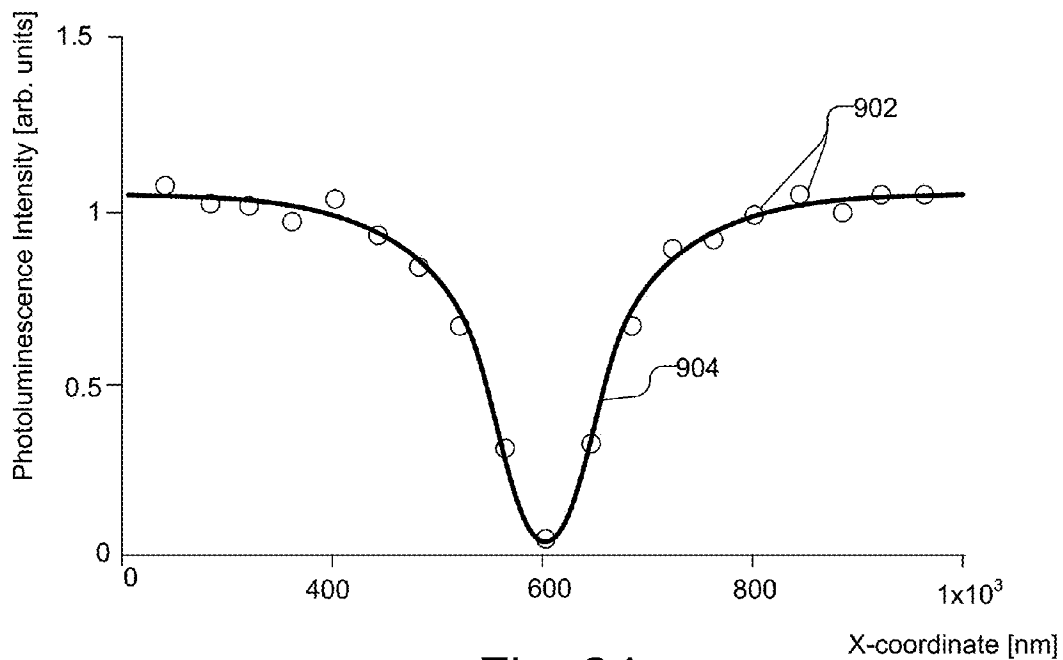

Fig. 24

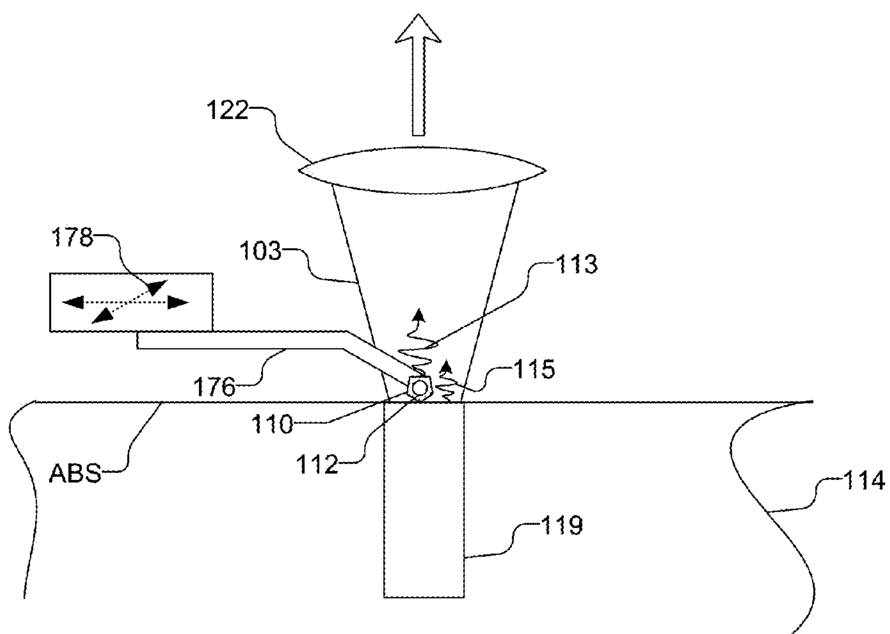

Fig. 25

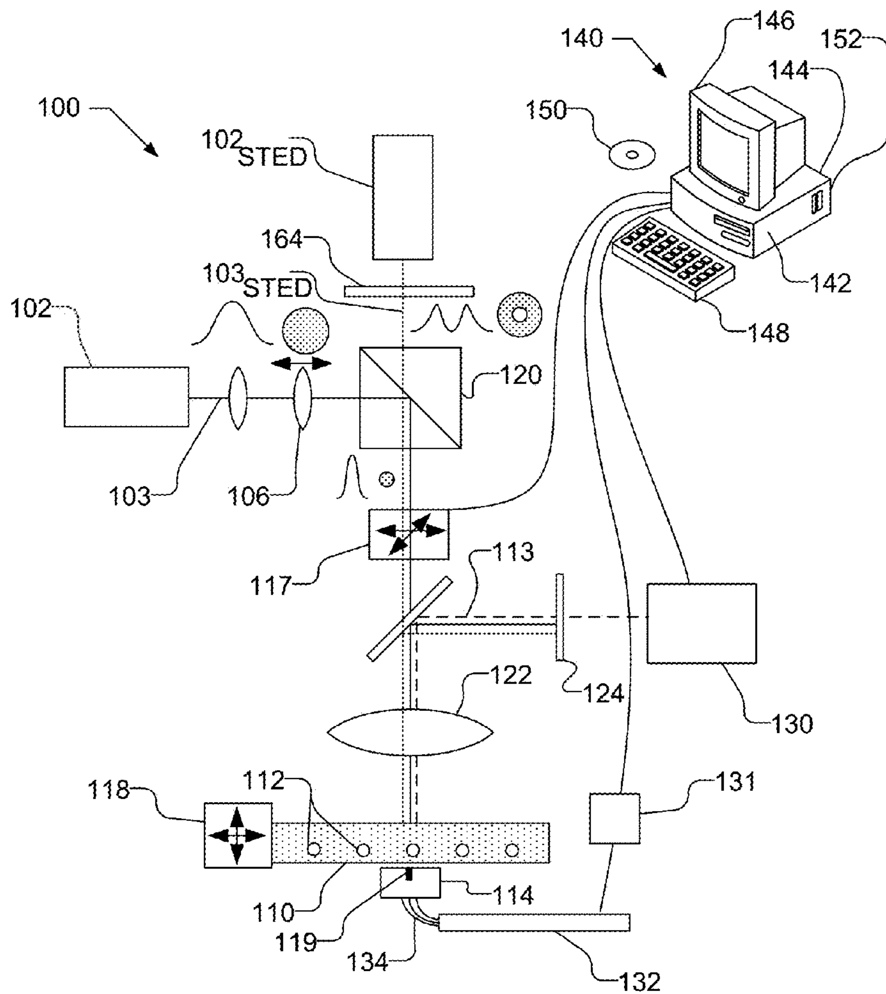

Fig. 26

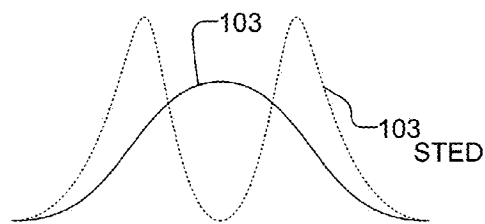

Fig. 27

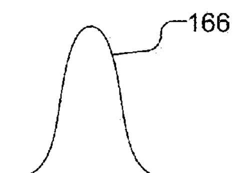

Fig. 28

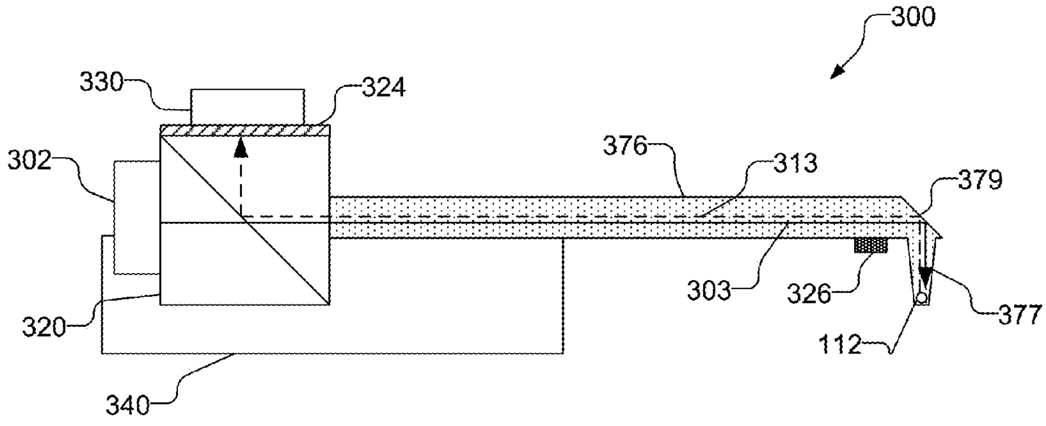

Fig. 29

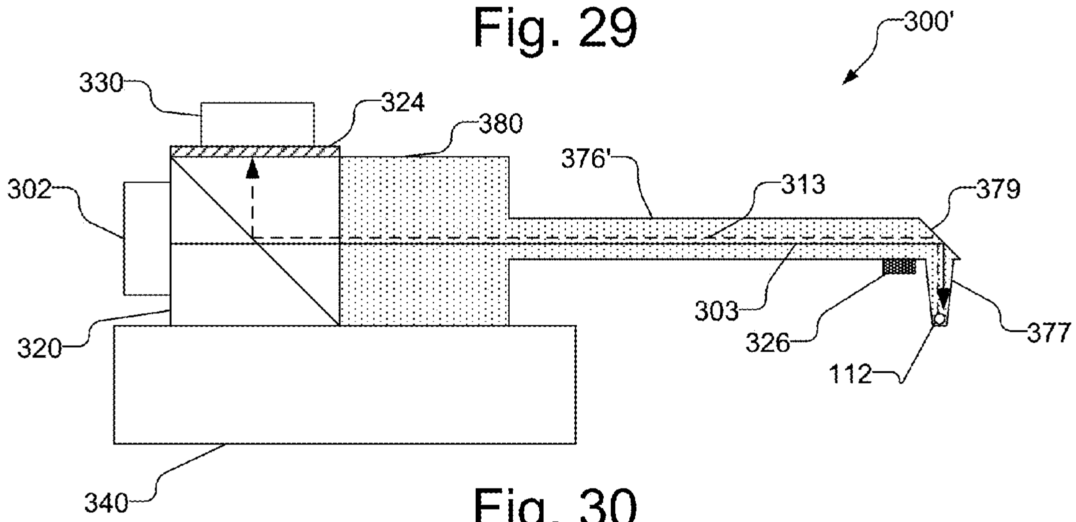

Fig. 30

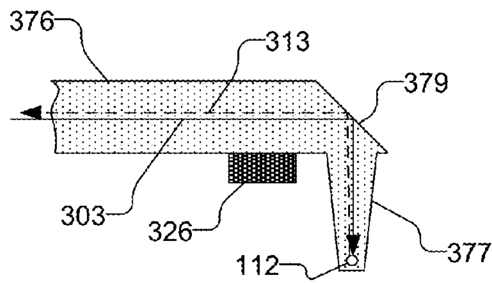

Fig. 31

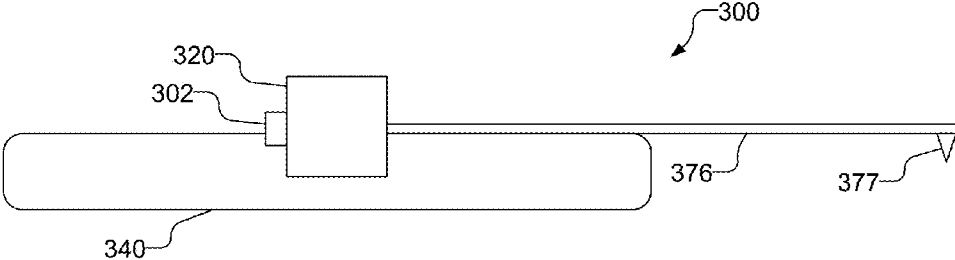

Fig. 32

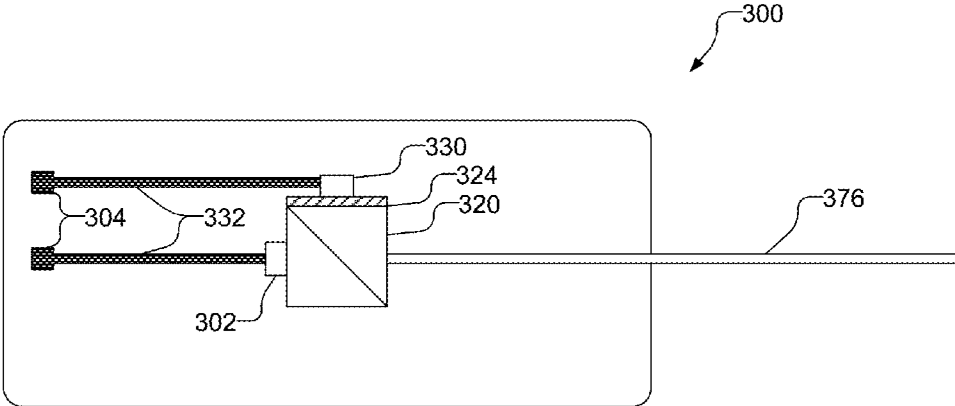

Fig. 33

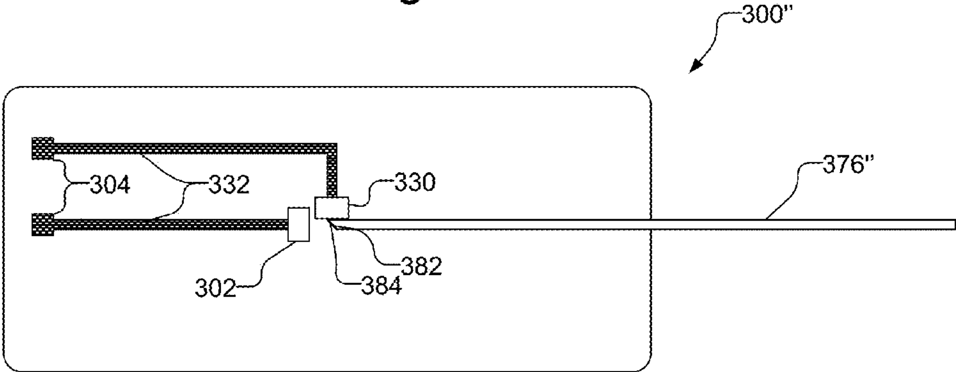

Fig. 34

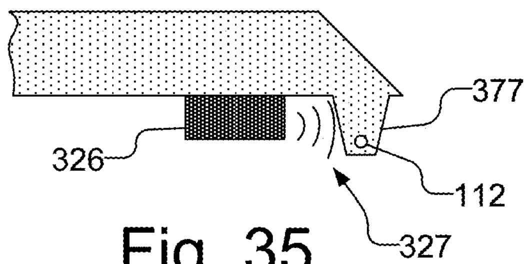

Fig. 35

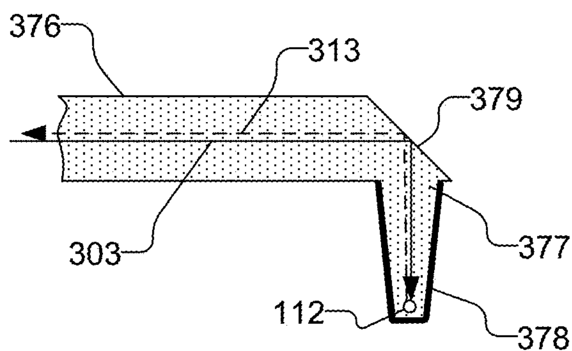

Fig. 36

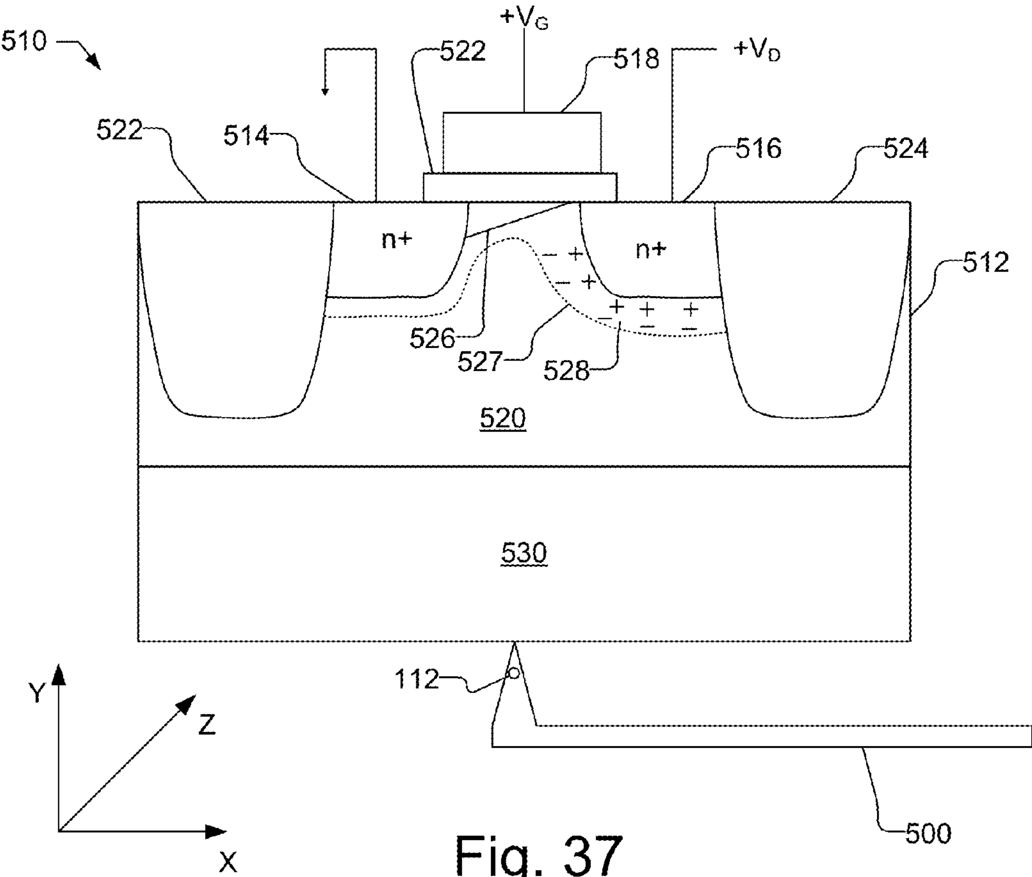

Fig. 37

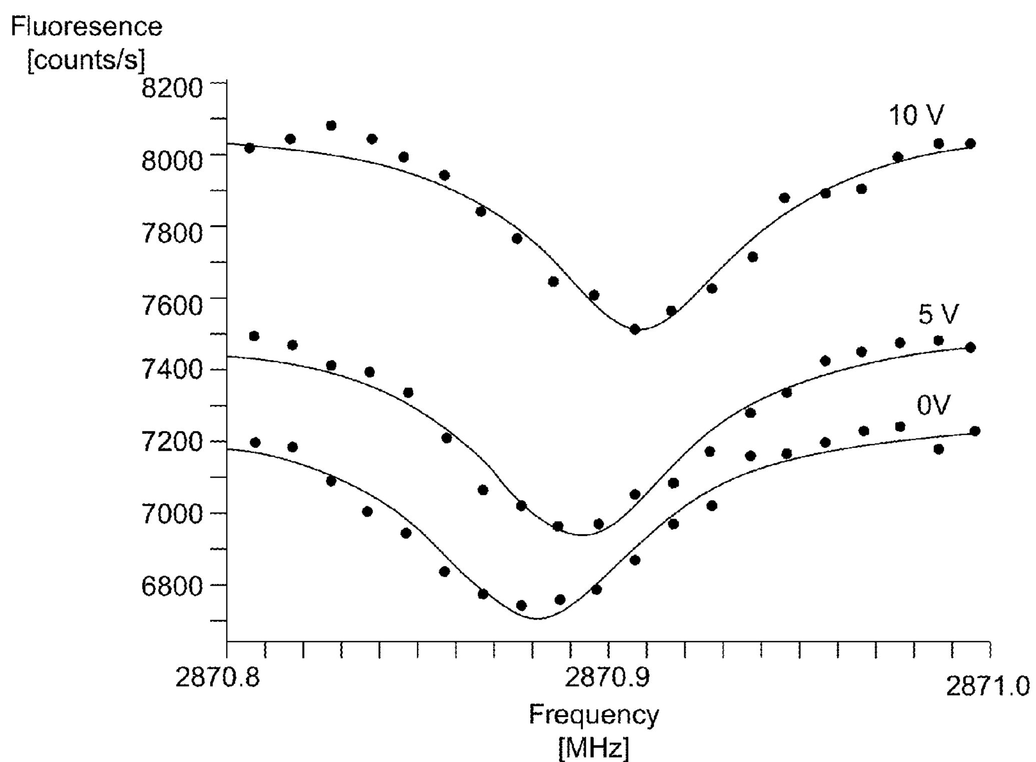

Fig. 38

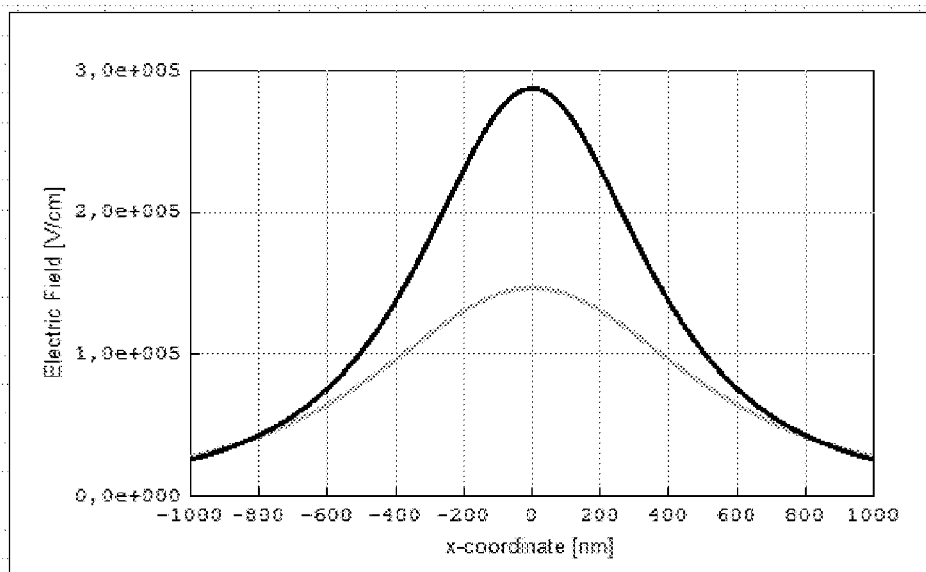

Fig. 39

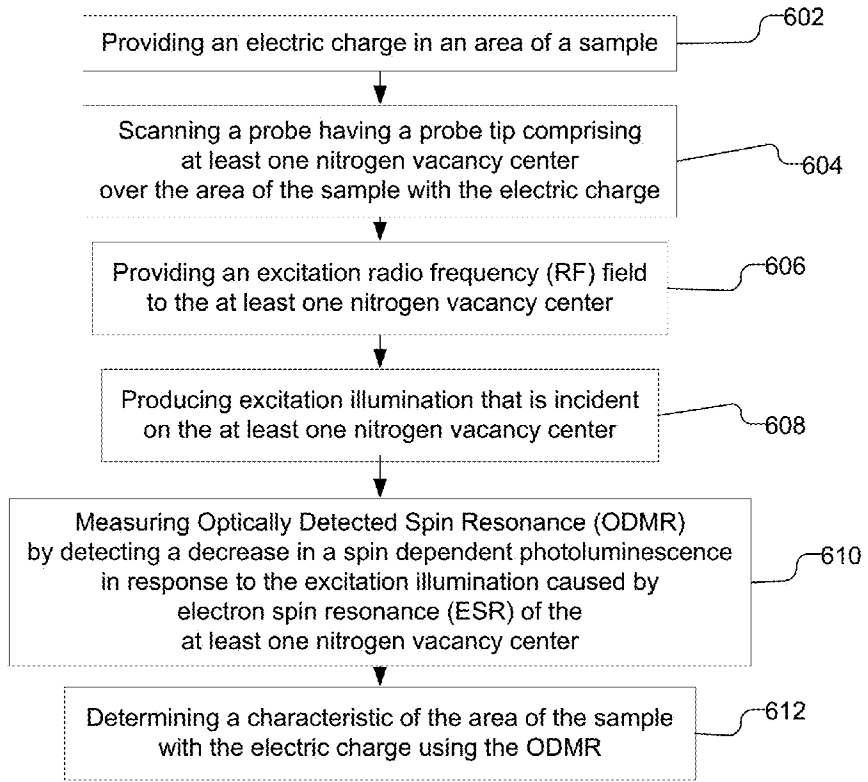

Fig. 40

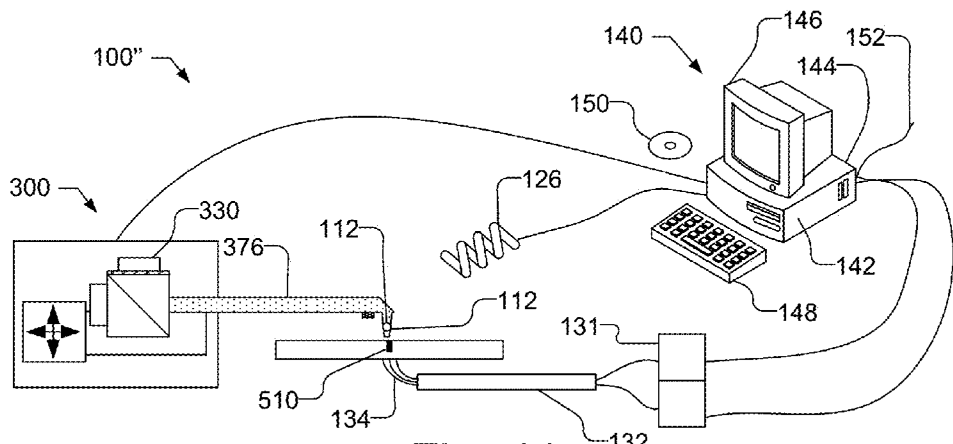

Fig. 41

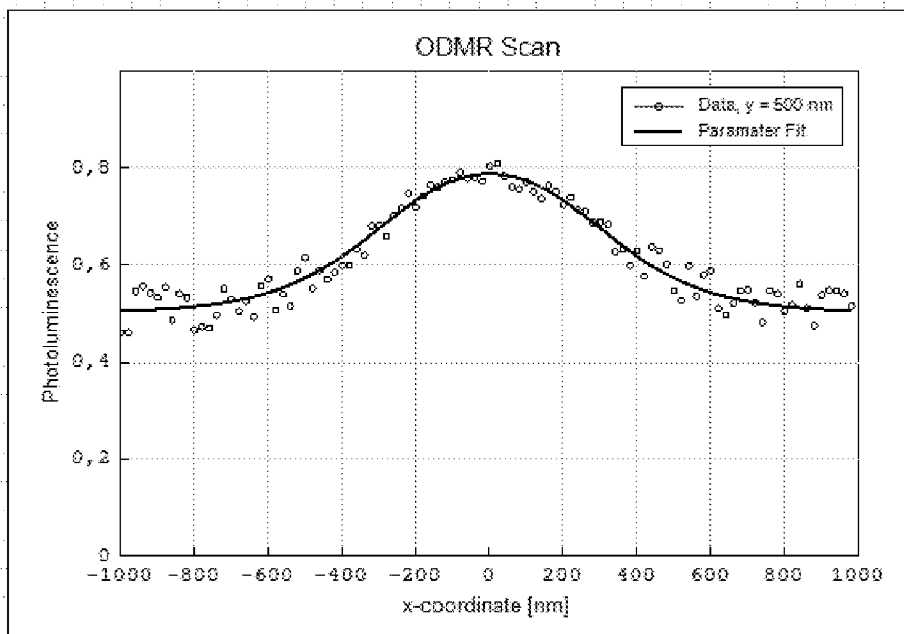

Fig. 42

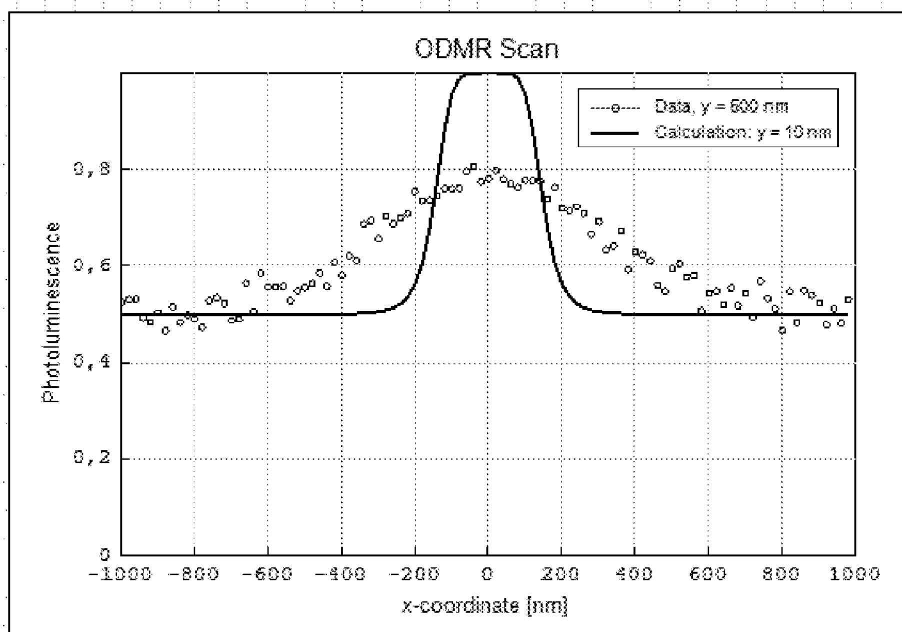

Fig. 43

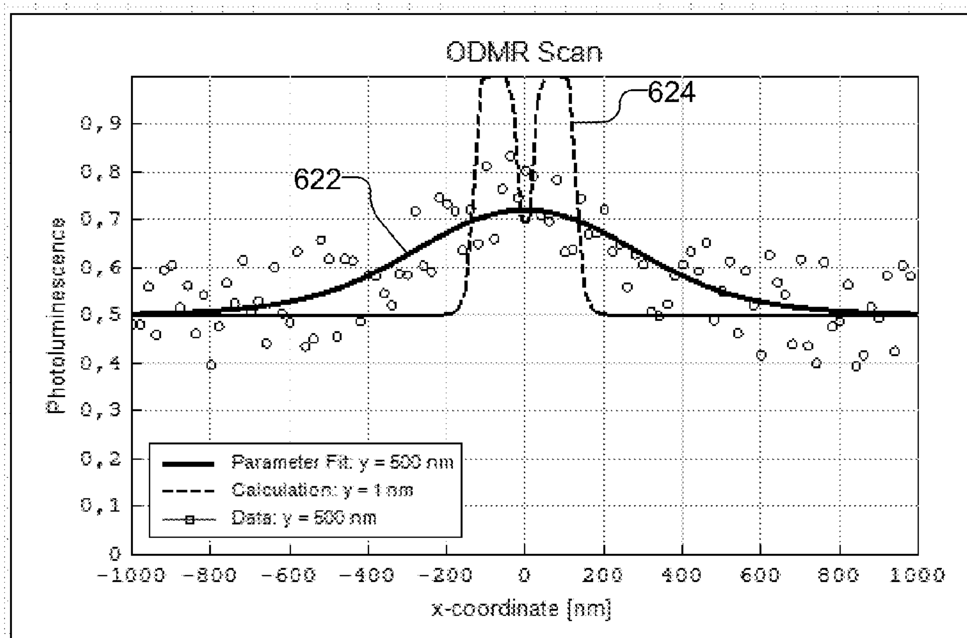

Fig. 44

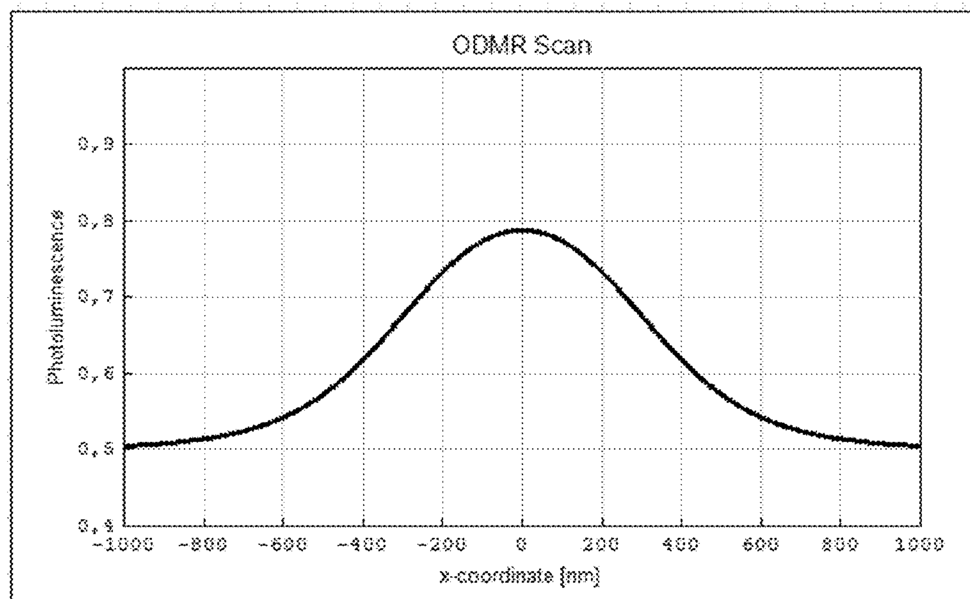

Fig. 45

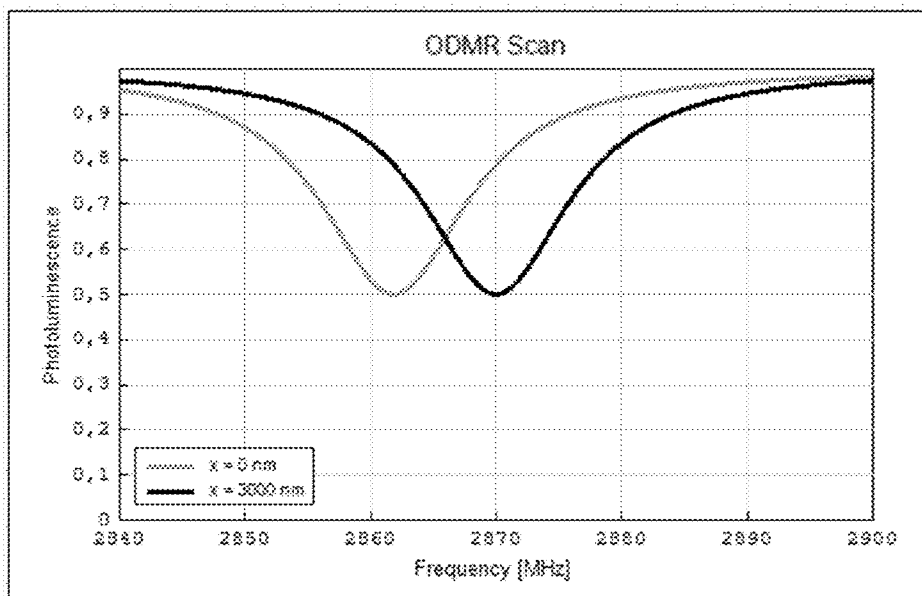

Fig. 46

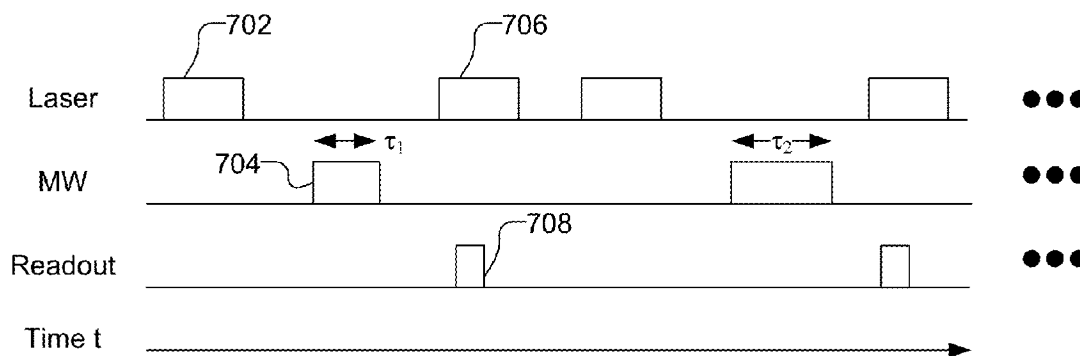

Fig. 47

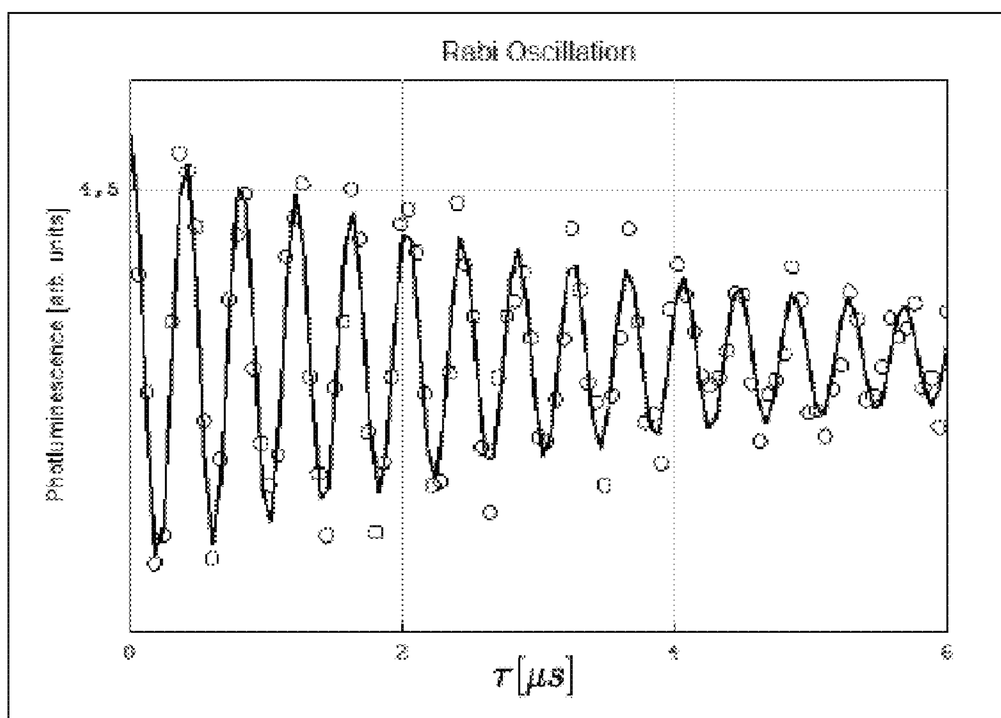

Fig. 48

INTEGRATED OPTICAL NANOSCALE PROBE MEASUREMENT OF ELECTRIC FIELDS FROM ELECTRIC CHARGES IN ELECTRONIC DEVICES

CROSS REFERENCE TO RELATED APPLICATIONS

[0001] This application is a continuation-in-part of U.S. application Ser. No. 14/952,852, filed Nov. 25, 2015, which is a continuation-in-part of U.S. application Ser. No. 14/542,410, filed Nov. 14, 2014, and a continuation-in-part of U.S. application Ser. No. 14/532,992, filed Nov. 4, 2014, which is a continuation-in-part of U.S. application Ser. No. 14/184,610, filed Feb. 19, 2014, now U.S. Pat. No. 8,885,301, and claims priority under 35 USC 119 to U.S. Provisional Application No. 61/950,596, filed Mar. 10, 2014, all of which are incorporated by reference herein in their entireties.

BACKGROUND

[0002] As critical dimensions in magnetic data storage systems, e.g. hard disk drives, are continuing to shrink to a few tens of nanometers, the development of characterization techniques that may be used in manufacturing or research and development has become increasingly demanding. For example, optical and magneto-optical metrology methods do not provide the spatial resolution required to determine properties of the write-field emanating from the write pole on the nanometer length scale. Magnetic Force Microscopy, on the other hand, has high spatial resolution but does not provide quantitative information about the magnetic field strength. In addition, current magnetic recording heads include other features that are on the nanometer length scale that are desirable to characterize, but that cannot be adequately measured using conventional metrology systems. By way of example, some magnetic recording heads include features such as optical near-field transducers for heat assisted magnetic recording (HAMR), for which characterization of the optical power in the near-field of these near-field transducers is desired. Accordingly, improved metrology methods for characterizing, e.g., magnetic recording heads is desired.

SUMMARY

[0003] A diamond probe is suitable to be attached to an Atomic Force Microscope and is created with a tip that incorporates a one or more Nitrogen Vacancy (NV) centers located near the end of the tip. The probe arm acts as an optical waveguide to propagate the emission from the NV center with high efficiency and a beveled end directs excitation light to the NV center and directs photoluminescence light emanating from the NV center into the probe arm. The probe tip is scanned over an area of a sample with an electric charge, such as a field effect transistor or flash memory. Optically Detected Spin Resonance (ODMR) is measured as the probe tip is scanned over the area of the sample, from which a characteristic of the area of the sample with the electric charge may be determined.

[0004] In one implementation, a method includes providing an electric charge in an area of a sample; scanning a probe having a probe tip comprising at least one nitrogen vacancy center over the area of the sample with the electric charge; providing an excitation radio frequency (RF) field to the at least one nitrogen vacancy center; producing excitation illumination that is incident on the at least one nitrogen vacancy center; measuring Optically Detected Spin Resonance (ODMR) as the probe tip is scanned over the area of the sample with the electric charge by detecting a decrease in a spin dependent photoluminescence in response to the excitation illumination caused by electron spin resonance (ESR) of the at least one nitrogen vacancy center; and determining a characteristic of the area of the sample with the electric charge using the ODMR.

[0005] In one implementation, an apparatus includes a biasing source configured to provide a bias signal; a probe card coupled to the biasing source and configured to be connected to a sample to provide an electric charge in an area of the sample; a probe having a probe tip comprising at least one nitrogen vacancy center, the probe configured to scan the probe tip across the area of the sample with the electric charge; a light source that produces excitation illumination that is incident on the at least one nitrogen vacancy center; a radio frequency antenna that provides an excitation field to the at least one nitrogen vacancy center; a detector configured to detect photoluminescence produced by the at least one nitrogen vacancy center in the probe tip; and at least one processor coupled to the detector and configured to measure Optically Detected Spin Resonance (ODMR) as the probe tip is scanned over the area of the sample with the electric charge by detecting a decrease in a spin dependent photoluminescence in response to the excitation illumination caused by electron spin resonance (ESR) of the at least one nitrogen vacancy center; and determine a characteristic of the area of the sample with the electric charge using the ODMR.

BRIEF DESCRIPTION OF THE DRAWINGS

[0006] FIG. **1** illustrates an optical metrology device capable of characterizing magnetic recording heads using photoluminescence produced by a substitutional impurity in a crystal.

[0007] FIG. **2** schematically illustrates the energy levels of a negatively charged nitrogen vacancy center in a diamond crystal.

[0008] FIG. **3** schematically illustrates a diamond film with a plurality of nitrogen vacancy centers that is positioned to be in a magnetic field produced by a write pole from a recording head.

[0009] FIG. **4** illustrates an optical metrology device that uses Stimulated Emission Depletion.

[0010] FIG. **5** illustrates the point spread function of excitation illumination and depletion illumination.

[0011] FIG. **6** illustrates the effective point spread function of the combined excitation illumination and depletion illumination from FIG. **5**.

[0012] FIG. **7** illustrates several waveforms used to measure Optically Detected Spin Resonance using depletion illumination.

[0013] FIG. **8** schematically illustrates the use of depletion illumination to measure Optically Detected Spin Resonance from a diamond film with a plurality of nitrogen vacancy centers that is positioned to be in a magnetic field produced by a write pole from a recording head.

[0014] FIG. **9** schematically illustrates the use of depletion illumination to measure Optically Detected Spin Resonance from a diamond film with a plurality of nitrogen vacancy centers that is in contact with the air bearing surface of the recording head.

[0015] FIG. **10** schematically illustrates a diamond film with a nitrogen vacancy center that is on an Atomic Force

Microscope arm positioned to be in a magnetic field produced by a write pole from a recording head.

[0016] FIGS. **11**A and **11**B illustrate the temperature dependence of the ESR frequency and resulting resonance lines at different temperatures, e.g., 300° K and 700° K.

[0017] FIG. **12** schematically illustrates a diamond film with a plurality of nitrogen vacancy centers that is positioned to measure a near-field transducers of a Heat Assisted Magnetic Recording write head.

[0018] FIG. **13** illustrates the temperature profile produced by a near field transducer used in a Heat Assisted Magnetic Recording write head.

[0019] FIG. **14** is an ESR spectrum that may be generated while measuring a near field transducer and that may be evaluated to extract temperature information.

[0020] FIG. **15** illustrates a temperature profile extracted from an ESR spectrum.

[0021] FIG. **16** illustrates an optical metrology device capable of characterizing a photon emitter on a nanometer length scale using photoluminescence (PL) produced by a substitutional impurity in a crystal film.

[0022] FIGS. **17**A and **17**B, by way of example, illustrate a side view and a back view, respectively, of recording head in contact with a crystal film.

[0023] FIG. **18** is a flow chart illustrating a method of determining one or more characteristics of a photon emitter using NV centers and an optical metrology device.

[0024] FIG. **19**, by way of illustration, shows a portion of a crystal film with a plurality of luminescing NV centers, illustrated as white spots.

[0025] FIG. **20** illustrates the quenching of the photoluminescence intensity produced by the NV centers caused by a near-infrared CW laser beam.

[0026] FIG. **21** illustrates a near field illumination profile for a near field photon emitter.

[0027] FIG. **22** illustrates an example of a photoluminescence quenching profile for the NV centers of a crystal film.

[0028] FIG. **23** shows in two dimensions the detected quenching of the intensity of the photoluminescence produced by the NV centers caused by near field illumination of a photon emitter.

[0029] FIG. **24** shows detected photoluminescence quenching data along with a fit curve illustrating a spatially resolved quenching profile.

[0030] FIG. **25** schematically illustrates one implementation in which a crystal film with one or more NV centers is held on the tip of an Atomic Force Microscope (AFM) arm to measure a photon emitter.

[0031] FIG. **26** illustrates an optical metrology device with additional light sources to produce STED illumination to improve resolution and to scan the photon emitter.

[0032] FIG. **27** illustrates the Gaussian point spread function of the excitation illumination from the optical metrology device in FIG. **26**.

[0033] FIG. **28** illustrates the effective point intensity distribution of the excitation illumination combined with the STED illumination.

[0034] FIG. **29** illustrates a probe arm assembly in which the NV center is positioned at the tip of a probe arm and the detector is attached to the probe arm, e.g., via a beam splitter.

[0035] FIG. **30** illustrates another embodiment of a probe arm assembly with an enlarged end of the probe arm.

[0036] FIG. **31** illustrates a closer view of the tip of the probe arm of the probe arm assembly showing the probe arm acting as a optical waveguide by means of total internal reflection.

[0037] FIGS. **32** and **33**, by way of example, illustrate a side view and a top view of the probe arm with a beam splitter mounted on a holder plate.

[0038] FIG. **34** illustrates a top view of another embodiment of a probe arm assembly with a probe arm connected directly to the detector.

[0039] FIG. **35** illustrates a closer view of the tip of the probe arm of the probe arm assembly with an RF antenna.

[0040] FIG. **36** illustrates a closer view of the tip of the probe arm of the probe arm assembly with an absorption layer.

[0041] FIG. **37** illustrates a probe arm scanning over a backside of a sample that includes an integrated electronic circuit, illustrated as a Field Effect Transistor (FET).

[0042] FIG. **38** illustrates the ESR-frequency shifted in the presence of an applied electric field (Stark-Effect).

[0043] FIG. **39** illustrates the calculated electric field of a line charge at 500 nm and 700 nm.

[0044] FIG. **40** is a flow chart illustrating a method of using at least NV center in a probe arm to characterize an area of a sample with an electric charge.

[0045] FIG. **41** illustrates an optical metrology device with a probe arm assembly with an NV center at the tip of a probe arm configured to characterize an area of a sample with an electric charge.

[0046] FIG. **42** illustrates the calculated ODMR in a plane 500 nm above a line charge.

[0047] FIG. **43** illustrates the calculated ODMR in a plane 10 nm above a line charge.

[0048] FIG. **44** illustrates the calculated ODMR for two line charges in planes 500 nm and 1 nm above the two line charges.

[0049] FIG. **45** illustrates a calculated ODRM for a fixed RF excitation as a function of the x-coordinate in a plane 500 nm above the electric charge.

[0050] FIG. **46** illustrates a frequency shift determined using ODMR in a plane 500 nm above the electric charge.

[0051] FIG. **47** illustrates a sequence of laser pulses and pulses of AC current to record the Rabi oscillation using ODMR.

[0052] FIG. **48** illustrates a graph of measured photoluminescence with respect to different durations of the pluses of AC current.

DETAILED DESCRIPTION

[0053] FIG. **1** illustrates an optical metrology device **100** capable of characterizing magnetic recording heads using photoluminescence produced by a substitutional impurity **112** in a crystal **110**. For example, one or more nitrogen vacancy centers (NV centers) in a diamond crystal may be used. An NV center is a naturally occurring or technically created impurity in a diamond crystal where a Nitrogen atom replaces a Carbon atom creating a vacancy next to the Nitrogen atom. The diamond crystal, by way of example, may have a (**111**) crystal orientation, but other crystalline orientations are possible. If desired, other substitutional impurities in crystals may be used, such as the Silicon-vacancy center in diamond (SiV-), but for the sake of simplicity, the present disclosure will refer to nitrogen NV centers in diamond. The crystal may be, e.g., a crystal film that contains a plurality of

NV centers or a crystal particle that contains a single (or a few) NV centers. If desired, a film may be produced that contains a plurality of crystal particles in a suspension forming a film on, e.g. a glass substrate, each crystal particle having one or more NV centers.

[0054] The NV centers, which are basically artificial atoms with distinct quantum energy levels, show unique extrinsic and intrinsic optical spin dynamics including stable photoluminescence (PL) based on radiating transitions between optically excited energy levels of their charged quantum states. The PL is temperature as well as magnetic field dependent. Further, Electron Spin Resonance (ESR) is excited in the NV center electronic spin system by an external radio frequency (RF)-field with frequencies resonant with the transitions between the energy sub-levels. At resonance, the PL intensity is measurably reduced. Moreover, the ESR is linearly dependent on an applied magnetic field and, thus, one or more NV centers may be used as a magnetic field sensor with nanometer resolution using optically detected ESR (sometimes referred to herein as ODMR (Optically Detected Magnetic Resonance) (ESR is paramagnetic resonance that falls into this category)). The ESR is also temperature dependent, so that for a fixed applied magnetic field, the shift in ESR is a measure of temperature. For both magnetic field and temperature measurements, the spatial resolution is determined fundamentally by the size of a single NV center which is on the Angstrom length scale. Accordingly, the optical metrology device **100** may optically detect the PL of one or more NV centers **112** in a crystal **110**, e.g. using photon counting by employing a photo detector or by using a camera with high sensitivity, to measure a variety of characteristics of a recording head that has features with a nanometer length scale.

[0055] The optical metrology device **100** may be, e.g., a microscope such as a confocal microscope or a wide-field microscope. For example, a confocal microscope may include a light source **102** that produces excitation illumination **103** that is incident on the crystal **110** with the substitutional impurities **112**. The use of a confocal detection system enables selection of PL coming from only a small volume of the crystal **110**, e.g., 1 μm^3, that is associated with the spot on the surface of the crystal **110** produced by the excitation illumination change. The light source **102** may be, e.g., a laser, light emitting diode (LED), etc., that excites the NV center with a continuous (CW) or pulsed excitation illumination, with one or more wavelengths in a range of 460 nm to 580 nm, and which may be, e.g., 532 nm. With pulsed excitation illumination, the pulse width may be, e.g., approximately 800 ps with a 4-MHz repetition rate. The light source **102** may have a power density of, e.g., 40 kW/cm^2, to polarize the NV center by pumping it between the ground and the excited levels. The light from the light source **102** may be provided to a collimator consisting of lenses **104** and **106** either directly or by way of an intervening optical element, e.g., fiber optics or a light pipe. The collimator **104**, **106** expands and collimates the light, which is focused by lens **122**, which is also used to collect the PL emanating from the NV centers. In an embodiment in which the device is a confocal microscope, the lens **106** (and/or other appropriate lens (es)) may be moved back and forth, as illustrated by arrow **108** and/or a 2-dimensional steering-mirror system could be used to move the excitation illumination **103** relative to the back-aperture plane of the objective lens **122** scanning the focused beam **103** in the sample plane. Additionally, appropriate apertures may be used in an embodiment in which the microscope is a confocal microscope. Moreover, if desired, additional light sources may be used along with light source **102**.

[0056] A beam splitter **120** receives the excitation illumination from the light source **102** and provides at least a portion of the excitation illumination to the objective lens **122**. The excitation illumination is focused on the surface of the crystal **110** by the objective lens **122**, which may have a high numerical aperture (NA=0.95) or an oil-immersion lens with an NA of, e.g. 1.3. The objective lens **122** may focus the excitation illumination on the crystal **110** at a normal angle of incidence. It should be understood, however, that an oblique angle of incidence of the excitation illumination may be used if desired. The objective lens **122** focuses the light onto the crystal **110** with one or more NV centers **112**. The crystal **110** and NV centers **112** are positioned to be in a magnetic field produced by the recording head **114**. The recording head **114** may be a magnetic recording head, such as that used in hard disk drives, and may be in any desired form factor including bar, slider, HGA (head gimbal assembly), and HSA (head stack assembly). Moreover, the recording head **114** may be a Heat Assisted Magnetic Recording (HAMR) write head or other type of magnetic recording head. The crystal **110** may be placed near or in contact with the recording head **114**, or if desired, deposited on the recording head **114**. Moreover, if desired, an intervening layer may be located between the crystal **110** and the recording head **114**, such as a layer of a magnetic recording medium or a layer of material with low thermal conductivity that may be heated by a thermal device on a HAMR write head, or a reflecting layer. The NV centers **112** in the crystal **110** may have a relatively low density such that the distance between adjacent NV centers **112** is greater than a width of the write pole **116** to be measured in the recording head **114**. Alternatively, a single NV center **112** may be used in the crystal **110**. In such an embodiment, relative movement between the recording head **114** and the crystal **110** may be produced, e.g., as illustrated by actuator **118**. Alternatively, the NV centers **112** in the crystal **110** may have a relatively high density such that the distance between adjacent NV centers **112** is similar to or less than the width of the write pole **116** to be measured in the recording head **114**. With a relatively high NV center density, relative movement between the crystal **110** and the recording head **114** may not be necessary. Moreover, in some embodiments, movement between the crystal **110** and the recording head **114** may not be possible, for example, if the crystal **110** is applied directly to the recording head **114**, e.g., during the manufacturing process. The optical metrology device **100**, however, may include additional optic elements to move the excitation illumination over the crystal **110**, e.g., in one or two dimensions. In another embodiment, no relative motion is employed, e.g., between the excitation illumination and the crystal or between the crystal and the write pole, but rather the integral ODMR signal is collected for varying excitation fields over an area that includes the write pole, and the magnetic field is derived from the ODMR spectrum using a high density NV film. In another embodiment, the magnetic field produced by the recording head **114** may be varied while maintaining the excitation field constant and the ODMR signal is detected to determine the magnitude of the bias signal necessary to produce a desired magnetic field from the recording head **114**. In another embodiment, the thermal device on the recording head **114** may be controlled to vary the heating of the layer of the magnetic recording medium or the layer of material with low thermal conductivity while maintaining the excitation

field constant and the ODMR signal is detected to determine the magnitude of the bias signal necessary to produce the desired heating.

[0057] During measurement, PL **113** produced by the NV centers **112**, illustrated by the dotted line, will be collected by the objective lens **122** and directed by the beam splitter **120** towards a detector **130**. As illustrated, a spectral filter **124**, such as a dichroic film, is positioned before the detector **130** to remove any reflected excitation illumination and to direct only the PL to the detector **130**. The spectral filter **124**, thus, may be a long-pass filter with a wavelength cut-off at, e.g., 580 nm, to filter out any remaining pump light. The detector **130** may be, e.g., a non-imaging photodetector, such as a silicon avalanche photodiode operating in the signal photon regime, which detects the optical intensity at a single spot. Alternatively a CCD camera can be used to detect the PL.

[0058] In addition, a radio wave frequency (RF) antenna **126** is positioned to provide an excitation field to the crystal **110**. The RF antenna **126** may produce a varying excitation field, e.g., that may be controlled to sweep the frequency in a continuous or stepped manner. A continuous or pulsed excitation field produced by the RF antenna **126** may have a power of, e.g., 1 W and a frequency ranging from 1 GHz to 5 GHz. The RF antenna **126** may also produce a constant excitation field. The excitation field produced by RF antenna **126** drives electron spin resonance which may be optically detected, e.g., ODMR, by detecting a drop in the spin dependent PL in response to the excitation illumination caused by electron spin resonance (ESR) of the nitrogen vacancy centers. The ODMR may be detected while varying the excitation frequencies of the excitation field while holding the magnetic field produced by the recording head **114** constant, while holding the excitation frequency of the excitation field constant while varying the magnetic field produced by the recording head **114**, or while varying both the excitation frequencies of the excitation field and the magnetic field produced by the recording head **114**.

[0059] The detector **130** is connected to a computer **140** and the computer **140** receives, stores, and analyzes the optically detected data provided by the detector **130**, along with the excitation frequencies provided by RF antenna **126** associated with the data. The computer **140** includes a processor **142** with memory **144**, as well as a user interface including e.g., a display **146** and input devices **148**. A non-transitory computer-usable storage medium **150** having computer-readable program code embodied may be used by the computer **140** for causing the processor **142** to control the optical metrology device **100** and to perform the functions including the analysis described herein. The data structures and software code for automatically implementing one or more acts described in this detailed description can be implemented by one of ordinary skill in the art in light of the present disclosure and stored, e.g., on a computer readable storage medium **150**, which may be any device or medium that can store code and/or data for use by a computer system such as processor **142**. The computer-usable storage medium **150** may be, but is not limited to, magnetic and optical storage devices such as disk drives, magnetic tape, compact discs, and DVDs (digital versatile discs or digital video discs). A communication port **152** may also be used to receive instructions that are used to program the computer **140** to perform any one or more of the functions described herein and may represent any type of communication connection, such as to the internet or any other computer network. Additionally, the functions described herein may be stored in memory **155** or embodied in whole or in part within the circuitry of an application specific integrated circuit (ASIC) or a programmable logic device (PLD), and the functions may be embodied in a computer understandable descriptor language which may be used to create an ASIC or PLD that operates as herein described.

[0060] As illustrated, the computer **140** may be coupled to the recording head **114**, via a probe card **132** which is connected to the recording head **114** using one or more probes **134**, which may be, e.g., pogopins, probes, or other contacts such as wires that are wire bonded. The probe card **132** may be coupled to a biasing source **131** that provides a bias signal, such as a current or voltage signal, which is provided to the recording head **114** via the probe card **132** and causes the recording head **114** to produce a magnetic field. The biasing source **131** may be connected to and controlled by the computer **140**. The computer **140**, thus, may control the magnetic field produced by the recording head **114**, e.g., by controlling the bias signal provided to the recording head. The biasing source **131** may provide a plurality of bias signals with different levels to the recording head **114**. Accordingly, the recording head **114** may be controlled via the biasing source **131** to produce a constant magnetic field, e.g., while the excitation field is varied, or to produce a varying magnetic field, while the excitation field is held constant (or varied). The varying magnetic field produced by the recording head **114** may vary continuously or in a stepped manner. The computer **140** may cause the biasing source **131** (or another biasing source) to further control any other desired features of the recording head **114**, such a thermal device, e.g., a high intensity light source, on the recording head **114**, when the recording head **114** is, e.g., a HAMR write head. Accordingly, the recording head **114** may be controlled via the biasing source **131** to produce a constant heat level, e.g., while the excitation field is varied, or to produce varying heat levels, while the excitation field is held constant (or varied). Additionally, when the recording head **114** includes a Dynamic-Flying Height (DFH) device, one of the probes **134** of the probe card **132** may be used to provide current to the microactuator device from a second circuit in the current or voltage source that is connected to the computer **140**. Write heads use a DFH device as an adjustment mechanism to internally bias the write pole closer to or further from the air bearing surface. The DFH device is typically in the form of a heater incorporated into the write head structure, with additional contact pads for external connection. By applying a bias to the additional contact pads via the probe card **132**, the position of the write pole can be adjusted towards or away from the air bearing surface of the write head. By adjusting the position of the write pole via the DFH device, the recording head **114** may be measured at different temperatures and/or vertical displacement from the crystal **110**.

[0061] Additionally, when the recording head **114** includes a microactuator device, one of the probes **134** of the probe card **132** may be used to provide current to the microactuator device. The source of the current may be a second circuit in the current or voltage source connected to the computer **140**. Write heads use a microactuator device as an adjustment mechanism to move the write pole in the cross-track direction to better align the write pole to the lands of a disk that is being written to. The microactuator device is incorporated into the write head structure, which includes additional contact pads for external connection. By applying a bias to the additional contact pads via the probe card **132**, the position of the write

pole can be adjusted in the cross-track direction. By adjusting the position of the write pole via the microactuator device during measurement with the device, the performance of the microactuator may be verified and the characteristics of the recording head **114** may be measured at different write pole positions.

[0062] The computer **140** is further coupled to control the RF antenna **126** to provide a desired excitation field (or varying excitation field) to the crystal **110** during measurement.

[0063] As discussed above, an NV center in diamond is a naturally occurring or technically created impurity in a diamond crystal where a Nitrogen atom replaces a Carbon atom creating a vacancy next to the Nitrogen atom. Nitrogen vacancy centers may be created in a diamond crystal, e.g., using a type-Ib HPHT single-crystal sample that is initially embedded with nitrogen impurities. For example, nitrogen impurities may be embedded by irradiation with a an ion-beam, e.g. N_2^+ ions at 5 keV, in case of a very high purity diamond film or by an electron beam in case the diamond film already has nitrogen impurities and annealing, e.g., for 2 hours at 850° C. The density of the NV centers within the crystal film may be controlled, e.g., by controlling the applied irradiation dose, or using appropriate masking techniques. For example, an ion beam fluence of 10^{11} cm^2 can result in density of 8×10^{10} NV cm^{-2}. Moreover, by controlling the energy of the implantation as well as the annealing process the depth of the NV centers implanted in the crystal may be controlled.

[0064] FIG. **2** schematically illustrates the energy levels of a negatively charged NV center in a diamond crystal. An NV center may be optically excited, e.g., with excitation illumination having a wavelength range from 460 nm to 580 nm, which yields an intense fluorescence emission from the NV center with lifetimes in the millisecond range. For example, as illustrated, the NV center may be excited with a laser at a wavelength of 532 nm and in response will emit a broadband luminescence with a zero phonon line at 637 nm, at room temperature. FIG. **2** further illustrates the mechanism of stimulated emission, in which an electron in an excited state gives energy to an incoming photon and is forced to the ground state before it can create photoluminescence by spontaneous emission. The ground state of the NV center has an electron spin triplet structure with a zero-field frequency splitting of 2.87 GHz between the m_S=0 and the degenerate m_S=±1 states. In the absence of an external magnetic field, e.g., from the recording head **114**, a drop of luminescence intensity is present at an excitation frequency of 2.88 GHz due to the induced change in populations of m_S=0 and m_S=±1 spin sublevels. Thus, the location of the NV center may be identified by an optically detected zero field magnetic resonance at ~2.88 GHz which has its origin in the crystal-field splitting of energy sub-levels. The magnetic resonance occurs between the m_s=0 and m_s=±1 spin sub-levels of the spin triplet ground state $^3A_2$ and can be detected by either conventional electron paramagnetic resonance (EPR) or optically detected magnetic resonance (ODMR). The optical detection of the magnetic resonances of the NV center is enabled by the differing fluorescence of the m_s=0 and ±1 spin projections, i.e. the fluorescence intensity is reduced when the spin system is in resonance due to the RF excitation.

[0065] In the presence of a magnetic field from the recording head **114**, the resonance peak will split due to the Zeeman effect. As illustrated in FIG. **2**, two resonance peaks may be identified, respectively corresponding to transitions between m_S=0 and m_S=−1, and between m_S=0 and m_S=+1 sublevels. The frequency of these resonance peaks is a function of the magnitude of the magnetic field and is called the Larmor frequency f given by

$$f = \frac{1}{2\pi}\gamma B \qquad \text{eq. 1}$$

[0066] where γ is the Gyromagnetic ratio and B the magnetic field, i.e. by measuring f, the magnetic field B may be determined. Thus, for magnetic field sensing applications, the magnetic field may be evaluated by measuring the Zeeman shifts of the NV center defect electron spin sub-levels through the optical detection of electron spin resonance (ESR), i.e., ODMR. The ODMR may be measured by detecting a decrease in the spin dependent PL caused by ESR of the NV centers while varying the excitation frequencies of the excitation field while holding the magnetic field produced by the recording head **114** constant, while holding the excitation frequency of the excitation field constant while varying the magnetic field produced by the recording head **114**, or while varying both the excitation frequencies of the excitation field and the magnetic field produced by the recording head **114**. One of the advantages of the use of NV center-based magnetometry is the possible combination of atomic-scale spatial resolution with high magnetic field sensitivity, e.g., below 10 nT $Hz^{-1/2}$, even under ambient conditions.

[0067] As illustrated in FIG. **2**, the m_S=0 spin state is dependent on temperature D(T), and consequently the ESR frequency is temperature dependent. Moreover, the PL intensity (I_{PL}) of an NV center and the relative I_{PL} difference between its spin states (ESR contrast), which strongly decrease above 550° K, may be used to measure temperature. Accordingly, one or more NV centers may serve as a nano-scale thermometer with sensitivities on the order of 100 mK/Hz between room temperature and 700° K. The high sensitivity and wide range of operating temperatures make NV centers an attractive candidate for a variety of thermo-sensing applications such as diamond-based scanning thermal microscopy. The impact of temperature versus magnetic field on the ESR spectrum may be distinguished using a pulsed RF excitation field with an appropriate pulse sequence (spin echo technique), as opposed to a continuous-wave RF excitation field. The thermal device of the recording head **114** may be controlled via the biasing source **131** to produce a constant temperature while the excitation frequency of the excitation field is varied or to produce different temperatures while holding the excitation frequency of the excitation field constant, or while varying both the temperature produced by the thermal device of the recording head **114** and the excitation frequencies of the excitation field.

[0068] In addition, the PL of an NV center may be turned "off" in time, when the 532 nm excitation pulse, e.g., with a duration of 60 ps, is followed by a longer wavelength pulse e.g. 775 nm and duration 3.2 ns, of sufficient intensity. This mechanism is known as Stimulated Emission Depletion (STED). Alternatively, STED with CW or quasi CW illumination may be employed. Spatial resolution may be improved using STED to functionally switch off a portion of NV centers, e.g., STED microscopy.

[0069] Additionally, if desired, Ground State Depletion (GSD) may be used, as opposed to STED. Similar to STED, GSD uses depletion illumination to functionally switch off a

portion of NV centers, but unlike STED, GSD uses the same wavelength for the excitation illumination and the depletion illumination.

[0070] Thus, one or more NV centers in a diamond film may be used to measure the write field of a recording head with nano-meter spatial resolution making use of the optically detected Electron Spin Resonance (ODMR), which frequency spectrum depends linearly on the magnetic field. Accordingly, characteristics of the recording head, including efficiency of the recording head, the strength of the magnetic field and physical dimensions of the write pole may be measured. This may be carried out by exercising the write portion of the recording head with a write current, which can be a DC or an AC current, to produce the magnetic field at the write pole. For example, the efficiency of the recording head may be determined by varying the bias signal to the recording head to vary the magnetic field while maintaining the excitation field at a constant frequency to determine the relationship between the applied bias signal and resulting magnetic field as provided by equation 1. In another example, the strength of the magnetic field may be determined for any scanned position based on the frequency of these resonance peaks, as provided by equation 1. Additionally, one or more NV centers in a diamond film may be used to measure the near-field power of a near-field transducer in a recording head used in thermally assisted magnetic recording with nano-meter spatial resolution making use of temperature dependence of the optically detected Electron Spin Resonance or the temperature dependency of the PL intensity. Moreover, the efficiency of the thermal device in the recording head may be determined by varying the bias signal to the thermal device to vary the temperature while maintaining the excitation field at a constant frequency to determine the relationship between the applied bias signal and resulting heat.

[0071] Thus, a characteristic of the recording head **114** may be determined based on the ESR as measured by the detector **130**, the frequency of excitation field produced by RF antenna **126**, and the bias applied to the recording head **114** by the biasing source **131** to control the magnetic field and/or the heat produced by the thermal device. For example, a graph may be generated for the excitation field with respect to the bias signal. The excitation field may be fixed and the bias signal may be swept to vary the magnetic field or heat produced by the recording head, or the bias signal may be fixed and the excitation field swept. This process may be repeated at multiple levels of the fixed excitation field or the fixed bias signal and the magnetic field determined from the ESR, e.g., based on equation 1. Additionally, an external thermal device may be used to calibrate the ESR with respect to heat for one or more excitation frequencies of the RF antenna **126**, and the heat produced by, e.g., a HAMR recording head **114**, at one or more bias levels may be determined by measuring the ESR.

[0072] FIG. **3**, by way of example, schematically illustrates a diamond film **110** with a plurality of NV centers **112** and that is positioned to be in a magnetic field B produced by a write pole **116** from a recording head **114**. As discussed above, a light source **102** (shown in FIG. **1**) produces excitation illumination **103** that is focused by objective lens **122** onto the diamond film **110** while an external RF excitation field is produced by the RF antenna **126** with varying excitation frequencies or pulse sequence. In response to the excitation illumination **103**, the NV center **112***a* produces spin dependent PL **113** that is collected by the objective lens **122** and provided to the detector **130** (shown in FIG. **1**). The Optically Detected Spin Resonance (ODMR) may be measured by detecting a decrease in the spin dependent PL **113** caused by electron spin resonance (ESR) of the NV centers at varying excitation frequencies of the excitation field. If desired, the magnetic field of the recording head **114** may be varied while maintaining a constant frequency of the excitation field (or varying the frequency of the excitation field) while measuring ODMR.

[0073] As illustrated in FIG. **3**, the write pole **116** has a width W, while the density of the NV centers **112** in the diamond film **110** is such that adjacent NV centers are separated by a distance d that is greater than the width W of the write pole **116**, i.e., d>W. In such a configuration, a single NV center may be positioned over the write pole **116**, as illustrated. Relative movement between the recording head and the diamond film **110** may be produced in two dimensions, e.g., by moving the recording head with respect to the diamond film **110**, thereby scanning a single NV center over the recording head in two dimensions, as illustrated by arrows **162**. The ODMR may be measured by detecting a decrease in the spin dependent PL **113** caused by electron spin resonance (ESR) of a single NV center at varying excitation frequencies of the excitation field and/or varying magnetic fields of the recording head as the NV center is scanned over the recording head in two dimensions. Accordingly, characteristics of the recording head **114** may be measured with nano-meter spatial resolution including the efficiency of the recording head, dimensions of write pole **116** and strength of the magnetic field B.

[0074] FIG. **4** illustrates an optical metrology device **100'** that is similar to the optical metrology device **100**, shown in FIG. **1**, like designated elements being the same, but that uses Stimulated Emission Depletion (or GSD) as discussed above. As illustrated, optical metrology device **100'** includes a second light source $\mathbf{102}_{DEPL}$ that produces depletion illumination $\mathbf{103}_{DEPL}$, with the same or different wavelength in the case of GSD or STED, respectively, and that is coincident on the diamond film **110** with the excitation illumination **103** from light source **102**. The light source **102** produces excitation illumination **103** that has a Gaussian point spread function and produces a relatively large diffraction limited spot on the diamond film **110**. FIG. **5**, by way of example, illustrates the Gaussian point spread function of the excitation illumination **103** with a solid line. The second light source $\mathbf{102}_{DEPL}$ produces light that passes through a vortex phase plate **164** to produce a ring shaped beam that has a central zero intensity at the focal plane. FIG. **5**, by way of example, illustrates a ring shaped point spread function distribution of the depletion illumination $\mathbf{103}_{DEPL}$ which is coincident with the excitation illumination **103**. The depletion illumination $\mathbf{103}_{DEPL}$ quenches PL in the NV centers **112** in the diamond film **110** that are off-center, so that the off-center NV centers only contribute a constant background, which may be subtracted from the ODMR signal, thereby providing a signal from only the NV centers in the center of the depletion illumination $\mathbf{103}_{DEPL}$. FIG. **6** illustrates the effective point spread function **166** of the combined excitation illumination **103** combined with the depletion illumination $\mathbf{103}_{DEPL}$. The coincident excitation illumination **103** and depletion illumination $\mathbf{103}_{DEPL}$ may be scanned over the diamond film **110** to measure characteristics of the recording head **114** in two dimensions, e.g., using one or more mirrors **117** in the beam path.

[0075] In the case of using GSD, the depletion illumination $\mathbf{103}_{DEPL}$ may have a wavelength of 532 nm, with increased

power. For example, a reduction in the photoluminescence may be achieved for depletion illumination $\mathbf{103}_{DEPL}$ with power greater than 2 MW/cm^2. The depletion illumination $\mathbf{103}_{DEPL}$ may be continuous (CW) or pulsed excitation, with a pulse width of, e.g. 150 ps, where a pulsed depletion illumination $\mathbf{103}_{DEPL}$ results in stronger photoluminescence reduction.

[0076] FIG. **7**, by way of example, illustrates several waveforms that may be used to measure ODMR using depletion illumination. As illustrated, a pulse of excitation illumination is provided along with the excitation field and followed by a pulse of depletion illumination. The RF excitation field need not be pulsed and may always be on, and one or both of the excitation field and the magnetic field produced by the recording head **114** may be varied. The intensity of the depletion illumination is much greater than the intensity of the excitation illumination in the case of case of GSD or has a longer wavelength in case of STED. The PL signal **168** is detected after the pulsed depletion illumination.

[0077] FIG. **8** schematically illustrates the measurement of ODMR from a diamond film **110** with NV centers **112** similar to FIG. **3**, but uses depletion illumination $\mathbf{103}_{DEPL}$, e.g., for either STED or GSD, and the diamond film **110** has an increased density of NV centers **112**. As illustrated in FIG. **8**, the density of the NV centers **112** in the diamond film **110** may be such that adjacent NV centers are separated by a distance d that is less than the width W of the write pole **116**, i.e., d<W. The density of NV centers may be chosen so that a plurality of NV centers, e.g. 10×10 NV centers, is located under the write pole **116**. The coincident excitation illumination **103** and depletion illumination $\mathbf{103}_{DEPL}$ enables a reduced number of NV centers to be resolved, e.g., only NV centers that fall within the ring minimum of the depletion illumination $\mathbf{103}_{DEPL}$ are resolved. The coincident excitation illumination **103** and depletion illumination $\mathbf{103}_{DEPL}$ may be scanned in two dimensions over the diamond film, as illustrated by arrows **174**, e.g., using an arrangement of mirrors in the beam path, thereby obviating the needs for an actuator to produce relative movement between the recording head and the diamond film **110**. The ODMR may be measured by detecting a decrease in the spin dependent PL **113** caused by electron spin resonance (ESR) of the NV center(s) that fall within the ring minimum of the depletion illumination $\mathbf{103}_{DEPL}$ at varying excitation frequencies of the excitation field and/or varying magnetic fields produced by the recording head **114** as excitation illumination **103** and depletion illumination $\mathbf{103}_{DEPL}$ are scanned over the recording head in two dimensions. Accordingly, characteristics of the recording head may be measured with nano-meter spatial resolution including dimensions of write pole **116** and strength of the magnetic field B.

[0078] If desired, the diamond film **110** may be in direct contact with the recording head **114**, e.g. in contact with the Air Bearing Surface (ABS) of the recording head. For example, a diamond film **110** with a relatively high density of NV centers **112**, e.g., such that there are a plurality of NVC centers located under the write pole, may be directly deposited on the ABS of the recording head. FIG. **9** schematically illustrates the measurement of ODMR from a diamond film **110** with NV centers **112**, similar to that shown in FIG. **8**, but with the diamond film **110** attached to the ABS of the recording head **114**, i.e., directly coupled to or coupled to with one or more intervening layers. As discussed above, the coincident excitation illumination **103** and depletion illumination $\mathbf{103}_{DEPL}$ may be scanned with respect to the recording head in two dimensions to measure ODMR at varying excitation frequencies of the excitation field and/or varying magnetic fields produced by the recording head **114** as excitation illumination **103** and depletion illumination $\mathbf{103}_{DEPL}$ are scanned over the recording head in two dimensions.

[0079] FIG. **10** is similar to FIG. **3** and schematically illustrates the measurement of ODMR from a diamond film **110** with an NV center **112** held on the tip of an Atomic Force Microscope (AFM) arm **176** and that is in contact with the ABS of the recording head **114**. As illustrated, the diamond film **110** may be a micron sized diamond particle that includes a single or several NV centers **112**. The AFM arm **176** is scanned over the recording head **114** in two dimensions, as illustrated by arrows **178** and the PL **113** from the NV centers is collected. The ODMR may be measured from the NV center(s) **112** in the diamond film **110** positioned at the tip of the AFM arm **176**, at varying excitation frequencies of the excitation field and/or varying magnetic fields produced by the recording head **114** as the AFM arm **176** is scanned over the recording head in two dimensions.

[0080] In addition to measuring characteristics such as physical dimensions of the write pole **116** and the strength of the magnetic field B, the NV centers **112** in a diamond film may be used to measure the heat produced by a bias controlled thermal device. In one embodiment, for example, the near-field power at the near-field transducer of a write head for Heat-Assisted Magnetic Recording (HAMR) may be tested, but it should be understood that characteristics of any device that produces heat using a bias controlled thermal device may be measured. Characteristics related to the thermal device that may be determined include, e.g., power, temperature with respect to bias signal, spatial extent of the thermal device, or near-field transducer, and heating characteristics such as the spatial extent of heating and the heating width produced by the device. These characteristics may be determined in the same manner as the write pole related characteristics discussed above, where heat as opposed to a magnetic field is used. As illustrated in FIG. **2**, the axial zero field splitting parameter D(T) of an NV center is temperature dependent. With increasing temperature the energy gap between the $m_s=0$ and $m_s=-1, +1$ spin states is reduced and consequently the ESR frequency is shifted to lower values. FIG. **11**A, by way of example, illustrates the temperature dependence of the ESR frequency with respect to temperature and FIG. **11**B illustrates resulting resonance lines at different temperatures, e.g., 300° K and 700° K. Thus, by employing ODMR, the NV center may be used to measure local temperatures on the recording head with high spatial resolution, and thus, is suitable to characterize, e.g., near-field power at a near field transducer of a HAMR write head.

[0081] FIG. **12**, by way of example, schematically illustrates the measurement of ODMR from a diamond film **110** with NV centers **112**, similar to FIG. **9**, with the diamond film **110** in contact with ABS of the recording head **114** having a near field transducer **180**, e.g., used with a HAMR write head. In heat assisted magnetic recording (HAMR), the recording medium is locally heated by a near-field emanating from the near field transducer with, e.g. d=30 nm width. The recording head that is used in HAMR includes both a write pole and a thermal device, e.g., laser light source, that illuminates a near-field transducer **180** and by exiting plasmon resonance in the near-field, the near-field emanates from the transducer heating the recording medium. As discussed above in refer-

ence to FIG. **1**, the thermal device of the recording head **114** instead of or in addition to the write pole may be controlled via the probe card **132** and the biasing source **131**. The biasing source **131** used to control the thermal device may be, e.g., pulsed or DC and may be a constant or varying magnitude. If desired, separate probe cards and/or biasing sources may be used to control the write pole and thermal device. For example, multiple probes from a single probe card **132** may be connected to multiple biasing sources in order to separately engage either the write or the HAMR thermal device, or both, in situ, and either in sequential or simultaneous operation. If desired, the measurement may be performed using a diamond film **110** with the NV center **112** held on the tip of an Atomic Force Microscope (AFM) arm **176**, as illustrated in FIG. **10**.

[0082] FIG. **13** illustrates the temperature profile produced by a near field transducer used in a HAMR write head. The NV centers **112** in the diamond film **110** may be used to measure the power of the near field at the transducer and/or the spatial extent of the transducer **180** in the same manner as the magnetic field and/or spatial extent of the write pole is measured. The diamond film **110** may be coated with a thin heat absorption layer **182**, e.g., a few nanometers thick, that has low thermal conductivity, e.g. SiO_2, that functions as the recording medium to be heated. The diamond film **110** may be held close to or in contact with the ABS of the recording head **114**. Moreover, the diamond film **110** may be deposited on the ABS of the recording head **114**. Further, if desired, the diamond film **110** may be on the tip of an AFM arm as discussed above. The diamond film **110** may be, e.g., implanted with the NV centers **112** or may be a film that is embedded with nano-diamonds having NV centers. The diamond film **110** may be a mono crystalline diamond film with a matrix of equally spaced NV centers to measure the spatial extent of the near field transducer **180** and its power. The diamond film **110** may be a mono crystalline diamond film with a random distribution of NV centers **112** to measure the heating power with an estimate of the spatial extent of the near field transducer **180**. If the diamond film **110** is a film with suspended nano-diamonds having a random distribution, the heating power of the near field transducer **180** may be measured.

[0083] As illustrated in FIG. **12**, the recording head **114**, including the transducer **180**, is brought into contact with or sufficiently near the heat absorption layer **182** on the diamond film **110** that the near-field emanating from the transducer **180** locally increases the temperature of the heat absorption layer **182**. The increase in temperature ΔT affects the electronic state of the NV centers **112** in the diamond film **110**. An example of a temperature profile across the near field transducer is depicted in FIG. **13**. As can be seen, the maximum heating occurs in the center of the spatial extent of the near-field transducer.

[0084] As discussed above, a light source **102** (shown in FIG. **1**) produces excitation illumination **103** that is incident on the diamond film **110** while in an external RF excitation field with varying excitation frequencies or pulse sequence produced by the RF antenna **126**. In response to the excitation illumination **103** and while the near-field is produced by transducer **180**, the NV center produces spin dependent PL **113** that is collected by the objective lens **122** and provided to the detector **130** (shown in FIG. **1**). If desired, depletion illumination $\mathbf{103}_{DEPL}$ may be scanned with respect to the recording head in two dimensions to measure ODMR. Moreover, as discussed above, a diamond film **110** with the NV center **112** held on the tip of an Atomic Force Microscope (AFM) arm **176**, as discussed, in FIG. **10** may be used in place of the depletion illumination. The integral PL emitted by the NVs is collected with a high numerical aperture objective lens **122** while applying an RF-field of varying frequency or a pulse sequence. A magnetic field may be produced by the write pole or an external magnetic field source, or no magnetic field may be used. Using a matrix of equally spaced NV centers, a frequency spectrum of the ODMR signal, such as that illustrated in FIG. **14**, may be generated and may be evaluated to extract temperature information, as illustrated in FIG. **15** in the same way as described for the write-field measurement, and using the known Temperature/ESR dependence, e.g., illustrated in FIGS. **11**A and **11**B. As can be seen in FIGS. **11**A and **11**B, temperature is inversely related to the ESR frequency, and thus, the minimum excitation frequency in the ESR spectrum is used to determine the maximum temperature. Additionally, because the maximum heating occurs at the center of the near-field transducer, the number of spectral lines in the ESR spectrum that are associated with the center of the near-field transducer may be used to determine the spatial extent of the near-field transducer. Moreover, if desired, the heat produced by the thermal device may be varied, e.g., by varying the applied bias signal to the thermal device, while producing a constant excitation frequency from the RF antenna **126**. For example, the excitation frequency of the RF antenna **126** may be set at a level at which a known good thermal device in a recording head heats an absorption layer **182** to a specific temperature, and sample recording heads may be tested at that excitation frequency to determine the bias signal necessary to produce same temperature. Thus, the efficiency of the thermal device in the recording head may be determined.

[0085] FIG. **16** illustrates an optical metrology device **100'**, similar to optical metrology device **100** shown in FIG. **1**, like designated elements being the same, and is capable of characterizing a photon emitter on a nanometer length scale using photoluminescence (PL) produced by a substitutional impurity **112** in a crystal film **110**. As optical metrology device **100'** characterizes a photon emitter, there is no need for the radio wave frequency (RF) antenna **126**, shown in FIG. **1**. As discussed above, one or more nitrogen vacancy centers (NV centers) in a diamond crystal may be used. The NV centers, which are basically artificial atoms with distinct quantum energy levels, show unique extrinsic and intrinsic optical spin dynamics including stable photoluminescence based on radiating transitions between optically excited energy levels of their charged quantum states. The photoluminescence may be produced by the NV centers in response to excitation illumination. Additionally, the photoluminescence of an NV center may be turned “off” or reduced by the light emitted from a photon emitter that is under test due to a mechanism known as Stimulated Emission Depletion (STED) or alternatively by Ground State Depletion (GSD) or Charge State Depletion (CSD). STED is used in super-resolution (SRM) microscopy to achieve spatial resolution beyond the optical diffraction limit using a laser light source for photoluminescence depletion. Other than in SRM as discussed below, the STED light source in the present disclosure is the device under test. The optical metrology device **100'** may optically detect the photoluminescence of one or more NV centers **112** in a crystal film **110**, e.g. using photon counting by employing a photo detector on a scanning microscope or by using a camera with

high sensitivity. By comparing the detected photoluminescence intensity produced in response to the excitation illumination when no STED illumination from the photon emitter under test is present and the detected photoluminescence intensity produced in response to the excitation illumination in the presence of STED illumination from the photon emitter, the quenching of the photoluminescence intensity may be determined, sometimes referred to herein simply as photoluminescence quenching. The characteristics of the photon emitter, including spatial and power characteristics, may be determined by analyzing the amount of photoluminescence quenching, e.g., by fitting the photoluminescence quenching to a model or comparing the photoluminescence quenching to a library of predetermined data.

[0086] The use of a confocal detection system enables detection of photoluminescence produced in response to the excitation illumination from only a small volume of the crystal film **110**, e.g., 1 μm^3. The light source **102** may be, e.g., a laser, LED, etc., that excites the NV center with a continuous (CW) or pulsed excitation illumination, with one or more wavelengths in a range of 460 nm to 580 nm, and which may be, e.g., 532 nm. With pulsed excitation illumination, the pulse width may be, e.g., approximately 800 ps with a 4-MHz repetition rate. The light source **102** may have a power density of, e.g., 40 kW/cm^2, to polarize the NV center by pumping it between the ground and the excited levels. The light from the light source **102** may be provided to a collimator consisting of lenses **104** and **106** either directly or by way of an intervening optical element, e.g., fiber optics or a light pipe. The collimator **104**, **106** expands and collimates the light, which is focused by lens **122**, which is also used to collect the photoluminescence emanating from the NV centers. In an embodiment in which the device is a confocal microscope, the lens **106** (and/or other appropriate lens(es)) may be moved back and forth, as illustrated by arrow **108** and/or a 2-dimensional steering-mirror system could be used to move the excitation illumination **103** in the back-aperture plane of the objective lens **122** scanning the focused excitation illumination **103** in the sample plane. Additionally, appropriate apertures may be used in an embodiment in which the microscope is a confocal microscope. Moreover, if desired and as discussed below, additional light sources may be used along with light source **102**.

[0087] A beam splitter **120** receives the excitation illumination from the light source **102** and provides at least a portion of the excitation illumination to the objective lens **122**. The excitation illumination is focused on the surface of the crystal film **110** by the objective lens **122**, which may have a high numerical aperture (NA=0.95) or an oil-immersion lens with an NA of, e.g. 1.3. The objective lens **122** may focus the excitation illumination on the crystal film **110** at a normal angle of incidence. It should be understood, however, that an oblique angle of incidence of the excitation illumination may be used if desired. The objective lens **122** focuses the light onto the crystal film **110** with one or more NV centers **112**. The crystal film **110** and NV centers **112** are positioned to be in a near field emission of the photon emitter **119** under test. By way of example, FIG. **16** illustrates the photon emitter **119** as a part of a Heat Assisted Magnetic Recording (HAMR) recording head **114**. The photon emitter **119**, for example, may be a thermal device that heats the recording medium using a laser light source and a near field transducer. It should be understood, however, that the photon emitter **119** under test may be any other type of device that produces a near field of illumination. In addition to near field emitters, the optical metrology device may be used for characterization of far field photon emitters with nanometer precision, which may be useful for characterizing a laser, e.g., the beam waist of a focused laser, or optical fibers. For example, a focal spot of a focused laser beam may be as small as 200 nm in diameter, which cannot easily be characterized by conventional methods. By scanning the focal spot from a focused laser beam over the NV centers **112** or an optical fiber on the crystal film **110**, for example, the profile of the laser beam or optical fiber may be resolved with nanometer resolution.

[0088] The crystal film **110** may be placed near or in contact with the photon emitter **119**, or if desired, deposited on the air bearing surface (ABS) of the recording head **114**, e.g., if the photon emitter **119** is part of the recording head. FIGS. **17**A and **17**B, by way of example, illustrate a side view and a back view, respectively, of recording head **114** in contact with crystal film **110**. As illustrated in FIG. **17**A, the recording head **114** includes a body, referred to as a slider **202**, with a write pole structure **204**, illustrated greatly enlarged, coupled to the back end of the slider **202**. A light source **208**, e.g. a laser diode, that is near the write pole structure **204** including the write pole **206** is integrated into the recording head **114**. Light from the integrated light source **208** is coupled to a near field transducer **212** at the ABS via an optical wave guide **210**. The near field illumination is produced by the near field transducer **212** at the air bearing surface AB. As can be seen in FIG. **17**B, the top surface of the crystal film **110** may be patterned, illustrated with notches **111**, forming islands with a width that is greater than a maximum dimension of the expected quenching profile, i.e., the area subject to photoluminescence quenching by STED near field illumination produced by the photon emitter **119**. For example, the island width may be approximately half the width of the slider **202** or less. The length of the island is optional and may be greater than the length of the slider **202**, and, in fact, may extend the length of the crystal film **110** if desired. The ABS of the recording head **114**, and more particularly, the near field transducer **212**, may be placed in contact with the crystal film **110** on a patterned island of the crystal film **110**.

[0089] The NV centers **112** in the crystal film **110** may be arranged in the form of a matrix and may have a uniform or a random distribution with a defined average density. Different average densities of the NV centers **112** in the crystal film **110** may be used depending on how the optical metrology device **100'** collects the photoluminescence. By way of example, however, an average density of the NV centers **112** may be, e.g. 200 NV centers per μm^2 or such that the distance between adjacent NV centers **112** is similar to or less than the dimension of the expected quenching profile, i.e., the area subject to photoluminescence quenching. Alternatively, the crystal film **110** may, in fact, include a number of small crystals, each containing a number of NV centers **112**. If desired, optical metrology device **100'** may include additional optic elements to move the excitation illumination over the crystal film **110**, e.g., in one or two dimensions. In one embodiment, as discussed below, a second light source may be provided that produces STED illumination with a ring shaped beam that has a central zero intensity at the focal plane that is coincident with the excitation illumination and which is scanned over the crystal film **110**. Alternatively, a single (or few) NV center **112** may be used in the crystal film **110**. In such an embodi-

ment, relative movement between the recording head **114** and the crystal film **110** may be produced, e.g., as illustrated by actuator **118** in FIG. **16**.

[0090] During measurement, photoluminescence **113** produced by the NV centers **112**, illustrated by the dotted line, will be collected by the objective lens **122** and directed by the beam splitter **120** towards a detector **130**. As illustrated, a spectral filter **124**, such as a dichroic film, is positioned before the detector **130** to remove any reflected excitation illumination and STED illumination from the photon emitter **119** and to direct only the photoluminescence to the detector **130**. The spectral filter **124**, thus, may be a long-pass filter with a wavelength cut-off at, e.g., 580 nm, or a narrow band pass filter with a center wave length of e.g. 637 nm, to filter out any remaining excitation illumination and STED illumination. The detector **130** may be, e.g., a non-imaging photodetector, such as a silicon avalanche photodiode operating in the signal photon counting regime, which detects the optical intensity at a single spot. Alternatively a CCD camera can be used to detect the intensity of the photoluminescence.

[0091] The detector **130** is connected to a computer **140** and the computer **140** receives, stores, and analyzes the optically detected data provided by the detector **130**. The computer **140** includes a processor **142** with memory **144**, as well as a user interface including e.g., a display **146** and input devices **148**. A non-transitory computer-usable storage medium **150** having computer-readable program code embodied may be used by the computer **140** for causing the processor **142** to control the optical metrology device **100'** and to perform the functions including the analysis described herein. The data structures and software code for automatically implementing one or more acts described in this detailed description can be implemented by one of ordinary skill in the art in light of the present disclosure and stored, e.g., on a computer readable storage medium **150**, which may be any device or medium that can store code and/or data for use by a computer system such as processor **142**. The computer-usable storage medium **150** may be, but is not limited to, magnetic and optical storage devices such as disk drives, magnetic tape, compact discs, and DVDs (digital versatile discs or digital video discs). A communication port **152** may also be used to receive instructions that are used to program the computer **140** to perform any one or more of the functions described herein and may represent any type of communication connection, such as to the internet or any other computer network. Additionally, the functions described herein may be stored in memory **144** or embodied in whole or in part within the circuitry of an application specific integrated circuit (ASIC) or a programmable logic device (PLD), and the functions may be embodied in a computer understandable descriptor language which may be used to create an ASIC or PLD that operates as herein described.

[0092] As illustrated, the computer **140** may be coupled to the recording head **114**, via a probe card **132** which is connected to the recording head **114** using one or more probes **134**, which may be, e.g., pogopins, probes, or other contacts such as wires that are wire bonded. The probe card **132** may be coupled to a biasing source **131** that provides a bias signal, such as a current or voltage signal, which is provided to the recording head **114** via the probe card **132** and controls the photon emitter **119**, i.e., a high intensity light source, on the recording head **114**. If the light source is separate from the recording head **114**, e.g., the probe card **132** may control the light source, which is remote from the recording head **114**, to produce illumination that is incident on the photon emitter **119**, which operates as a near field transducer.

[0093] The biasing source **131** may be connected to and controlled by the computer **140**. The computer **140**, thus, may control the illumination produced by the photon emitter **119** on the recording head **114**, e.g., by controlling the bias signal provided to the recording head (or separate illumination source). The biasing source **131** may provide a plurality of bias signals with different levels to the recording head **114**. Accordingly, the recording head **114** may be controlled via the biasing source **131** to produce near field illumination with a desired intensity that is constant or varying with a desired pulse width and frequency. The varying near field illumination produced by the photon emitter **119** may vary continuously or in a stepped manner.

[0094] Accordingly, the recording head **114** may be controlled via the biasing source **131** to produce a constant or varying near field illumination. Additionally, when the recording head **114** includes a Dynamic-Flying Height (DFH) device, one of the probes **134** of the probe card **132** may be used to provide current to the microactuator device from a second circuit in the current or voltage source that is connected to the computer **140**. Write heads use a DFH device as an adjustment mechanism to internally bias the write pole structure, including the photon emitter, closer to or further from the air bearing surface. The DFH device is typically in the form of a heater incorporated into the write head structure, with additional contact pads for external connection. By applying a bias to the additional contact pads via the probe card **132**, the position of the photon emitter**114** can be adjusted towards or away from the air bearing surface of the write head. By adjusting the position of the photon emitter **119** via the DFH device, the performance of the photon emitter **119** may be measured at different vertical displacement from the crystal film **110**.

[0095] Additionally, when the recording head **114** includes a microactuator device, one of the probes **134** of the probe card **132** may be used to provide current to the microactuator device. The source of the current may be a second circuit in the current or voltage source connected to the computer **140**. Write heads use a microactuator device as an adjustment mechanism to move the write pole structure, including the photon emitter, in the cross-track direction to better align the write pole structure to the lands of a disk that is being written to. The microactuator device is incorporated into the write head structure, which includes additional contact pads for external connection. By applying a bias to the additional contact pads via the probe card **132**, the position of the photon emitter **119** can be adjusted in the cross-track direction. By adjusting the position of the photon emitter **119** via the microactuator device during measurement with the device, the performance of the microactuator may be verified and the characteristics of the photon emitter **119** may be measured at different positions. Additionally, with an adequate density of NV centers, e.g., a low NV center density, and sufficient movement caused by the microactuator device, the microactuator device may be used to produce relative movement between the crystal film **110** and the photon emitter **119** during measurement.

[0096] As discussed above, the crystal film **110** contains one or more substitutional impurities **112**, such as NV centers. An NV center in diamond is a naturally occurring or technically created impurity in, e.g., a diamond crystal where a Nitrogen atom replaces a Carbon atom creating a vacancy

next to the Nitrogen atom. Nitrogen vacancy centers may be created in a diamond crystal, e.g., using a type-Ib HPHT single-crystal sample that is initially embedded with nitrogen impurities. For example, nitrogen impurities may be embedded by irradiation with a an ion-beam, e.g. N_2^+ ions at 5 keV, in case of a very high purity diamond film or by an electron beam in case the diamond film already has nitrogen impurities and annealing, e.g., for 2 hours at 850° C. The density of the NV centers within the crystal film may be controlled, e.g., by controlling the applied irradiation dose, or using appropriate masking techniques. For example, an ion beam fluence of 10^{11} cm^2 can result in a density of 8×10^{10} NV cm^{-2}. Moreover, by controlling the energy of the implantation as well as the annealing process the depth of the NV centers implanted in the crystal may be controlled.

[0097] An NV center may be optically excited, e.g., with excitation illumination having a wavelength range from 460 nm to 580 nm, which yields an intense photoluminescence emission from the NV center with lifetimes in the millisecond range. For example, the NV center may be excited with a laser at a wavelength of 532 nm and in response will emit a broadband luminescence with a zero phonon line at 637 nm, at room temperature. In the mechanism of stimulated emission, an electron in an excited state gives energy to an incoming photon and is forced to the ground state before it can create photoluminescence by spontaneous emission.

[0098] In addition, the photoluminescence of an NV center may be turned "off" or the intensity reduced in time when the pulse of excitation illumination is followed by a longer wavelength, or with the same wavelength, pulse of sufficient intensity, e.g., from the photon emitter **119** under test, due to a mechanism known as Stimulated Emission Depletion (STED). By way of example, the excitation illumination may have a wavelength of 532 nm and a duration of 60 ps followed by a longer wavelength pulse from the photon emitter **119** under test, e.g. 830 nm, with a duration 3.2 ns, of sufficient intensity to quench the intensity of the photoluminescence. If desired, STED with a continuous (CW) or quasi CW illumination may be employed.

[0099] Thus, one or more NV centers in a crystal film may be used to measure characteristics of the photon emitter, including spatial and power characteristics by detecting quenching of the photoluminescence intensity produced by NV centers caused by the near field illumination of the photon emitter. The photoluminescence quenching data may be analyzed, e.g., by fitting to a model or comparing a library of data, to determine the desired characteristics of the photon emitter.

[0100] FIG. **18**, by way of example, is a flow chart illustrating a method of determining one or more characteristics of a photon emitter using NV centers and an optical metrology device, such as the optical metrology device **100'**. As illustrated, excitation illumination is produced, e.g., by the optical metrology device **100'**, and is incident on a crystal film with the one or more NV centers (**302**). As discussed above, the NV centers produce photoluminescence having an intensity in response to the excitation illumination. Illumination is produced from the photon emitter, where the illumination is incident on the crystal film with the one or more NV centers (**304**). The illumination produced by the photon emitter quenches the intensity of the photoluminescence from the one or more nitrogen vacancy centers. The illumination from the photon emitter may be near field illumination or far field illumination. For example, the illumination may be produced by providing a bias signal to the photon emitter, which causes the photon emitter to generate near field illumination. Where the photon emitter is a laser diode, a bias current may be used, but a bias voltage may be used for other types of light sources if appropriate. For example, if the photon emitter may include a laser light source and near field transducer on a recording head, the bias current may be provided to the recording head via the probe card **132** to cause the photon emitter to emit the near field illumination. Alternatively, the light source may be remote from the photon emitter, e.g., as illustrated with the near field transducer **114** in FIG. **17**A, where light from the remote light source is provided to the near field transducer, which produces the near field illumination in response. The illumination may be far field illumination, such as that produced by a laser or fiber optics.

[0101] The amount of quenching of the intensity of the photoluminescence produced by the one or more NV centers caused by the illumination of the photon emitter is detected (**306**). The amount of quenching of the intensity of the photoluminescence may be detected by subtracting the background photoluminescence intensity. In other words, a first photoluminescence intensity may be detected from the one or more NV centers in response to the excitation illumination without the presence of the illumination produced by the photon emitter. A second photoluminescence intensity may be detected from the one or more NV centers in response to the excitation illumination in the presence of the illumination produced by the photon emitter, i.e., while the illumination from the photon emitter quenches the intensity of the photoluminescence from the NV centers. The amount of quenching of the intensity of the photoluminescence may then be determined based on a difference between the first photoluminescence intensity and the second photoluminescence intensity.

[0102] The amount of quenching of the intensity of the photoluminescence is analyzed to determine the one or more characteristics of the photon emitter (**308**). For example, the amount of quenching of the intensity of the photoluminescence may be analyzed by fitting the detected amount of quenching of the intensity of the photoluminescence to a photoluminescence quenching model. By way of example, the detected amount of photoluminescence quenching may be used in a non-linear, multi parameter fit to a model of a photoluminescence quenching distribution profile to determine the desired characteristics of the photon emitter. Additionally, or alternative, the amount of quenching of the intensity of the photoluminescence may be analyzed by comparing the amount of quenching of the intensity of the photoluminescence to a library of data, which is pre-generated and stored, e.g., in memory of the metrology device. The pre-generated data in the library may be produced, e.g., using the photoluminescence quenching model or in any other desired manner, such as empirically. The amount of quenching of the intensity of the photoluminescence may be analyzed in other manners as will be evident to those of ordinary skill in the art in light of the present disclosure. Characteristics that may be determined by analyzing the amount of quenching of the intensity of the photoluminescence, for example, may be the peak power or a width of the distribution profile. The width of the profile, for example when using a Lorentzian, may be the Full Width Half Magnitude (FWHM) or FWHM Half Magnitude (HWHM) or other equivalent measure, but for the sake of ease of reference will be referred to herein as FWHM. The characteristics of the photon emitter may be determined for different bias currents provided to the photon emitter. Moreover, the quenching data may be detected as a function of the

bias current provided to the photon emitter and analyzed, e.g., by fitting to a photoluminescence quenching model of an integrated photoluminescence quenching profile or comparing to a library of data to determine characteristics such as the width of the distribution profile and a power scaling factor. Again, the library of data may be produced, e.g., using the photoluminescence quenching model of an integrated photoluminescence quenching profile or in any other desired manner, such as empirically.

[0103] FIG. **19**, by way of illustration, shows a portion of a crystal film with a plurality of luminescing NV centers **402**, illustrated as white spots, only a couple of which are labeled **402**. As can be seen, the distribution of NV centers **402** may be inhomogeneous, i.e., non-uniform, but a crystal film with a homogeneous, i.e., uniform, distribution of NV centers may be used if desired. The crystal film, by way of example, may be a single crystal with a number of NV centers or a plurality of nano-crystals combined into the film, each nano-crystal containing one or more NV centers. The NV centers are in the same x/y plane and may have a defined average density, e.g., of 200 NV centers per square micron, or an average spacing of 60 nm±30 nm, but other average densities and/or average spacing may be used depending on the physical characteristics of the photon emitter under test. The spatial resolution is determined by the distance between the near-field illumination and the NV centers. Accordingly, for nanometer scale resolution, the NV centers should be relatively close to the top surface of the crystal film, e.g., a distance of 5 nm or less.

[0104] As discussed above, the NV centers are excited with excitation illumination at a wavelength of 532 nm, and luminesce at 637 nm, which may be collected, e.g., using a wide-field microscope with a CCD camera or a scanning microscope with a photodetector. The illumination from the photon emitter, however, will quench, i.e., turn off or reduce the intensity photoluminescence of the NV centers, due to STED. FIG. **19** illustrates a photon emitter **404** under test as a spot and further illustrates a diffraction limited spot **406** of the imaging system as a reference. By way of example, the photon emitter **404** may have a wavelength of, e.g., 700 nm to 900 nm and may be a continuous wave (CW) or pulsed light emitter.

[0105] The crystal film with NV centers has a characteristic dependence of STED on the power of the quenching light source. FIG. **20**, by way of example, illustrates the quenching of the photoluminescence intensity produced by the NV centers, i.e., the background subtracted photoluminescence intensity, caused by a near-infrared CW laser beam, where the y-axis represents photoluminescence intensity in arbitrary units, and the x-axis represents the laser power of the quenching light source in mW. The photoluminescence quenching dependence DP is described by an exponential function as follows:

$$DP(I)=m(I-I_0)^n+\text{const} \quad \text{eq. 2}$$

[0106] where "I" represents the general intensity, which may be uniform or locally varying, of the quenching light source, m is the quenching scaling factor and n the quenching exponent, and const is the asymptotic depletion value for very high depletion light intensity, for example, at 300 mW illustrated in FIG. **20**. The power dependence of the crystal film has to be measured once to determine the parameters I_0, m, n and const. The calibration of the power dependence of the crystal film may be performed using an external laser light source, e.g., laser, with known intensity I to produce data such as that shown in FIG. **20**. Preferably, the calibration of the power dependence of the crystal film is performed at the location on the crystal film that will be used to test photon emitters, but if the average density of NV centers is uniform over the entire crystal film, calibration of the power dependence of the crystal film may be performed anywhere on the crystal film.

[0107] The photon emitter may be characterized based on its peak power and its spatial distribution. FIG. **21**, by way of example, illustrates a near field illumination profile for a near field photon emitter, where the y-axis represents power of the photon emitter in mW and the x-axis represents the x-coordinate in nm. The peak power of the near field illumination profile is illustrated by line **602** and the FWHM is illustrated by arrows **604**. The near field illumination profile NF is described by a Lorentzian function with a parameter w that is the FWHM of the near-field distribution determined by the aperture size and the peak power (P) of the photon emitter as follows:

$$NF(x, y, P) = P\frac{w^2}{4[(x-x_0)^2+(y-y_0)^2]+w^2} \quad \text{eq. 3}$$

[0108] where x_o and y_0 are the coordinates with the peak power P. A Lorentzian function is used in a model as an example but this could also be a Gaussian or any other function that can describe the near-field distribution. The use of different model functions may yield different or additional characteristic parameters of the photon source related to the extent and geometry of the near-filed distribution.

[0109] FIG. **22** illustrates an example of a photoluminescence quenching profile for the NV centers of a crystal film, where the y-axis represents photoluminescence intensity in arbitrary units and the x-axis represents the x-coordinate in nm. As can be seen with a comparison of FIGS. **6** and **7**, the FWHM of the photoluminescence quenching profile (illustrated by arrows **704**) may be larger than the FWHM of the near field illumination profile. The locally varying photoluminescence quenching I_{STED} may be using equation 3 and equation 2 as follows:

$$I_{STED}(x,y,P)=DP(NF(x,y,P)) \quad \text{eq. 4}$$

[0110] Substituting NF(x,y,P) in equation 3 for the intensity I in equation 2, results in the following:

$$I_{STED}(x, y) = m\left[P\frac{w^2}{4[(x-x_0)^2+(y-y_0)^2]+w^2} - I_0\right]^n \quad \text{eq. 5}$$

[0111] where $I_{STED}(x, y)$ is the locally varying amount of quenching of the intensity of the photoluminescence with const=0, and P and w are fitting parameters of the peak power and the FWHM of the near field illumination profile, respectively, for a rotationally symmetric distribution.

[0112] FIG. **23**, by way of illustration, shows in two dimensions the detected quenching of the intensity of the photoluminescence produced by the NV centers **802** caused by near field illumination of a photon emitter. In FIG. **23**, the NV centers are illustrated as spots, with darker spots representing increased quenching. The near field illumination produced by the photon emitter interacts with the NV centers **802** turning off or reducing the intensity of the photoluminescence for

individual NV centers when the near field illumination at the individual NV centers is greater than a characteristic threshold value. The photoluminescence quenching of FIG. **23** may be determined as the difference in the measured photoluminescence intensity from the NV centers without the quenching illumination from the photon emitter and the measured photoluminescence intensity from the NV centers in the presence of the quenching illumination from the photon emitter. The intensity of the photoluminescence from the NV centers may be measured using, e.g., a wide-field microscope with a CCD camera or a scanning microscope with a photodetector, which may be scanned in the x and y coordinates. Once the photoluminescence quenching is detected, it may be analyzed, e.g., by fitting to a photoluminescence quenching model or compared to a library of data, to determine the desired characteristics of the photon emitter.

[0113] FIG. **24**, by way of illustration, shows detected photoluminescence quenching data, i.e., the amount of quenching of the intensity of the photoluminescence from the NV centers, as spots **902**, along with a fit curve **904** illustrating a spatially resolved quenching profile. The photoluminescence quenching data may be detected along a horizontal line **804** in FIG. **23**. The center line **804** may be determined from a two-dimensional distribution of the photoluminescence quenching data as a line that extends through the point or area with the strongest quenching. The two-dimensional distribution of the photoluminescence quenching data may be produced from a two-dimensional scan of the photon emitter. Alternatively, a one-dimensional scan of the photon emitter may be used to produce the photoluminescence quenching data from the NV centers if the scan passes through the point or area with the strongest quenching. The detected photoluminescence quenching data may be analyzed, e.g., by fitting to a photoluminescence quenching model, such as equation 5, or compared to a library of data, which may be produced using the model or empirically, to determine the one or more characteristics of the photon emitter. Thus, for example, a non-linear, multi parameter fit to the photoluminescence quenching profile model may be used to determine the peak power P and the width of the near field illumination profile. For example, the parameter fit such as that illustrated in FIG. **24** may provide a FWHM of 29.03 nm and a peak power P of 3083 [a.u.] for the near field illumination profile.

[0114] Additionally, by varying the separation between the photon emitter and the NV centers, the decay of the near-field power in the z-direction may also be measured. The separation between the photon emitter and the NV centers may be controlled by moving the crystal film, e.g., using a Atomic Force Microscope (AFM) or other actuator holding the crystal film and/or by moving the photon emitter, e.g., using a dynamic fly height (DFH) adjustment on the recording head.

[0115] If desired, the photoluminescence quenching may be detected for varying bias currents that are applied to the photon emitter and the peak power and FWHM of the near field illumination profile may be determined for different bias currents.

[0116] The optical metrology device **100'** shown in FIG. **16** may detect the quenching of the intensity of the photoluminescence caused by a near field photon emitter in various manners. For example, FIG. **25** schematically illustrates one implementation in which a crystal film **110** with one or more NV centers **112** is held on the tip of an Atomic Force Microscope (AFM) arm **176** to measure a photon emitter **119**. The embodiment shown in FIG. **25** is similar to the embodiment shown in FIG. **10**, without the RF antenna **126**, like designated elements being the same. The crystal film **110** with one or more NV centers **112** on the tip of the arm **176** is in contact with or at a controlled distance from the photon emitter **119** on the recording head **114**. The crystal film **110** may be a micron sized diamond particle that includes a single or several NV centers **112**. The AFM arm **176** may be scanned over the photon emitter **119** on the recording head **114** in one or two dimensions, as illustrated by arrows **178**. The use of a crystal film **110** with one or more NV centers **112** is held on the tip of an Atomic Force Microscope (AFM) arm **176** may be used in place, e.g., of the STED illumination embodiments discussed herein. As discussed above, a light source **102** (shown in FIG. **16**) produces excitation illumination **103** that is focused by the objective lens **122** onto the crystal film **110**. In response to the excitation illumination **103**, the NV center **112** produces photoluminescence **113** that is collected by the objective lens **122** and provided to the detector **130** (shown in FIG. **16**). As the crystal film **110** is scanned across the recording head **114**, including the photon emitter **119** and ABS, at each measurement position, the intensity of the photoluminescence **113** is measured with and without the near field illumination **115** from the photon emitter **119** to detect the quenching of the intensity of the photoluminescence at each measuring position. With the photoluminescence quenching detected at a plurality of measuring positions, a one dimensional line profile or two-dimensional distribution of the photoluminescence quenching may be determined. With a two-dimensional distribution of the photoluminescence quenching, the line profile through the strongest quenching point may be used to derive the peak power or the width of the near field illumination profile of the photon emitter by analyzing the amount of quenching of the intensity of the photoluminescence, e.g., by fitting to a photoluminescence quenching model, or compared to a library of data, which may be produced using the model or empirically, as discussed above. If desired, the scan may be repeated for different values of the bias current supplied to the light source, or equivalently, different values of the bias current may be supplied to the light source at each position during a single scan of the crystal film **110**.

[0117] Moreover, as discussed above, by varying the separation between the photon emitter and the NV centers, the decay of the near-field power in the z-direction may also be measured. The separation between the photon emitter and the NV centers may be controlled by moving the crystal film, e.g., using an actuator holding the crystal film and/or by moving the photon emitter, e.g., using a dynamic fly height (DFH) adjustment on the recording head. Further, the photoluminescence quenching may be detected for varying bias currents that are applied to the photon emitter and the peak power and width of the near field illumination profile may be determined for different bias currents.

[0118] In another implementation, the photoluminescence quenching of the intensity of the photoluminescence produced by a near field photon emitter may be detected without using relative movement between the photon emitter and the crystal film. For example, the optical metrology device may use scanning external STED illumination while the photon emitter and crystal film are held stationary with respect to each other.

[0119] FIG. **26** illustrates, by way of example, the optical metrology device **100'** with additional light sources to produce STED illumination to improve resolution and to scan the

photon emitter. The optical metrology device **100'** in FIG. **26** is similar to the embodiment shown in FIG. **4**, without the RF antenna **126**, like designated elements being the same. As illustrated, optical metrology device **100'** includes a second light source $\mathbf{102}_{STED}$ that produces STED illumination $\mathbf{103}_{STED}$ having a different wavelength as the light source **102**, and that is coincident on the crystal film **110** with the excitation illumination **103** from light source **102**. The light source **102** produces excitation illumination **103** that has a Gaussian point spread function and produces a relatively large diffraction limited spot on the crystal film **110**. FIG. **27**, by way of example, illustrates the Gaussian point spread function of the excitation illumination **103** with a solid line. The second light source $\mathbf{102}_{STED}$ produces light that passes through a vortex phase plate **164** to produce a ring shaped beam that has a central zero intensity at the focal plane. FIG. **27**, by way of example, illustrates a ring shaped point intensity distribution of the STED illumination $\mathbf{103}_{STED}$, which is coincident with the excitation illumination **103**. The STED illumination $\mathbf{103}_{STED}$ quenches the intensity of the photoluminescence produced by the NV centers **112** in the crystal film **110** that are off-center relative to the excitation illumination **103**, so that the off-center NV centers only contribute a constant background, which may be subtracted from the photoluminescence quenching signal produced by the photon emitter **119** under test, thereby providing a photoluminescence quenching signal from only the NV centers in the center of the STED illumination $\mathbf{103}_{STED}$. FIG. **28** illustrates the effective point intensity distribution **166** of the excitation illumination **103** combined with the STED illumination $\mathbf{103}_{STED}$. The coincident excitation illumination **103** and STED illumination $\mathbf{103}_{STED}$ may be scanned over the crystal film **110** at the region of interest by two-dimensional deflection in the back aperture of the objective lens **122** to detect the photoluminescence quenching caused by the photon emitter **119** in two dimensions, e.g., using one or more mirrors **117** in the beam path, which may be controlled by the computer **140**.

[0120] The STED illumination $\mathbf{103}_{STED}$ may have a wavelength greater than the excitation illumination **103**, e.g., greater than 532 nm, and with increased power. For example, a reduction in the photoluminescence may be achieved for STED illumination $\mathbf{103}_{STED}$ with power greater than 2 MW/cm^2. The STED illumination $\mathbf{103}_{STED}$ may be continuous (CW) or pulsed excitation, with a pulse width of, e.g. 150 ps, where a pulsed STED illumination $\mathbf{103}_{STED}$ results in stronger quenching of the intensity of the photoluminescence.

[0121] By determining the characteristics of the photon emitter, e.g., the peak power or power conversion factor and the aperture diameter determined, a finished photon emitter may be verified. For example, where the photon emitter is on a recording head, e.g., a HAMR head, each finished slider (or a sampling of finished sliders) may be verified by comparing the determined characteristics to an acceptable threshold. Recording heads with photon emitters having a peak power, a power conversion factor, or aperture diameter that is not within acceptable levels may be rejected.

[0122] Additionally, the characteristics of the photon emitter may be used in the process of attaching photon emitters to sliders, in the case of a HAMR head, or other types of devices. For example, the characteristics of the photon emitter, e.g., peak power, may be detected while actively aligning the laser light source to the slider, thereby enabling an optimum alignment between the laser light source and the slider, or other types of devices.

[0123] Additionally, the photon emitter discussed herein is a near field illumination source, such as the type used in recording heads. However, if desired, other near field illumination photon emitters may be tested, including optical fibers, plasmon tips for optical near field microscopy (SNOM), nano-photonics devices, optical wave-guides, laser-diodes, laser focal spot (beam waist) characterization. Moreover, it is possible to measure characteristics of far field emitters, such as a laser or fiber optics. For example, the process may be used to profile a laser beam produced by a laser or characterize fiber optics with a high degree of precision, i.e., on a nanometer length scale.

[0124] In another embodiment, a probe resembling, e.g., an Atomic Force Microscope (AFM) probe in shape and size and that is suitable to be attached to an AFM, may be created from a diamond film. The probe includes a tip that incorporates a single or a multitude of NV centers located near the end of the tip facing the device under test. A beveled portion at the end of the probe arm directs excitation light to the NV center and directs photoluminescence light emanating from the NV center into the probe arm. The probe arm acts as an optical waveguide to propagate the emission from the NV center with high efficiency. Various optical components may be mounted to the probe, e.g., via a beam splitter, including the light source (or a portion of the light source), a detector, as well as an RF antenna, if used. The integrated components enable excitation of photoluminescence in the NV center as well as optically detected Electron Spin Resonance (ODMR) and temperature measurements. Further, the probe may serve as a light probe utilizing the physical effect of Stimulated Emission Depletion (STED) caused by light from the light source under test acting on the photoluminescence radiation emanating from the NV center.

[0125] By way of example, FIG. **29** illustrates a probe arm assembly **300** in which the NV center **112** is positioned at the tip of a probe arm **376**, similar to the arm **176** discussed in reference to FIGS. **10** and **25**. As illustrated, the arm **376** and the tip **377** are produced from a crystal film, such as a diamond film. The NV center **112** is produced to be in the tip **377**, as illustrated in FIG. **29**. Thus, the arm is a crystal arm with the crystal probe tip at one end with the at least one nitrogen vacancy center in the crystal tip. A beam splitter **320** is connected to the arm **376** and a light source **302** to produce the excitation illumination **303** and a detector **330** for the photoluminescence **313** produced by the NV center **112** are connected to the beam splitter **320**. The beam splitter **302** may be is composed of e.g. two micro prisms. The beam splitter **302** may be a dichroic beam splitter, e.g., including optical coatings so that light emitted from the light source **302**, e.g., having a wavelength shorter than 600 nm, is transmitted into the probe arm **376** and photoluminescence **313** produced by the NV center **112**, e.g., having a wavelength greater than 600 nm, is reflected to the detector **330**. Advantageously, the beam splitter **320** and arm **376** may be directly connected, i.e., with no intervening focusing optics disposed between the beam splitter **320** and the arm **376**. Moreover, the light source **302** and detector **330** may be connected to the beam splitter **320** so that no intervening focusing optics need be disposed between the light source **302** and the beam splitter **320** and/or the detector **330** and the beam splitter **320**. Thus, the excitation illumination from the light source **302** is introduced into an

end of the crystal arm **376** that is opposite the end of the crystal arm **376** with the probe tip **377**.

[0126] FIG. **30** illustrates another embodiment of a probe arm assembly **300'**, that is similar to probe arm assembly **300**, like designated elements being the same. The arm assembly **300'** of FIG. **30**, however, includes an arm **376'** that includes an enlarged end **380** that is coupled to the beam splitter **320**. The enlarged end **380** enables a greater surface area of the arm **376'** to be coupled to the beam splitter **320** thereby a larger interface through which excitation illumination **303** and photoluminescence **313** may be coupled into and out of the arm **376'**.

[0127] The arm **376** may be produced using a diamond film with NV centers implanted to a desired depth. Lithography, such as electron-beam lithography, may be used to define in a SiO_2 mask the probe tip **377** and the enlarged end **380**, if used. The diamond film may be etched, e.g., using reactive ion etching (RIE) to define the probe tip **377** and enlarged end **380** if used. Another mask deposition, lithography, and etch process may be used to define the opposite side of the arm **376** including the surface to be mounted to the holder plate **340** and the enlarged end **380**, if used. The bevel **397** on the probe arm **376** may be produced, e.g., through isotropic wet-etching with a sacrificial layer, mechanical polishing, anisotropic wet-etching, or focused ion-beam etching. The arm **376** may be cut through the diamond film, e.g., using an etching process. With a sparse implantation of NV centers in the initial diamond film, the resulting probe tip **377** may have only a limited number of NV centers **112**. Post processing testing of the probe tip **377** for photoluminescence may be used to ensure the presence and number of NV centers in the probe tip **377**.

[0128] The light source **302** for either arm assembly **300** or arm assembly **300'**, collectively referred to herein as arm assembly **300**, may be, e.g., a laser diode or LED chip that is mounted to the beam splitter **320**. If desired, the light source **302** may include a fiber optic or a light pipe that connects a light emitter, such as a laser or LED, to the beam splitter **320**. As discussed previously, the light source **302** may excite the NV center with a continuous (CW) or pulsed excitation illumination, with one or more wavelengths in a range of 460 nm to 580 nm, and which may be, e.g., 532 nm. With pulsed excitation illumination, the pulse width may be, e.g., approximately 800 ps with a 4-MHz repetition rate. The light source **302** may have a power density of, e.g., 40 kW/cm^2, to polarize the NV center by pumping it between the ground and the excited levels.

[0129] The detector **330** may be e.g., a non-imaging photodetector, such as a silicon avalanche photodiode operating in the single photon regime, i.e., using photon counting, which detects the optical intensity at a single spot. If desired, a CCD or CMOS array may be used, but because the photoluminescence is not being imaged, a CCD or CMOS array is unnecessary. The use of a camera, e.g., using a CCD or CMOS array to provide an overview of the sample during testing, however, may be desirable. As illustrated, a spectral filter **324**, such as a dichroic film, may be positioned between the detector **330** and the beam splitter **320**. The spectral filter **324** may be an integral part of the beam splitter **320**, e.g., an optical coating. The spectral filter **324** removes any reflected excitation illumination **303** and directs only the photoluminescence **313** to the detector **330**. The spectral filter **124**, thus, may be a long-pass filter with a wavelength cut-off at, e.g., 580 nm, to filter out any remaining pump light. Thus, the detector **330** is physical connected to the beam splitter **320**, either directly or with a spectral filter **324** disposed between the detector **330** and the beam splitter **320**, with no intervening focusing optics disposed between the beam splitter **320** and the detector **330**. The filter **324** may be an integral part of the beam splitter **320**,

[0130] The beam splitter **320** may be, e.g., a micro-prism or a combination of two micro-prisms, that passes the excitation illumination **303** from the light source **302** to the arm **376** and reflects the returning photoluminescence **313** towards the detector **330**. If desired, the beam splitter **320** may be configured to reflect the excitation illumination **303** from the light source **302** and transmit the returning photoluminescence **313** to the detector **330**. If desired, the beam splitter **320** may be a dichroic beam splitter which may eliminate the need for the spectral filter **324** before the detector **330**.

[0131] As illustrated in FIG. **29**, as shown more closely in FIG. **31**, arm **376** acts as an optical waveguide by means of total internal reflection. The end **379** of the arm **376** may be beveled to direct the excitation illumination **303** into the tip **377** and to direct the photoluminescence **313** from the NV center **112** into the length of the arm **376**. Thus, the excitation illumination **303** from the light source **302** is introduced into the arm **376** via the beam splitter **320**, without focusing optics, is guided along the length of the arm **376** via total internal reflection and the arm **376** is configured to reflect the light, e.g., 90°, into the tip **377** to the NV center **112**. The arm **376** is configured to reflect photoluminescence **313** from the NV center **112** in the tip **377**, e.g., 90°, out of the tip **377** into the arm **376**, and the photoluminescence **313** is guided along the length of the arm **376** via total internal reflection until it is received by detector **330**, via the beam splitter **320**, without focusing optics.

[0132] The arm **376** with beam splitter **320** may be mounted on a holder plate **340**, which is mounted to the AFM during operation. For example, the arm **376** and beam splitter **320** may be glued to the holder plate **340**. For example, the arm **376** may be glued onto the holder plate **340** referenced to an edge on the holder plate **340** or placed in a trench in the holder plate **340**. FIGS. **32** and **33**, by way of example, illustrate a side view and a top view of the arm **376** with beam splitter **320** mounted on the holder plate **340**. The light source **302** and detector **330** may also be mounted on the holder plate **340** if desired and the holder plate **340** may include conductive pads and leads **304** and **332** for the desired electrical connections. Alternatively, one or both the light source **302** and detector **330** may be mounted on the beam splitter **320**, which is then mounted on the holder plate **340**. For example, FIG. **33** illustrates the detector **330** coupled to the side of the beam splitter **230**, along with spectral filter **324**, and thus, detector **330** may be mounted to the holder plate **340**. FIG. **29**, on the other hand, illustrates the detector **330** coupled to the top of the beam splitter **230**, and thus, the detector **330** may be mounted to the beam splitter **230**, via intervening spectral filter **324**.

[0133] FIG. **34** illustrates another embodiment of an arm assembly **300"** that is similar to arm assembly **300**, e.g., illustrated in FIG. **33**, except that a separate beam splitter **320** is not used with arm assembly **300"**. As illustrated, the end **382** of the probe arm **376"** that is nearest the light source **302** and detector **330** may be beveled, to reflect photoluminescence light to the detector **330**. It will be understood that the photoluminescence light is reflected by the beveled portion of the end **382** and is extracted through the side of the probe arm

376" at the end **382**, and therefore is referred to herein as being extracted through the end **382**. The detector **330** is in direct contact with the side of the probe arm **376"** at the end **382** to receive the photoluminescence light that is reflected by the beveled portion of the end **382**. A dichroic filter **384** may be deposited on the beveled portion of the end **382** to assist in the reflection of the photoluminescence light but allowing the excitation illumination from light source **302** to enter the probe arm **376"**. The light source **302** may be separated from the probe arm **376"**, e.g., by approximately half the width of the detector **330**. The apertures of the light source **302** and the detector **330** are centered on the beveled portion of the end **382**.

[0134] The arm assembly **300** may be used in the same manner as arm **176** discussed in reference to FIG. **10** to characterize magnetic recording heads. If desired, an RF antenna **326** may be located on the arm **376** to provide an excitation field to the NV center **112**. The RF antenna **326** may produce a desired excitation field as discussed above. The RF antenna **326** may be configured, e.g., by positioning and orientation, to produce the desired excitation field that is incident on the NV center **112** but will have little impact on the recording head being tested. For example, with the RF antenna **326** being located close to the NV center **112**, a reduced RF excitation field may be used. Moreover, as illustrated in FIG. **35**, the RF antenna **326** may be oriented and configured to focus the excitation field **327** on the tip **377** with the NV center **112**, and accordingly, little or no excitation field will be directly incident on the recording head. With the presence of the RF antenna **326**, the holder plate **340** may include conductive pads and leads for the desired electrical connections. If desired, however, the RF antenna **326** may be separate from the arm **376**, e.g., as illustrated in FIG. **10**. Thus, the arm **376** may be scanned over the recording head **114** (as illustrated in FIG. **10**) in two dimensions and the photoluminescence **113** from the NV center(s) **112** is collected. It should be understood that scanning is performed by producing relative movement between the arm **376** and the sample, e.g., the arm **376** may move in two dimensions and the sample held stationary or the sample may move in two dimensions while the arm **376** is held stationary, or both the arm **376** and sample may move. Additionally, the arm **376** and/or sample may move in the vertical dimension to place the tip **377** in contact with or near the sample. Thus, the tip **377** with the NV center(s) **112** may be in contact with or at a controlled distance from the recording head **114**. The ODMR may be measured from the NV center(s) **112** at the tip **377** of the arm **376**, at varying excitation frequencies of the excitation field and/or varying magnetic fields produced by the recording head **114** as the arm **376** is scanned over the recording head in two dimensions.

[0135] Additionally, the arm assembly **300** may be used in the same manner as arm **176** discussed in reference to FIG. **25** to characterize a photon emitter. If the arm assembly **300** is used to characterize a photon emitter, the RF antenna **326** is not needed. Again, the arm **376** may be scanned over the device being tested, e.g., the photon emitter **119** (shown in FIG. **25**) in one or two dimensions and the photoluminescence **113** from the NV center(s) **112** is collected, while the tip **377** with the NV center(s) **112** is in contact with or at a controlled distance from the photon emitter **119**. It should be understood that scanning is performed by producing relative movement between the arm **376** and the sample, e.g., the arm **376** may move in two dimensions and the sample held stationary or the sample may move in two dimensions while the arm **376** is held stationary, or both the arm **376** and sample may move. Additionally, the arm **376** and/or sample may move in the vertical dimension to place the tip **377** in contact with or near the sample. The light source **302** produces excitation illumination **303** that is directed to the NV center **112** in the tip **377** via the beam splitter **320** and arm **376**. In response to the excitation illumination **103**, the NV center **112** produces photoluminescence **113** that is directed back through the arm **376** and provided to the detector **330** via the beam splitter **320**. As the arm **376** is scanned across the recording head **114**, including the photon emitter **119** and ABS, at each measurement position, the intensity of the photoluminescence **113** is measured with and without the near field illumination **115** from the photon emitter **119** to detect the quenching of the intensity of the photoluminescence at each measuring position. With the photoluminescence quenching detected at a plurality of measuring positions, a one dimensional line profile or two-dimensional distribution of the photoluminescence quenching may be determined. With a two-dimensional distribution of the photoluminescence quenching, the line profile through the strongest quenching point may be used to derive the peak power or the width of the near field illumination profile of the photon emitter by analyzing the amount of quenching of the intensity of the photoluminescence, e.g., by fitting to a photoluminescence quenching model, or compared to a library of data, which may be produced using the model or empirically, as discussed above. If desired, the scan may be repeated for different values of the bias current supplied to the light source, or equivalently, different values of the bias current may be supplied to the light source at each position during a single scan of the arm **376**.

[0136] With the use of arm assembly **300**, with the detector **330** connected to arm **376** via beam splitter **320** to receive photoluminescence **313** without focusing optics, the efficiency of light extraction is improved. Accordingly, the signal to noise ratio is improved and fewer NV centers **112** are required with arm assembly **300**, thereby improving spatial resolution. Moreover, measuring time may be decreased as loss of the resulting photoluminescence **313** from the NV centers **112** is reduced or eliminated by guiding the photoluminescence **313** to the detector **330**.

[0137] Additionally, the probe arm **376** may be configured to determine a characteristic of the recording head using measured ODMR based on the heating of the probe tip **377** by a thermal device and near-field transducer in a recording head, such as a HAMR head, as the probe arm **376** is scanned over the sample, as discussed above. For example, a bias signal may be provided to the thermal device, which causes the near-field transducer to heat the probe tip **377**. The ODMR may be measured from the NV center(s) **112** at the tip **377** of the arm **376**. The increase in temperature caused by the thermal device and near-field transducer affects the electronic state of the NV centers **112**, from which a desired characteristic may be determined, as discussed above. Moreover, if desired, as illustrated in FIG. **36**, a heat absorption layer **378**, similar to the absorption layer **118** discussed above, may be coated on the tip **377** of the probe arm **367**, where the thermal device and near-field transducer heat the absorption layer **378** as the probe arm **376** is scanned over the sample.

[0138] NV centers may be used to directly detect electric fields emanating from small areas of a sample, such as an integrated circuit. For example, small, e.g., nanometer sized,

static electric charges located in a transistor or a flash memory cell may be detected using NV centers. Moreover, the electromagnetic fields generated by varying the electric charges, e.g., by switching the transistor or producing a current in an electric device, may be detected using NV centers.

[0139] Currently, testing and failure analysis through integrated circuit metrology is based on Laser Voltage Probing" (LVP) and "Laser Voltage Imaging" (LVI). Conventionally, LVP and LVI are used to dynamically test signal integrity, e.g., in transistors, by tracing the signal through the device. In LVP and LVI, infra-red laser light is focused on an active area of the sample, e.g. a Field Effect Transistor (FET). LVI is basically, a two-dimensional implementation of LVP. In LVP, the laser light is introduced into the FET from the backside of the wafer substrate. Based on the reflected optical signal, LVP detects changes in the refractive index of the materials in the transistor that is caused by changes in the free carrier density (FCD) when the transistor is switched on and off. The modulation of the reflected optical signal caused by changes in the FCD, unfortunately, is convoluted with a number of different contributions other than FCD, such as heating, the Kerr effect, the Pockels effect, geometrical effects, (the topology of the device under test), electro refraction, interference and more. In general, the underlying physical effects in LVP are not well understood. Due to the complexity of interpretation of the optical signal, LVP is not applicable to quantitative static probing of the FCD. Moreover, the light must penetrate the sample and accordingly relatively long wavelengths for the optical probing is used, which limits the spatial resolution to approximately 1 micron.

[0140] While conventional LVP and LVI are unsuitable for quantitative analysis of electrical devices, particularly, on a small scale, e.g., nanometer scale, NV centers may be used, advantageously, to provide such a quantitative analysis.

[0141] FIG. **37** illustrates a probe arm **376**, as discussed above, scanning over a backside of a sample **510** that includes an integrated electronic circuit, illustrated as a Field Effect Transistor (FET) **512**. The probe arm **376** includes a tip with a crystal film, such as a diamond film, that includes at least one NV center **112** and may be integrated with a light source **302** and detector **330**, as discussed above. The integrated electronic circuit, illustrated as FET **512**, may be, e.g., any conventional electronic circuit in which a static or dynamically charge is located. For example, FET **512**, is illustrated with a source **514**, drain **516**, and gate **518** terminals. The FET **512** may further include a substrate **520** terminal that biases the transistor into operation and a gate dielectric **522** between the gate **518** and the substrate **520**. The FET **512** is further illustrated as including isolation trenches **524**. In operation, a voltage applied to the gate **518** induces a channel charge **526** between the source and drain contacts via the field effect with an depletion charge **528** accumulating at the drain **516**. When the gate voltage is zero, there is a small depletion charge **528**. With increasing gate voltage, the channel charge **526** region under the gate **518** grows (channel pinching) and the depletion charge **528** accumulates on one side of the gate in the channel, as illustrated. The size of the area of the depletion charge **528** may be small, e.g., on the order of nanometers.

[0142] The probe arm **376** is illustrated as being brought into contact with the backside of a substrate **530** on which the FET **512** is located. The substrate **530** may be thinned, if necessary, using conventional techniques, such as ion milling. By way of example, the substrate **530** may have a thickness of 500 nm. As discussed above, excitation illumination from light source **302** and a radio frequency field from RF antenna **326**, e.g., with variable frequency, may be applied to the NV center **112** in the tip of the probe arm **376**. As discussed above, a photodetector **330** optically detects a decrease in spin dependent photoluminescence in response to the excitation illumination caused by electron spin resonance (ESR) of the at least one nitrogen vacancy center **112** at varying excitation frequencies of the radio frequency field to measure Optically Detected Spin Resonance (ODMR). A characteristic of the electronic component may then be determined using the ODMR.

[0143] The at least one NV center **112** in the tip of the probe arm **376** has distinct quantum energy levels that show unique extrinsic and intrinsic optical spin dynamics including stable photoluminescence based on radiating transitions between optically excited energy levels of their charged quantum states. Further, Electron Spin Resonance (ESR) is excited in the NV center electronic spin system by an external radio frequency (RF)-field with frequencies resonant with the transitions between the energy sub-levels. At resonance, the photoluminescence intensity is measurably reduced. The resonance frequency depends on the electric- and magnetic fields acting on the NV center **112**. The ESR-frequency is shifted in the presence of an applied electric field (Stark-Effect), e.g., as illustrated in FIG. **38**. Accordingly, the one or more NV centers **112** may be used as an electric field sensor with nanometer resolution using optically detected ESR (sometimes referred to herein as ODMR (Optically Detected Magnetic Resonance) (ESR is paramagnetic resonance that falls into this category)). The spatial resolution is determined fundamentally by the size of a single NV center **112** which is on the Angstrom length scale and, practically, by the distance between the electric field source or charge and the NV center **112**. Accordingly, the optical metrology device using, e.g., the probe arm **376** may optically detect the photoluminescence of one or more NV centers **112** in the crystal tip of the probe arm **376** using photon counting by employing a photo detector, **330**, or by using a camera with high sensitivity, to measure a variety of characteristics of an electronic circuit of sample **510** that has features with a nanometer length scale.

[0144] The at least one NV center **112** of the probe arm **376** directly measures the electric field produced by the electronic circuit of the sample **510**, and accordingly, the measurement is not convolved with other physical effects, unlike conventional LVP. By way of example, FIG. **39** illustrates the calculated perpendicular (y-component) electric field of a line charge of 50 nm length and a charge density of $1.6\ 10^{-8}$ Coulomb/m at a distance of 500 nm (curve **552**) and a distance of 700 nm (curve **554**). The line charge is a geometrically simplified representation of depletion charge **528**. The spin resonance of the NV center **112** is solely influenced by the electric field and thus, there is no convolution of other physical effects. Accordingly, the measurement by the NV center **112** in the probe arm **376** is quantitative. Further, because the measurement does not evaluate an optical image the method is not diffraction limited.

[0145] FIG. **40**, by way of example, is a flow chart illustrating a method of using at least one NV center **112** in a probe arm **376** to characterize an area of a sample with an electric charge. An electric charge is provided in an area of the sample (**602**). For example, a transistor may be turned on (or off) or a flash memory cell may be written to produce a desired static charge. Moreover, the electric charge may be dynamically changing, e.g., by turning a transistor on and off, by changing

the gate voltage e.g., in a FET transistor, or by moving the electric charge through a conductor, e.g., providing an electric current, which may be alternating or direct. The NV center **112** may be used to measure the electric field produced by the charge and/or the magnetic field produced by the dynamically changing electric charge.

[0146] A probe having a probe tip with at least one nitrogen vacancy center is scanned over the area of the sample with the electric charge (**604**). For example, as illustrated in FIG. **37**, the NV center **112** in the probe arm **376** may be scanned over the sample **510**. The NV center **112** in the probe arm **376** may be scanned in a plane with a known distance from the electric field source or electric charge. The plane may be defined, e.g., by the backside of the substrate **530** of the sample **510**. If necessary, the substrate **530** may be thinned, e.g., using ion milling or other appropriate means, to define a plane with a known distance from the electric field source. As illustrated in FIG. **37**, the scan may be performed in one dimension (X) or two dimensions (X, Z) with nanometer resolution.

[0147] An excitation radio frequency (RF) field is provided to the at least one nitrogen vacancy center (**606**) and excitation illumination is produced that is incident on the at least one nitrogen vacancy center (**608**). The excitation RF field may be produced by an external RF antenna, such as RF antenna **126** illustrated in FIG. **10** or RF antenna **326** illustrated in FIG. **29**, in the case where a static electric field measurement is made. If the electric charge is dynamically changing, the excitation RF field may be produced by a dynamically changing magnetic field in the sample that is produced by the dynamically changing electric charge. The Optically Detected Spin Resonance (ODMR) is measured as the probe tip is scanned over the area of the sample with the electric charge by detecting a decrease in a spin dependent photoluminescence in response to the excitation illumination caused by electron spin resonance (ESR) of the at least one nitrogen vacancy center (**610**). A characteristic of the area of the sample with the electric charge is determined using the ODMR (**612**).

[0148] FIG. **41** illustrates, by way of example, the optical metrology device **100"** with a probe arm assembly **300** with an NV center **112** at the tip of a probe arm **376**, configured to characterize an area of a sample **510** with an electric charge. The optical metrology device **100"** may include an external RF antenna **126** or, alternatively, may have an RF antenna **326** on the probe arm **376**. The probe arm assembly **300**, including actuator **118** to produce relative movement between the sample **510** and the NV center **112**, is controlled by computer **140**. The computer **140** is also coupled to the sample **510** via a probe card **132** which is connected to the sample **510** using one or more probes **134**, which may be, e.g., pogopins, probes, or other such contacts. The probe card **132** may be coupled to a biasing source **131** that provides a bias signal to the sample **510**and a voltage source **133** that provides a gate control voltage to the sample **510**. The biasing source **131** and voltage source **133** are controlled by computer **140**. As discussed above, the computer **140** includes at least one processor **142** that is configured to perform the functions including the analysis described herein. The at least one processor **142** for example, may be coupled to the detector **330** and may be configured to measure Optically Detected Spin Resonance (ODMR) as the probe tip is scanned over the area of the sample with the electric charge by detecting a decrease in a spin dependent photoluminescence in response to a received excitation radio frequency (RF) field and the excitation illumination caused by electron spin resonance (ESR) of the at least one nitrogen vacancy center; and determine a characteristic of the area of the sample with the electric charge using the ODMR.

[0149] A static electric field measurement may be made, for example, with knowledge of the distance in the Y dimension of the NV center **112** from the electric charge Q, the characteristics of the charge can be determined by parameter fitting of the measured field distribution to model equations. For example, an electric field of a charge segment may be written as equation 6, where i and j are unit vectors in the direction of the position vector pointing to E(x, y), while the perpendicular filed of a line charge with length L and charge density X=Q/L is written as equations 7 and 8.

$$dE = \frac{k \cdot \lambda}{((x-x_0)^2 + y^2)^{\frac{3}{2}}} \cdot (x-x_0) \cdot i + y \cdot j \qquad \text{eq. 6}$$

$$E_y = \int_{-\frac{L}{2}}^{\frac{L}{2}} \frac{k \cdot \lambda \cdot y}{((x-x_0)^2 + y^2)^{\frac{3}{2}}} dx_0 \qquad \text{eq. 7}$$

$$E_y(x; y) = -\frac{k \cdot 4^{\frac{3}{2}} \cdot \left((L+2 \cdot x) \cdot \sqrt{L \cdot (L-4 \cdot x) + 4 \cdot (y^2+x^2)} + (L-2 \cdot x) \cdot \sqrt{L \cdot (L+4 \cdot x) + 4 \cdot (y^2+x^2)}\right) \cdot \lambda}{8 \cdot y \cdot \sqrt{L \cdot (L-4 \cdot x) + 4 \cdot (y^2+x^2)} \cdot \sqrt{L \cdot (L+4 \cdot x) + 4 \cdot (y^2+x^2)}} \qquad \text{eq. 8}$$

[0150] The frequency shift caused by electric field E_y is written as equation 9. The resonance curve of the ESR resonance line with width γ is written as equation 10. The photoluminescence P(x,y) along x at a height y for a fixed RF excitation frequency is written as equation 11. Here C_p is the frequency shift parameter, A is the RF field amplitude, γ is ESR line width, and C_{ODMR} is the ODMR contrast parameter, which is a characteristic constant of the NV center **112** and may be determined once for an individual diamond film or tip.

$$\Delta f(x; y) = C_p \cdot E_y(x; y) \qquad \text{eq. 9}$$

$$f_r(x) = \frac{A}{\pi \cdot \gamma} \cdot \left(\frac{\gamma^2}{(x-x_0)^2 + \gamma^2}\right) \qquad \text{eq. 10}$$

$$P(x; y) = 1 - \frac{A}{\pi \cdot \gamma} \cdot \left(\frac{\gamma^2}{(x + \Delta f(x; y) - x_0)^2 + \gamma^2}\right) \cdot C_{ODMR} \qquad \text{eq. 11}$$

[0151] Equation 11 describes the photoluminescence contrast in two dimensions, x and y. The x coordinate is along the length of the geometrically simplified line-charge and the y coordinate is the distance between the line-charge and a parallel plane that contains the NV center. For the measurement, the distance γ is known, based on the known amount of thinning of the substrate **530** and the known geometry of the device in y-direction i.e. the thicknesses of any thin film layers. The parameter fit of the measured data to P(x,y) is performed for this known distance, e.g. y=500 nm, and results in the charge length L and charge density X=Q/L, from which the charge Q can be determined (which are implicit in equation 11 from equations 8 and 9), which are characteristic quantities of the device under test.

[0152] FIG. **42**, by way of example, illustrates a parameter fit of the photoluminescence distribution P(x,y) using equation 11 (and implicitly from equations 8 and 9) for simulated measured data from an ODMR scan measured in a plane that is at a height y=500 nm above a line charge, where the resulting charge Q is determined to be 8.6912×10^{-16} C, γ is 1.7382×10^{-8} A s/m and the charge length is determined to be L=50 nm. While the curve for the parameter fit illustrated in FIG. **42** does not appear to depict the charge length L, this is due to the height at which the measurement data was obtained, i.e., y=500 nm. Nevertheless, the measured data is adequate to accurately determine the charge length L and charge Q. By way of example, knowing the charge Q and charge length L from the parameter fit of P(x,y) to the data measured at height y=500 nm, one can calculate P(x,y) at a much closer measurement height y by plugging the calculated parameters into the equation 11, to produce a curve that provides a clearer depiction of the line charge. For example, the curve in FIG. **43** represents a photoluminescence distribution calculated by equation 11 assuming a height of y=10 nm and the fit parameters Q and L obtained from the data measured at y=500 nm (as illustrated in FIG. **42**) to more clearly depict the geometry of the line charge. Thus, while the parameter fit illustrated in FIG. **42** does not clearly depict the geometry of the line charge due to the height at which the measurement data was obtained, FIG. **43** illustrates that using the charge Q and the charge length L determined from the parameter fit with the measured data, if the photoluminescence distribution is calculated from equation 11 at a closer height, the calculated photoluminescence distribution more clearly depicts the geometry of the line charge as expected.

[0153] FIG. **42** illustrates a parameter fit of the photoluminescence distribution for measured data from an ODMR scan for a single line charge. The same process may be used for more than one line charge. For example, if there are two adjacent devices or electric charges, the measured data may be used to find the charge length L and charge Q for both line charges, where the photoluminescence P(x,y) along x at a height y for a fixed RF excitation frequency for the two line charges may be written as equation 12, where the space between the line charges is (x2−x1)>L, and x1 and x2 are the respective centers of the two line charges.

$$P2(x,y)=P(x,y)=P(x,y)|_{x0=x1}+P(x,y)|_{x0=x2} \quad \text{eq. 12}$$

[0154] By fitting the measured data, at the known measurement height (e.g., y=500 nm) to the equation 12, the charge length L and charge Q for both line charges can be determined. FIG. **44**, by way of example, illustrates a curve **622** produced by parameter fit of the photoluminescence distribution P(x,y) using equation 12 for simulated measured data from an ODMR scan measured at a height y=500 nm. The parameter fit produced by curve **622** accurately determines the charge Q and charge length L for two line charge, despite not clearly depicting the geometry of the line charges, similar to FIG. **42**. Curve **624**, on the other hand, is a calculated photoluminescence distribution based on the measured data and the charge Q and charge length L for the two line charges determined based on curve **622**, but assuming a measurement height y=1 nm, which is much closer to the line charges than the actual measurement height. As with FIG. **43**, curve **624** more clearly depict the geometry of the two line charges illustrating the measurement data and the parameter fit **622** may be relied upon to accurately determine the characteristics of the two line charges. Thus, two adjacent devices separated by a distance smaller than the optical diffraction limit can be resolved even though the individual charges are not discriminable in data taken at y=500 nm.

[0155] Thus, to characterize an area of a sample with a static electric charge or charges, e.g., in an electronic device, such as an integrated circuit, FET and the flash-memory cell, etc., the ODMR may be measured at a fixed RF excitation frequency while the NV center **112** in the probe arm **376** is scanned over the area that contains the electric charge or charges. The photoluminescence may be parameter fit, as discussed above to determine the charge Q and the charge length L. FIG. **45**, by way of example, illustrates a calculated photoluminescence distribution from an ODMR scan for a fixed RF excitation as a function of the x-coordinate, x=0 being the center of the line where the e-field has a maximum, at a plane 500 nm above the electric charge. Alternatively, the RF excitation frequency may be varied at scan locations of the NV center **112** in the probe arm **376** and the resonance frequency may be determined using ODMR. FIG. **46**, by way example, illustrates a frequency shift determined using ODMR, which occurs at a plane 500 nm above the electric charge for two locations x along the line charge. The frequency shift will be largest at the center of the charge (x=0) where the e-field is a maximum and zero far away from the charge (x=3000 nm) where the e-field is zero. Known parameters that can be entered into the model equations are the NV center to charge distance y, the ESR line-width γ, the electric field line shift constant C_p, and the ODMR contrast constant C_{ODMR}.

[0156] Thus, the charge Q and the charge length (L in the one-dimensional case of a line charge) may be measured. For example, in the case of the FET and the flash-memory cell, the length L is the channel length and the charge Q is determined by the electron density in the channel. The measured ODMR signal is determined by the charge Q and charge length L by means of the E-field, the charge Q and charge length L may be derived from a parameter fit to the ODMR data. (i.e. the local frequency shift or the ODMR signal distribution for a fixed RF-excitation).

[0157] A dynamic electro-magnetic field measurement from the sample may also be made with the NV center **112** in the probe arm **376**. The electric charge or charge location will change dynamically when e.g., the transistor device is switching. The moving charge generates an AC electro-magnetic field orthogonal to the direction of motion of the charge, which can be detected using the NV center **112** in the probe arm **376** as a magnetic field sensor. For example, when the switching of the transistor is driven by a continuous AC current with a microwave MW frequency f_{MW}. The resulting electro-magnetic field with a frequency f_{MW} and an amplitude B_{MW} resonant with the $|0\rangle \rightarrow |-1\rangle$ transition of the NV center **112** and drives an oscillation between these spin states. With f_0 being the zero field resonance frequency of the NV center **112**, applying a static magnetic field B_z of appropriate magnitude will shift the ESR to the frequency f_{MW} of the applied MW-field, as shown in equation 13, where γ is the gyromagnetic ratio.

$$f_{MW}=f_0+\gamma B_z \quad \text{eq. 13}$$

[0158] The method makes use of the fact that a microwave field can drive coherent Rabi oscillations between the energy levels $|0\rangle$ and $|\pm1\rangle$ of the two level NV quantum system. The

Rabi frequency f_R is proportional to the amplitude B_{MW} of the electro-magnetic field being measured, as described in equation 14.

$$f_R(B_{MW}) = \gamma B_{MW} \quad \text{eq. 14}$$

$$\gamma = \frac{28\ \text{kHz}}{\mu\text{Tesla}}$$

[0159] Therefore, the electro-magnetic field amplitude B_{MW} may be determined by detecting the Rabi oscillation.

[0160] FIG. **47** illustrates a sequence for recording the Rabi oscillation using ODMR by applying laser pulses to the NV center **112** and pulses of AC current with a MW frequency to the sample with varying durations. The RF field generated by the sample is the excitation field for the NV center **112**, and thus, no external RF field is necessary. As illustrated, a sequence includes providing a first pulse **702** of the excitation illumination, e.g., from the light source **302** shown in FIG. **29**, that is incident on the at least one NV center. The first pulse **702** of excitation illumination pumps the spin system of the NV center into the $|0\rangle$ state, which has the higher photoluminescence intensity. A pulse **704** of AC current with MW frequency is then applied to the sample. The pulse **704** has a duration τ that may be varied in each sequence, and thus, is illustrated with duration τ_1 in the first sequence. A second pulse **706** of the excitation illumination that is incident on the nitrogen vacancy center is applied following the pulse **704** of AC current, and the spin dependent photoluminescence is measured **708** in response to the second pulse **706** of the excitation illumination. As illustrated in FIG. **47**, the sequence repeates with different durations of the pulse of AC current illustrated as duration τ_2 in the second sequence. By measuring the photoluminescence for an appropriate range of durations τ of the AC current with MW frequency, the Rabi oscillation is recorded. FIG. **48**, by way of example, illustrates a graph of measured photoluminescence with respect to different durations τ of the AC current with MW frequency. The Rabi oscillation **720** may be determined based on the spin dependent photoluminescence measured at the different durations τ of the pulse of the AC current, e.g., by curve fitting the data points. The Rabi frequency is 2_7*B_{MW}, where B_{MW} is the un-known, which is determined by parameter fitting. A parameter fit to equation 15 may be used to yield the Rabi frequency and, thus, the amplitude B_{MW} of the microwave electro-magnetic field being generated by the sample in response to the AC current with the microwave frequency, where τ_R is the Rabi decay time, C is the contrast parameter, F_0 is the fluorescence in the $|0\rangle$ state, F_1 is the fluorescence in the $|1\rangle$ state, B_{MW} is the RF field amplitude, and γ is the gyromagnetic ratio.

$$f(B_{MW};\tau) = C\cdot\frac{F_0}{2}\cdot\left(\cos(2\cdot\pi\cdot\gamma\cdot B_{MW}\cdot\tau)\cdot e^{-\frac{\tau}{\tau_R}}\right) + F_0\cdot\left(1-\frac{C}{2}\right) \quad \text{eq. 15}$$

for the $|0\rangle \to |-1\rangle$ transition

$$C = \frac{F_0 - F_1}{F_0}$$

[0161] This process is repeated for each measurement location on the sample, i.e., after performing the plurality of sequences to record the Rabi oscillation, the probe arm **376** is moved to the next location on the sample and the process is repeated.

[0162] Although the present invention is illustrated in connection with specific embodiments for instructional purposes, the present invention is not limited thereto. Various adaptations and modifications may be made without departing from the scope of the invention. Therefore, the spirit and scope of the appended claims should not be limited to the foregoing description.

What is claimed is:

1. A method comprising:

providing an electric charge in an area of a sample;

scanning a probe having a probe tip comprising at least one nitrogen vacancy center over the area of the sample with the electric charge;

providing an excitation radio frequency (RF) field to the at least one nitrogen vacancy center;

producing excitation illumination that is incident on the at least one nitrogen vacancy center;

measuring Optically Detected Spin Resonance (ODMR) as the probe tip is scanned over the area of the sample with the electric charge by detecting a decrease in a spin dependent photoluminescence in response to the excitation illumination caused by electron spin resonance (ESR) of the at least one nitrogen vacancy center; and

determining a characteristic of the area of the sample with the electric charge using the ODMR.

2. The method of claim **1**, wherein the sample is an integrated circuit device.

3. The method of claim **1**, wherein the characteristic of the area of the sample with the electric charge comprises at least one of an electric field distribution of the electric charge and a width of the area of the sample with the electric charge.

4. The method of claim **1**, wherein scanning the probe having the probe tip over the area of the sample with the electric charge comprises scanning the probe tip in two dimensions over the area of the sample with the electric charge.

5. The method of claim **1**, wherein an amplitude and frequency of the excitation RF field provided to the at least one nitrogen vacancy center is constant as the probe tip is scanned over the area of the sample with the electric charge.

6. The method of claim **1**, wherein scanning the probe having the probe tip over the area of the sample with the electric charge comprises moving the probe tip to a plurality of locations over the area of the sample with the electric charge and temporarily holding the probe tip stationary at each location of the plurality of locations;

wherein the excitation RF field provided to the at least one nitrogen vacancy center is varied at each location of the plurality of locations while the probe tip is temporarily held stationary; and

wherein the determining the characteristic of the area of the sample with the electric charge comprises determining a resonance frequency using the ODMR.

7. The method of claim **1**, wherein the electric charge is a static electric charge.

8. The method of claim **1**, wherein the electric charge is dynamically changing and wherein the excitation RF field is produced by a dynamically changing magnetic field in the sample produced by the electric charge that is dynamically changing.

9. The method of claim **8**, wherein the electric charge is dynamically changing by moving through the area of the sample to produce a current in the area of the sample.

10. The method of claim **9**, wherein the current is an alternating current.

11. The method of claim **10**, wherein determining the characteristic of the area of the sample with the electric charge using the ODMR comprises:

detecting a Rabi oscillation of the at least one nitrogen vacancy center, the Rabi oscillation having a Rabi frequency;

determining an amplitude of a magnetic field produced by the alternating current using the Rabi frequency.

12. The method of claim **11**, wherein the providing an electrical charge, the producing the excitation illumination, and the measuring ODMR comprises:

producing a plurality of sequences including producing a pulse of pump illumination that is incident on the at least one nitrogen vacancy center followed by producing a pulse of the alternating current followed by producing a pulse of the excitation illumination that is incident on the at least one nitrogen vacancy center and measuring the spin dependent photoluminescence in response to the pulse of the excitation illumination; wherein different durations of the pulse of the alternating current is used in each sequence;

wherein detecting the Rabi oscillation comprises using the spin dependent photoluminescence measured at the different durations of the pulse of the alternating current.

13. The method of claim **1**, wherein the probe tip comprises a crystal particle and the at least one nitrogen vacancy center is in the crystal particle, further comprising:

focusing the excitation illumination on the crystal particle; and

receiving the spin dependent photoluminescence from the at least one nitrogen vacancy center with a microscope.

14. The method of claim **1**, wherein the probe comprises a crystal arm and the probe tip is at a first end of the crystal arm and the at least one nitrogen vacancy center is in the probe tip.

15. The method of claim **14**, wherein producing the excitation illumination that is incident on the at least one nitrogen vacancy center comprises introducing the excitation illumination at a second end of the crystal arm that is opposite the first end of the crystal arm, wherein the excitation illumination is guided via total internal reflection through the crystal arm and is reflected into the probe tip.

16. The method of claim **15**, wherein introducing the excitation illumination at the second end of the crystal arm is performed without focusing the excitation illumination.

17. The method of claim **15**, wherein introducing the excitation illumination at the second end of the crystal arm comprises one of transmitting or reflecting the excitation illumination into the crystal arm by a beam splitter that is directly connected to the second end of the crystal arm.

18. The method of claim **17**, wherein measuring the ODMR by detecting the decrease in the spin dependent photoluminescence in response to the excitation illumination caused by ESR of the at least one nitrogen vacancy center comprises detecting photoluminescence from the at least one nitrogen vacancy center with a detector that is physical connected to the beam splitter either directly or with a spectral filter disposed between the detector and the beam splitter.

19. The method of claim **15**, wherein measuring the ODMR by detecting the decrease in the spin dependent photoluminescence in response to the excitation illumination caused by ESR of the at least one nitrogen vacancy center comprises detecting photoluminescence produced by the at least one nitrogen vacancy center in the probe tip and that is reflected into the crystal arm and extracted through the second end of the crystal arm.

20. The method of claim **19**, wherein the spin dependent photoluminescence extracted through the second end of the crystal arm is detected without focusing the spin dependent photoluminescence.

21. The method of claim **19**, wherein the spin dependent photoluminescence extracted through the second end of the crystal arm is reflected by the second end of the crystal arm to a detector, and wherein introducing the excitation illumination at the second end of the crystal arm comprises transmitting the excitation illumination into the crystal arm through the second end of the crystal arm.

22. The method of claim **14**, wherein the excitation RF field is produced by a radio frequency antenna on the crystal arm.

23. The method of claim **1**, wherein the ODMR is measured at varying excitation frequencies of the excitation RF field.

24. An apparatus comprising:

a biasing source configured to provide a bias signal;

a voltage source to provide a gate control voltage;

a probe card coupled to the biasing source and the voltage source and is configured to be connected to a sample to provide an electric charge in an area of the sample and to provide the gate control voltage;

a probe having a probe tip comprising at least one nitrogen vacancy center, the probe configured to scan the probe tip across the area of the sample with the electric charge;

a light source that produces excitation illumination that is incident on the at least one nitrogen vacancy center;

a detector configured to detect photoluminescence produced by the at least one nitrogen vacancy center in the probe tip; and

at least one processor coupled to the detector and configured to measure Optically Detected Spin Resonance (ODMR) as the probe tip is scanned over the area of the sample with the electric charge by detecting a decrease in a spin dependent photoluminescence in response to a received excitation radio frequency (RF) field and the excitation illumination caused by electron spin resonance (ESR) of the at least one nitrogen vacancy center; and determine a characteristic of the area of the sample with the electric charge using the ODMR.

25. The apparatus of claim **24**, wherein the sample is one of a Field Effect Transistor or Flash memory.

26. The apparatus of claim **24**, wherein the characteristic of the area of the sample with the electric charge comprises at least one of an electric field distribution of the electric charge and a width of the area of the sample with the electric charge.

27. The apparatus of claim **24**, wherein the probe is configured to scan the probe tip over the area of the sample with the electric charge in two dimensions.

28. The apparatus of claim **24**, wherein an amplitude and frequency of the excitation RF field received by the at least one nitrogen vacancy center is constant as the probe tip is scanned over the area of the sample with the electric charge.

29. The apparatus of claim **24**, wherein the probe is configured to scan the probe tip over the area of the sample with the electric charge by being configured to move the probe tip to a plurality of locations over the area of the sample with the

electric charge and temporarily hold the probe tip stationary at each location of the plurality of locations;

wherein the excitation RF field received by the at least one nitrogen vacancy center is varied at each location of the plurality of locations while the probe tip is temporarily held stationary; and

wherein the at least one processor is configured to determine the characteristic of the area of the sample with the electric charge by being configured to determine a resonance frequency using the ODMR.

30. The apparatus of claim **24**, the apparatus further comprising a RF antenna that produces the excitation RF field received by the at least one nitrogen vacancy center, wherein the electric charge is a static electric charge.

31. The apparatus of claim **24**, wherein the electric charge is dynamically changing and wherein the excitation RF field received by the at least one nitrogen vacancy center is produced by a dynamically changing magnetic field in the sample produced by the electric charge that is dynamically changing.

32. The apparatus of claim **31**, wherein the electric charge is dynamically changing by moving through the area of the sample to produce a current in the area of the sample.

33. The apparatus of claim **32**, wherein the current is an alternating current.

34. The apparatus of claim **33**, wherein the at least one processor is configured to determine the characteristic of the area of the sample with the electric charge using the ODMR by being configured to:

detect a Rabi oscillation of the at least one nitrogen vacancy center, the Rabi oscillation having a Rabi frequency;

determine an amplitude of a magnetic field produced by the alternating current using the Rabi frequency.

35. The apparatus of claim **34**, wherein the at least one processor is further configured to:

produce a plurality of sequences including produce a pulse of pump illumination that is incident on the at least one nitrogen vacancy center followed by producing a pulse of the alternating current followed by producing a pulse of the excitation illumination that is incident on the at least one nitrogen vacancy center and measuring the spin dependent photoluminescence in response to the pulse of the excitation illumination; wherein different durations of the pulse of the alternating current is used in each sequence;

wherein the at least one processor is configured to detect the Rabi oscillation by being configured to use the spin dependent photoluminescence measured at the different durations of the pulse of the alternating current to detect the Rabi oscillation.

36. The apparatus of claim **24**, wherein the probe tip comprises a crystal particle and the at least one nitrogen vacancy center is in the crystal particle, further comprising:

at least one lens configured to focus the excitation illumination on the probe tip and to project photoluminescence produced by the at least one nitrogen vacancy center on the detector.

37. The apparatus of claim **24**, wherein the probe comprises a crystal arm and the probe tip is at a first end of the crystal arm and the at least one nitrogen vacancy center is in the probe tip.

38. The apparatus of claim **37**, wherein the excitation illumination from the light source is introduced into a second end of the crystal arm that is opposite the first end of the crystal arm, wherein the excitation illumination is guided via total internal reflection through the crystal arm, and wherein the crystal arm is configured to reflect the excitation illumination into the probe tip.

39. The apparatus of claim **38**, wherein the excitation illumination from the light source is introduced into the second end of the crystal arm without focusing optics to focus the excitation illumination.

40. The apparatus of claim **38**, further comprising a beam splitter that is directly connected to the second end of the crystal arm, wherein the beam splitter transmits or reflects the excitation illumination from the light source into the crystal arm.

41. The apparatus of claim **40**, wherein the detector is physical connected to the beam splitter either directly or with a spectral filter disposed between the detector and the beam splitter.

42. The apparatus of claim **38**, wherein the crystal arm is configured to reflect the spin dependent photoluminescence produced by the at least one nitrogen vacancy center in the probe tip into the crystal arm and the spin dependent photoluminescence is guided via total internal reflection through the crystal arm and is extracted through the second end of the crystal arm.

43. The apparatus of claim **42**, wherein the spin dependent photoluminescence extracted through the second end of the crystal arm is detected by the detector without intervening focusing optics.

44. The apparatus of claim **42**, wherein the second end of the crystal arm is configured to reflect the spin dependent photoluminescence to the detector, and wherein the excitation illumination from the light source is introduced into the crystal arm by transmitting the excitation illumination through the second end of the crystal arm.

45. The apparatus of claim **37**, the apparatus further comprising a RF antenna on the crystal arm that produces the excitation RF field received by the at least one nitrogen vacancy center.

46. The apparatus of claim **24**, wherein the ODMR is measured at varying excitation frequencies of the excitation field.

47. A method comprising:

controlling a sample to produce a magnetic field;

scanning a probe having a probe tip comprising at least one nitrogen vacancy center through the magnetic field produced by the recording head;

producing excitation illumination that is incident on the at least one nitrogen vacancy center;

measuring Optically Detected Spin Resonance (ODMR) by detecting a decrease in a spin dependent photoluminescence in response to a received excitation radio frequency (RF) field and the excitation illumination caused by electron spin resonance (ESR) of the at least one nitrogen vacancy center; and

determining a characteristic of the recording head using the ODMR.

48. The method of claim **47**, wherein the sample is a recording head that includes a write pole to produce the magnetic field and wherein the excitation RF field is produced by an external RF antenna.

49. The method of claim **47**, wherein the sample is an is an integrated circuit device that produces a dynamically changing electric charge, and wherein the magnetic field is a

dynamically changing magnetic field produced by the dynamically changing electric charge, and wherein the excitation RF field is produced by the dynamically changing magnetic field.

* * * * *